**Distribution Agreement**

In presenting this thesis or dissertation as a partial fulfillment of the requirements for an advanced degree from Emory University, I hereby grant to Emory University and its agents the non-exclusive license to archive, make accessible, and display my thesis or dissertation in whole or in part in all forms of media, now or hereafter known, including display on the world wide web. I understand that I may select some access restrictions as part of the online submission of this thesis or dissertation. I retain all ownership rights to the copyright of the thesis or dissertation. I also retain the right to use in future works (such as articles or books) all or part of this thesis or dissertation.

Signature:

_____ _____

Yanjun Feng Date

CASPASE-8 SHAPES THE PATTERNS OF
ANTIVIRAL CD8 T CELL AND NATURAL KILLER CELL RESPONSES

By

Yanjun Feng
Doctor of Philosophy

Graduate Division of Biological and Biomedical Science
Immunology and Molecular Pathogenesis

_____
Edward S. Mocarski, Ph.D.
Advisor

_____
Lisa Daley-Bauer, Ph.D.
Committee Member

_____
Mandy L. Ford, Ph.D.
Committee Member

_____
Jacob E. Kohlmeier, Ph.D.
Committee Member

_____
Mehul Suthar, Ph.D.
Committee Member

_____
Edmund K. Waller, MD, PhD.
Committee Member

Accepted:

_____
Lisa A. Tedesco, Ph.D.
Dean of the James T. Laney School of Graduate Studies

_____
Date

CASPASE-8 SHAPES THE PATTERNS OF
ANTIVIRAL CD8 T CELL AND NATURAL KILLER CELL RESPONSES

By

Yanjun Feng
B.S., Wuhan University, 2008
M.S., George Washington University, 2011

Advisor: Edward S. Mocarski, Ph.D.

An abstract of
A dissertation submitted to the Faculty of the
James T. Laney School of Graduate Studies of Emory University
in partial fulfillment of the requirements for the degree of
Doctor of Philosophy
in
Graduate Division of Biological and Biomedical Science
Immunology and Molecular Pathogenesis
2019

## Abstract

CASPASE-8 SHAPES THE PATTERNS OF
ANTIVIRAL CD8 T CELL AND NATURAL KILLER CELL RESPONSES

By Yanjun Feng

An optimal lymphocyte response against virus infection is dictated by a delicate balance between cell proliferation and death. Infection triggers lymphocytes to undergo a dramatic proliferation resulting in an exponential accumulation. This process must be tightly regulated to prevent immunoproliferative diseases. As the central mediator of extrinsic death, caspase-8 (Casp8) can initiate apoptosis, suppress necroptosis, and regulate death-independent signaling transduction. Understanding of Casp8 function in lymphocyte activation was confounded by an unleashing of RIPK3-mediated necroptosis in the absence of Casp8. *Casp8*$^{-/-}$*Ripk3*$^{-/-}$ (DKO) mice that lack this dysregulation open the way to study Casp8 function in lymphocytes. In this dissertation, murine cytomegalovirus (MCMV) is utilized to trigger a natural and robust adaptive Ly49H$^{+}$ natural killer (NK) and T cell responses. I describe my work evaluating the role of Casp8 in the generation of antiviral immunity, and demonstrate an unexpected death-independent function of Casp8 in suppressing NK and CD8 T cell expansion.

DKO mice are immunocompetent and capable of controlling MCMV infection; however, detailed characterizations of innate and adaptive immune responses have not been reported. I found that Casp8 and RIPK3 signaling is dispensable for the generation of antiviral immunity against MCMV. Enhanced NK and T cell expansion indicates that Casp8 normally dampens the accumulation of these cells during the acute phase of MCMV infection.

Elimination of Casp8 (together with RIPK3) leads to virus-specific CD8 T cell hyperaccumulation. I found that this is due to an increase in proliferation due to Casp8-deficiency in T cells independent of environmental cues in DKO mice following infection. Notably, the Ly49H$^{+}$ NK cell response drives this hyperaccumulation by promoting the T cell survival. This study highlights an antiviral natural killer cell function that promotes effector T cell expansion unless kept in check by T cell-autonomous Casp8 function.

The function of Casp8 in NK cell regulation beyond suppressing necroptosis remains unknown. I found that Casp8 has a Ly49H$^{+}$ NK cell-autonomous function in restricting expansion. Strikingly, NK cell responses are ablated once RIPK1 is eliminated along with Casp8 and RIPK3. Thus, Casp8 and RIPK1 dictate the magnitude of this NK cell subset following MCMV infection.

# CASPASE-8 SHAPES THE PATTERNS OF ANTIVIRAL CD8 T CELL AND NK CELL RESPONSES

By

Yanjun Feng
B.S., Wuhan University, 2008
M.S., George Washington University, 2011

Advisor: Edward S. Mocarski, Ph.D.

A dissertation submitted to the Faculty of the
James T. Laney School of Graduate Studies of Emory University
in partial fulfillment of the requirements for the degree of
Doctor of Philosophy
in
Graduate Division of Biological and Biomedical Science
Immunology and Molecular Pathogenesis
2019

## Acknowledgments

PhD is a long journey. And I could never get through it without the help and support from a lot of people. I would like to first thank my supervisor Ed for the freedom he gave me to develop my own projects and collaborations. He has taught me how to seek the simple but crucial questions that fill the gap in knowledge. He has been constantly challenging me in science, which pushes me to become a better and confident scientist. His passion in science is always inspiring and reminds me why I wanted to do Ph.D. at the beginning.

I would like to express my deepest gratitude and respect to my mentor Lisa. Lisa is a brilliant immunologist who has a keen vision in science. I want to thank her for guiding me through my projects, teaching me immunology techniques, giving me critiques, talking me out of difficulties in work and in life.

And I want to thank Linda, the "mother" in lab. She oversees the lab to make sure everyone getting what she or he needs. She is always there for me and reminds me that there is someone who backs me up. I would also like to thank all the present and previous members of Mocarski lab, especially Modi, Heather, Pratyusha, Hongyan, and Zach, for the support they offered and the joyful moments we shared.

There is no way I can make through grad school without my friends. Ching-wen, Tiger, Jeffrey, Alice, Lynnett, Paul, Mary, Catlin, and Monika, thank you for the fun/drinking/gossip/cursing moments we created together and for always being there with me. Thank rock climbing, and thank my climbing partners for holding ropes to secure my life.

All I can say to my parents is thank you. You have always been supporting any of the decision I have made, encouraging me to embrace the challenges and uncertainty in life.

Finally, I would like to show my deepest gratitude and love to my husband Guanyu. Life brought us together after we knowing each other for more than ten years. I never stop appreciating the beautiful and difficult moments we have experienced, the moments letting us grow as a strong team in life.

## Table of Contents

**Abstract**…. iv

**Acknowledgments** vi

**Table of Contents** vii

**List of Figures** ix

**Abbreviations** x

**Chapter 1: Introduction** 1

**1.1 T cell responses following MCMV infection** 1

1.1.1 Priming MCMV-specific CD8 T cell responses 1

1.1.2 Features of MCMV-specific CD8 T cell responses 3

1.1.3 CD4 T cell responses following MCMV infection. 10

1.1.4 Tissue-resident CD8 T cells following MCMV infection. 11

**1.2 NK cell responses following MCMV infection.** 13

1.2.1 NK cell activation is determined by the balance between activating and inhibitory receptor signals 13

1.2.2 Adaptive immune features of NK cells 15

**1.3 Cell death pathways** 18

1.3.1 Intrinsic cell death pathway 18

1.3.2 Extrinsic apoptotic pathway. 18

1.3.3 Necroptosis 20

1.3.4 Extrinsic cell death and host defense 23

1.3.5 Death-independent function of Casp8 23

**1.4 Casp8 and extrinsic death pathway in the regulation of T cells and NK cells** 25

1.4.1 Intrinsic death regulates T cell and NK cell during homeostasis and infection. 26

1.4.2 Casp8 and extrinsic death pathway in the regulation of T cell homeostasis. 27

1.4.3 Casp8 and extrinsic death pathway in the regulation of virus-specific T cell responses. 29

1.4.4 Casp8 and extrinsic death pathway in proliferation. 31

**1.5 Figures and Figure Legends.** 34

**Chapter 2: Remarkably Robust Antiviral Immune Response Despite Combined Deficiency in Caspase-8 and RIPK3.** ……37

**2.1 Abstract** 38

**2.2 Introduction** 39

**2.3 Results** 43

**2.4 Discussion** 52

**2.5 Materials and Methods** 57

**2.6 Figures and Figure Legends** 62

**Chapter 3: Caspase-8 Restricts Natural Killer Cell-triggered Antiviral CD8 T Cell Hyperaccumulation ..... 73**
**3.1 Abstract ..... 74**
**3.2 Introduction ..... 75**
**3.3 Results ..... 79**
**3.4 Discussion ..... 89**
**3.5 Materials and Methods: ..... 95**
**3.6 Figures and Figures Legends ..... 99**
**Chapter 4: Caspase-8 Restricts Ly49H+ NK cell expansion following Murine Cytomegalovirus Infection ..... 113**
**4.1 Abstract ..... 114**
**4.2 Introduction ..... 115**
**4.3 Results ..... 118**
**4.4 Discussion ..... 123**
**4.5 Materials and Methods ..... 126**
**4.6 Figures and Figure Legends ..... 128**
**Chapter 5: Discussion and future directions ..... 137**
**References: ..... 151**

## List of Figures

Figure 1.1 Overview of conventional and inflationary CD8 T cell kinetics during the acute and latent phases of MCMV infection. ..... 34
Figure 1.2 Casp8 determines the outcomes of extrinsic pathway. ..... 35

Figure 2.1 Age-dependent impact of Casp8 and RIPK3 deficiency on myeloid cell homeostasis. ..... 62
Figure 2.2 Impact of Casp8 and RIPK3 deficiency on T cell homeostasis at different ages. ..... 64
Figure 2.3 Impact of Casp8 and RIPK3 deficiency on DC activation following MCMV infection. ..... 66
Figure 2.4 Impact of Casp8 and RIPK3 deficiency on NK cell responses following MCMV infection. ..... 68
Figure 2.5 Impact of Casp8 and RIPK3 deficiency on T cell antiviral responses. ..... 70
Figure 2.6 Impact of Casp8 and RIPK3 deficiency on Ab levels following MCMV infection. .. 72

Figure 3.1 Impact of Casp8 on antiviral T cell responses during the acute phase of virus infection. ..... 99
Figure 3.2 Impact of Casp8 on antiviral T cell responses during long-term infection. ..... 101
Figure 3.3 Patterns of antiviral CD8 T cell responses when antigen levels are compromised... 103
Figure 3.4 Assessment of CD8 T cell proliferation and death. ..... 104
Figure 3.5 Impact of m157-driven NK cells on antiviral CD8 T cell responses. ..... 106
Figure 3.6 Impact of WT m157-driven NK cells on antiviral CD8 T cell responses. ..... 108

Figure 4.1 NK cell expansion, contraction, and differentiation during the acute phase of MCMV infection. ..... 128
Figure 4.2 Patterns of NK cell responses when antigen levels were compromised. ..... 130
Figure 4.3 Cell-autonomous impact of Casp8 on NK cell expansion and contraction during the acute phase of MCMV infection. ..... 132
Figure 4.4 Impact of Casp8 on NK cell proliferation and death. ..... 133
Figure 4.5 Assessment of NK cell responses in another Casp8-deficienct strain and the contribution of RIPK1 to the response. ..... 135
Figure 4.6 Phenotype of NK cells in long-term infected Casp8-deficient mice. ..... 136

Figure 5.1. Assessment of signaling mechanism following TCR stimulation. ..... 146
Figure 5.2 CD4 T cell proliferation and cytokine production following TCR stimulation. ..... 147
Figure 5.3 Assessment of the abnormal T cell and virus titers in long-term infected mice. ..... 149
Figure 5.4 Schematic of how Casp8 regulates CD8 T cell and NK cell. ..... 150

## Abbreviations

Ab: antibody
ADCC: antibody-dependent cellular cytotoxicity
APC: Antigen presenting cell
BMDC: bone marrow-derived DC
Casp: caspase
$Casp8^{DA/DA}$: Casp8 auto-processing mutant
$C8^{-/-}R3^{K51A}$: *$Casp8^{-/-}Ripk3^{K51A/K51A}$*
cDC: more mature $CD3^{-}CD11c^{+}MHC\text{-}II^{hi}$ cDC
cDC2: $CD8\alpha^{-}CD11b^{+}$ cDC
cDC1: $CD8\alpha^{+}CD11b^{-}$ cDC
CDV: cidofovia
cFLIP: cellular Fas-associated death domain-like interleukin-1-β-converting enzyme-inhibitory protein
CMV: cytomegalovirus
DC: dendritic cell
DD: death domain
DED: death effector domain
DISC: death-inducing signaling complex
DKO: *$Casp8^{-/-}Ripk3^{-/-}$*
DPEC: double positive effector cell
DR: death receptor
EAE: Experimental autoimmune encephalomyelitis
EEC: early effector cell
EOMES: eomesodermin
FADD: Fas-associated protein with death domain
FLICA: fluorescent-labeled inhibitor of caspases
FVS: fixable viability staining
GSDM: gasdermin
HET: *$Casp8^{+/-}Ripk3^{-/-}$*
hpi: hours post-infection
HSV-1: herpes simplex virus 1
ICCS: intracellular cytokine staining
IM: inflammatory monocyte
IKK: IκB kinases
IMS: mitochondrial intermembrane space
ITAM immunoreceptor tyrosine-based activation motif
ITIM: immunoreceptor tyrosine-based inhibitory motif
KD: kinase domain
KLRG1: killer cell lectin-like receptor G1
KIR: killer cell immunoglobulin-like receptor
LAMP-1: lysosomal associated membrane glycoprotein-1
LCMV: lymphocytic choriomeningitis virus
LILR: leukocyte immunoglobulin-like receptor
Macs: macrophages

MHV-68: murine γ-herpesvirus-68
MLKL: mixed lineage kinase domain like pseudokinase
MOMP: mitochondria outer membrane permeabilization
MPEC: memory precursor effector cell
pDC: plasmacytoid DC
PD-1: Programed death 1
PM: patrolling monocyte
pre-DC: precursor-like $CD3^{-}CD11c^{+}MHC\text{-}II^{lo}$ cDC
$R3^{K51A}$: *Ripk3*$^{K51A/K51A}$
RIPK: Receptor interacting protein kinase
RHIM: RIP homotypic interaction motif
RT: room temperature
SG: salivary gland
short-lived effector cell, SLEC
Tcm: T central memory
Tem: T effector memory
TLR: Toll-like receptor
TRADD: TNFR1-associated death domain protein
TRAIL: TNF- related apoptosis-inducing ligand
Trm: tissue-resident memory T cell
vICA: viral inhibitor of caspase 8 activation
vIRA: viral inhibitor of RIP activation
ZBP: Z-form nucleic acid binding protein

# Chapter 1: Introduction

## 1.1 T cell responses following MCMV infection

Human (h) cytomegalovirus (CMV) is a betaherpesvirus that infects overwhelming majority of the world's population by adulthood, with age of acquisition trending older in more developed countries. This virus establishes a life-long persistence in immunocompetent hosts (1). Although HCMV infection is generally asymptomatic, it can cause substantial pathology in immunocompromised hosts, such as AIDS patients and organ transplantation recipients (1). In addition, it is the most common congenital virus infection that can cause neurological defects in neonates (1). Therefore, understanding the mechanism that regulates anti-CMV immune response has significant clinical relevance. The understanding of virology and immunology of HCMV has been significantly enhanced by murine (M)CMV infection models in mice (1). MCMV is a natural mouse pathogen that reliably simulates disease and antiviral responses observed with HCMV in human. Both viruses use similar mechanisms to counteract the immune surveillance and help establish lifelong persistence in the host. Importantly, both HCMV and MCMV infection result in the hallmark T cell memory inflation (2). The phenotype, kinetics, and function of HCMV- and MCMV-specific T cell responses are similar, indicating that MCMV is an outstanding tool to explore immune mechanisms controlling HCMV infection. In this section, we are going to discuss the phenotypes of MCMV-specific CD8 T cells and the key factors that regulate this response.

### *1.1.1 Priming MCMV-specific CD8 T cell responses*

The first cells infected by MCMV following intraperitoneal inoculation are splenic marginal zone stromal cells (3). Infection of these stromal cells results in a rapid burst of type I IFN in serum at around 8 hours post-infection (hpi) produced by infected cells through a

lymphotoxin-β-dependent pathway (4). The second wave of type I IFN occurs between 36-48 hr and is mainly produced by plasmacytoid(p) DCs and $CD8\alpha^{-}CD11b^{+}$ conventional DC (cDC2) (5-7). Type I IFNs are potent antiviral cytokines that can act directly on the infected cells to inhibit virus replication and can trigger NK cell activation (5-7), a critical innate immune cell for early control of MCMV (8). In addition, MCMV infection induces proinflammatory cytokines (such as IL-12 and IL-18), which improves innate and adaptive immune cell activation (3).

DCs are critical for activating the CD8 T cell antiviral immune response. The magnitude of this response and phenotype of T cells are dictated by i) TCR stimulation by epitope-bounded MHC class molecules, ii) co-stimulation and iii) cytokine milieu. MCMV has evolved to encode viral-inhibitors that suppress DC antigen presentation and co-stimulation (1). Numerous *in vitro* co-culture studies have shown that MCMV infection paralyzes DC function, leading to impaired T cell proliferation (9). To impair antigen presentation in DCs, MCMV encodes m04, m06 and m152 viral proteins to retain the MHC-I molecules in ER/Golgi (10). Additionally, the MCMV is also capable of suppressing expression of co-stimulation. The virus-encoded m138 protein prevents CD80 expression on cell surface by retaining CD80 inside the lysosomal associated membrane glycoprotein-1 $(LAMP\text{-}1)^{+}$ intracellular compartment (11). Viral protein m147.5 inhibits CD86 expression on infected cell surface (12). Furthermore, CD40 is downregulated by viral glycoprotein m155 (13). While the virus restricts co-stimulatory molecule expression, the infection leads to an upregulation of programmed death ligand-1 (PD-L1) (14). Combined, MCMV inhibits antigen presentation and alters the balance between co-stimulatory and co-inhibitory molecules to impair priming of adaptive immune responses.

Although virus inhibitors severely impair antigen presentation, nevertheless the infection elicits robust T cell responses that are capable of controlling the infection. This begs the question

- how does the host immune system generate a powerful CD8 T cell response when the infected DCs are functionally paralyzed? MCMV infects a small fraction of DCs, less than 5% of DCs *in vivo* (15), allowing for the majority of these cells remain functional and successfully upregulate MHC class molecules and co-stimulatory molecules. These uninfected DCs, especially conventional $CD8\alpha^{+}CD11b^{-}$ cDC (cDC1) subsets, cross-present viral antigens to trigger a robust antiviral CD8 T cell expansion during the acute phase of MCMV infection (16-20). This is supported by data showing that bulk splenic DCs from infected animals trigger T cells undergoing robust proliferation in culture (9). The importance of cross-presentation has been further reinforced by the observation that a spread-defective MCMV mutant is able to trigger robust antiviral CD8 T cell responses. BATF3 is a critical transcriptional factor for cDC1 development (18). The impaired acute CD8 T cell responses observed in MCMV-infected *Batf3*$^{-/-}$ mice strongly support the role of cross-presenting cDC1 for CD8 T cell priming. Important to note, a later work has shown that cDC1 in *Batf3*$^{-/-}$ mice is restored in certain infection setting via a BATF2-dependent pathway (21), an important caveat that may affect the interpretation of the contribution of cDC1 during long-term MCMV infection in the setting of using *Batf3*$^{-/-}$ mice. Besides cDC1, the tissue-localized $CD103^{+}$ DC is another subset capable of cross-presentation (18); however, the contribution of this population during MCMV infection remains unclear (16). Taken together, cDC1s cross-present viral antigens to trigger MCMV-specific CD8 T cell responses. This is an effective host counterstrategy to the viral immune-suppressing functions.

### *1.1.2 Features of MCMV-specific CD8 T cell responses*

A classical pattern of virus-specific CD8 T cell responses includes stages of expansion, contraction, and memory formation. Virus infection triggers CD8 T cells to undergo an exponential expansion and differentiation into highly heterogeneous subsets in term of effector function,

differentiation plasticity and longevity (22). Different virus-specific CD8 T cell subsets can be loosely defined by the expression levels of killer cell lectin-like receptor G1 (KLRG1) and IL-7Rα (or CD127). KLRG1 was first recognized as a terminal differentiation marker on NK and activated T cells (23, 24) and later studies demonstrated its function in cell cycle inhibition (25). IL-7 is a critical cytokine for CD8 T cell survival during homeostasis and following infection. CD8 T cells expressing CD127, which is the high-affinity α chain of IL-7 receptor, exhibit an enhanced response to this pro-survival cytokine (26). Upon activation, $KLRG1^{lo}CD127^{hi}$ naïve CD8 T cells downregulate CD127 to become $KLRG1^{lo}CD127^{lo}$ early effector cells (EECs) (27, 28). These EECs have potential to differentiate into $KLRG1^{hi}CD127^{lo}$ short-lived effector cells (SLEC), or $KLRG1^{hi}CD127^{lo}$ memory precursor effector cells (MPEC), or $KLRG1^{hi}CD127^{hi}$ double positive effector cells (DPEC) (28, 29). SLECs differentiation is promoted by cumulative T cell receptor signals and proinflammatory cytokines (28, 30, 31). Adoptive transfer analysis has shown the limited differentiation plasticity of the SLEC subset (30, 32, 33). In contrast, $KLRG1^{lo}CD127^{hi}$ MPECs display increased survival and retain the differentiation potential to become EECs or SLECs (28). While SLECs and MPECs both exhibit a comparable capacity of cytotoxicity and IFNγ production (28, 34), the majority of SLECs contract following the peak of the acute phase, leaving MPECs to further differentiate into memory T cells that protect the host from subsequent infection (32). Although DPECs were initially thought of as terminally differentiated (28), a recent study highlights that these cells can down-regulate KLRG1 and differentiate into different memory lineages (33). Conventionally, memory CD8 T cells are grouped into T effector memory (Tem) cells and T central memory (Tcm) cells, based on their distinct features such as effector function, localization, migration and longevity (35). Tcm cells display high expression of CD62L and CCR7 but low levels of CCR5, suggesting that this subset preferentially homes to secondary lymphoid

organs. In contrast, Tem cells express low levels of CD62L and CCR7 but high levels of CCR5, and preferentially migrate to non-lymphoid tissues. Further, Tcm cells have higher proliferation capacity and can give rise to effector cells following stimuli; whereas, Tem cells have lower proliferation capacity but can mount fast responses to invading pathogens with high cytotoxicity capacity (36). These two subsets circulate through different organs and function complementary fashion in the antiviral host defense. Taken together, this highly heterogeneous effector and memory pool confers protective antiviral-immunity during acute and chronic/persistent phases of virus infection.

MCMV infection triggers CD8 T cell responses against a broad spectrum of epitopes. In C57BL/6 mice, CD8 T cells specific to more than 26 viral epitopes from 18 viral proteins have been identified (19). The epitopes recognized by T cells are categorized as either conventional or inflationary subset based on their distinct antiviral response patterns (19). Conventional epitope-specific CD8 T cells follow a classical pattern of expansion, contraction and stable memory (37). They predominantly exhibit SLEC phenotype during the acute phase, with 15% to 20% of the population as MPECs (37). Following the peak of the acute phase, the majority of the $KLRG1^{hi}$ subsets contract, leaving MPECs, DPECs, and the remaining SLECs differentiated into the memory subsets (37). Most of these cells exhibit $CD62L^{hi}KLRG1^{lo}CD127^{hi}$ Tcm phenotype in latently infected mice. Inflationary epitope-specific cells may also expand during the acute phase (19); however, unlike conventional CD8 T cells, inflationary cells continue to expand during latency, that is to say in the absence of active virus replication in any organ (19, 37). This subset mostly displays $CD62L^{lo}KLRG1^{hi}CD127^{lo}$ Tem phenotype, reflecting the continuous recruitment from naïve or Tcm pool (37). This is consistent with the memory inflation observed in HCMV serologically positive humans. An infected healthy adult may commit as much as 30% of total

peripheral blood CD8 T cells to HCMV specific epitopes, although the percentages vary widely between individuals (38). Similar to inflationary populations during MCMV infection, HCMV-specific memory cells display a Tem phenotype, including upregulated expression of T cell activation and differentiation markers CD57, KLRG1, and CD45RA, downregulated expression of CD27 and CD28; however, theses HCMV-specific memory T cells lack classical signs of T cell exhaustion as the MCMV-specific T cells (39).

The essential role of CD8 T cells in the control of MCMV infection has been clarified in different mouse strains. In BALB/c mice, IE1 is the dominant epitope that triggers CD8 T cell responses with an inflationary pattern (40). A recombinant vaccine containing IE1 epitope confers sufficient antiviral CD8 T cell immunity to protect against MCMV challenge (41). In line with this observation, transferring the inflationary M38-specific CD8 T cells is sufficient for virus control in C57BL/6 mice. In contrast, the conventional M45-specific CD8 T cells fail to control the infection *in vivo* (42), even though M45 is the immunodominant epitope that triggers a robust CD8 T cell expansion during the acute phase of MCMV infection in C57BL/6 mice. Importantly, this conventional subset confers protection to Δm152 MCMV mutant that lacks an MHC-I evasion gene (42), suggesting that the failure of protection is attributable to the susceptibility of this conventional epitope to MCMV immunoevasive inhibitors. In other words, efficient presentation of inflationary epitopes (e.g., M38 or IE1) on the infected cells results in recognition by the corresponding inflationary epitope-specific CD8 T cell subsets. The differences between conventional and inflationary subsets indicate another competing strategy between host and MCMV – while the host develops epitope-specific CD8 T cells in order to kill virus infected cells, the virus evolves a counterstrategy by luring its host to mount robust CD8 T cell responses that recognize certain epitopes not present on infected cells. Two-photon confocal microscopy reveals

a similar scenario (43), where multiple CD8 T cells collaborate to effectively kill an MCMV-infected cell, even though infection-induced MHC-I downregulation delays the target cell from being recognized and killed. Human CD8 T cell antiviral function also plays a critical role in controlling HCMV infection. This is supported by studies that adoptive transferring HCMV-specific CD8 T cells effectively ameliorates HCMV-related diseases in immunocompromised patients (44).

Antigen stimulation is essential for priming and sustaining conventional and inflationary CD8 T cell responses. cDC1-dependent cross-presentation triggers antiviral CD8 T cell expansion during the acute phase but is dispensable for the memory inflation (17, 20). Instead, infected non-hematopoietic cells in lymph nodes directly present viral antigens to simulate the epitope-specific inflationary cells to undergo proliferation, differentiation, and migration out of lymph nodes. This mechanism is thought to maintain the inflationary population at high levels in blood circulation and non-lymphoid organs (37). A recent study, however, suggests that circulating inflationary cells may be maintained by the latently infected endothelial cells that line the interior surface of blood vessel (45), consistent with previous studies showing endothelial cells are a major site for MCMV latency (46). These two models are not necessarily mutually exclusive; instead, both embrace the importance of direct presentation in support of memory inflation. In addition, the magnitude of this response is positively correlated to inoculum dose (16, 17, 47) and is enhanced upon each successive challenge (48).

In response to MCMV infection, only certain antigen-specific CD8 T cells undergo memory inflation, whereas others follow more classical kinetics. Understanding the mechanism behind these two response patterns is important for developing any CMV-based vaccine. One theory is that gene expression kinetics determine which epitope-specific CD8 T cells undergo

inflation. This is supported by a study showing that fusing a herpes simplex virus (HSV)-1 protein to different MCMV gene induces conventional or inflationary responses. Fusion to the *ie3* gene, a conventional inflationary epitope, lead to HSV-1-specific CD8 T cells undergoing memory inflation; whereas fusion to the *m45* gene, which follows a conventional pattern lead to a conventional response pattern to the same HSV-1 epitope (49). This result is consistent with the fact that *ie3*, like its splice variant *ie1*, is an immediate early gene expressed sporadically in latently infected cells (50), contrasting to *m45* as an early gene. A second theory is that the dependence on immunoproteasome determines whether an epitope triggers conventional or inflationary response. Processing of conventional epitopes is highly dependent on the immunoproteasome compared to inflationary epitopes (51). A study shows that moving the conventional HGIRNASFI[1] M45 epitope to the C-terminus of this protein triggers a robust inflationary response, because processing of this C-terminus-localized peptide does not require the immunoproteasome (52).

In addition to antigen presentation, co-stimulation plays an important role in regulating the magnitude and kinetics of MCMV-specific CD8 T cell responses. Most co-stimulatory molecules belong to immunoglobulin superfamily (e.g., the CD28 and CD80/CD86 family) or TNFR superfamily (e.g., CD40 and CD40L, OX40 and OX40L, 4-1BB and 4-1BBL). Interactions between CD80/86 and CD28 are required for the robust expansion of both conventional and inflationary subsets during the acute phase but are dispensable for memory inflation during latency (53). In contrast, engagement of OX40 with OX40L has no impact on the MCMV-specific CD8 T cell response magnitude during the acute phase; however, the interaction is crucial for the optimal inflationary responses (54). In addition, interactions between CD70 and CD27 (55), 4-1BBL and 4-1BB (56) support both conventional and inflationary subsets during the acute and latent phases.

[1] HGIRNASFI is the amino acid sequence of the epitope.

Interestingly, elimination of 4-1BB enhances CD8 T cell levels during the acute phase but leads to a decrease in memory inflation during long-term infection, suggesting a unique bi-phasic role of this co-stimulatory receptor in regulating MCMV-specific CD8 T cells. These data together indicate the importance of co-stimulation for regulating MCMV-specific CD8 T cell responses.

Appropriate signaling generated by the cytokine milieu and transcriptional regulation are important regulatory mechanism in the generation of MCMV-specific CD8 T cell responses. For example, IL-12 promotes MCMV-specific CD8 T cell responses (5), whereas IL-10 and IL-33 suppress the magnitude of this adaptive immune response (57, 58). Signal through IL-2 amplifies TCR signaling and improves virus-specific T cell proliferation. Elimination of IL-2 receptor lead to a decrease in the numbers of MCMV-specific CD8 T cells during both acute and latent phases (59), re-enforcing the crucial contribution of this cytokine for driving a robust MCMV-specific CD8 T cell response. The pro-survival cytokine IL-15 rather than IL-7 supports T cell levels during latency, through a CD122-mediated, STAT5 transcription factor-dependent mechanism (60). CD8 T cell differentiation is determined by the balance of distinct transcriptional factors, which have been mostly studied in models of infection, such as lymphocytic choriomeningitis virus (LCMV) (22). Transcription factors T-bet and eomesodermin (EOMES) function together to program effector cell fates. T-bet drives SLEC differentiation, while EOMES is required for MPEC differentiation. While neither is the suppressor for the other molecule, T-bet: EOMES ratio or the gradient of expression levels of both proteins determines cell differentiation fate. Transcriptional factors that are involved in MCMV-specific T cell regulation remain to be explored. However, a recent study has shown that elimination of transcription factor FOXO1 results in a hypo-response of MCMV-specific CD8 T cells during the acute phase and long-term infection, attributed to an increase in cell death rather than defective proliferation (61). In addition, MCMV-specific *Foxo1*$^{-}$

$^{-/-}$ T cells exhibit an impaired Tcm phenotypes during latency, an alteration that is also observed in LCMV-specific CD8 T cells (62). These data indicate that some established understanding of transcription factors in other infection models may inspire the work of MCMV. The contribution of T-bet and EOMES to MCMV-specific T cell differentiation remain unclear. Notably, loss of FOXO1 alters T-bet:EOMES ratio in CD8 T cells following MCMV infection, suggesting the importance of these two transcriptional factors for MCMV-specific CD8 T cell differentiation. Future studies in T-bet- or EOMES-modulated mice is required for evaluation.

### *1.1.3 CD4 T cell responses following MCMV infection.*

Following MCMV infection, CD4 T cells can function in three ways – i) act as helper cells to promote CD8 T cell function, ii) promote antibody (Ab) production, and iii) act directly on infected cells for virus control. In contrast to the large numbers of MCMV-specific CD8 T cells following the inflationary response pattern, most of CD4 T cells follow the classical kinetics, with the exception of the m09 epitope-specific CD4 T cells in C57BL/6 strain that are low during the acute phase but increase substantially by 40 dpi (63). MCMV-specific CD4 T cells produce IL-2, IFNγ, and TNF. CD4 T cells drive memory inflation through secreting IL-2 and through engagement of 4-1BBL and 4-1BB (56, 59). Moreover, these cells improve Ab production from B cells through CD28-CD80/86 interactions (64). The importance of CD4 T cells for MCMV control was initially shown in BALB/c mice, where CD4 T cell depletion lead to continuous viral replication in salivary gland (SG)s (65), a major site of MCMV shedding. The importance of IFNγ in inhibiting virus replication in SGs was shown by using bone marrow chimera (66). MCMV infection leads to MHC class I molecule downregulation from the surface of acinar glandular epithelial cells in SGs to avoid CD8 T cell immunosurveillance (66). Thus, the study proposed that bystander APCs that express MHC class II molecules activate tissue-resident CD4 T cells to

produce IFNγ for virus control. Additionally, granzyme B producing MCMV-specific CD4 T cells was shown to directly kill infected cells within the liver but not in spleen or lungs (67). In accordance, adoptive transfer of CD4 T cells specific to the MCMV epitope M25 confers sufficient protection to MCMV infection (68). The importance of CD4 T cells has also been shown in HCMV studies. Adoptively transferring *ex vivo* activated CD4 T cells into transplant recipients conferred sufficient protection against HCMV reactivation (69). Together, CD4 T cells are important for controlling the infection of MCMV and HCMV.

### *1.1.4 Tissue-resident CD8 T cells following MCMV infection.*

Increasing amounts of literature have emphasized the importance of resident memory T (Trm) cells in controlling CMV infection. Trm is a group of memory T cell localizing in a specific tissue and conferring first-line protection (35). In contrast to the circulating memory subsets, Trm cells show limited levels of re-circulation to blood and preferentially migrate and take up residence in tissues. HCMV-specific CD8 T cells reside in diverse tissue sites, including spleens, bone marrow, lymph nodes, lungs, colon and so on (70). These cells all exhibit a prompt cytotoxic cytokine production upon stimulation. Consistently, MCMV infection induces both CD8- and CD4-positive Trm cell accumulation in multiple organs (71). Tissue-specific homing receptors direct Trm cells to these specific organs. $CD69^{+}CD103^{-}$ lung-resident CD8 Trm cells are observed following MCMV infection (72). MCMV infection in all organs can be effectively controlled within two to three weeks, with the exception of SG where active virus replication persists for more than a month. Previous studies have emphasized that viral control in the SG is specifically dependent on CD4 T cells rather than CD8 T cells (65, 66), based on the result that has showed CD4 T cell-depletion lead to virus persistent replication in SGs. This observation is consistant with the effective MHC-I molecule down-regulation on infected acinar glandular epithelial cells of the

SG (66, 73). A recent study defines the SG-resident CD4 and CD8 Trm cells following MCMV infection (74). These cells exhibit upregulated expression of CD103 and/or CD69, and have lower turnover rate in comparison with lung- or spleen-resident cells (74, 75). The formation of the SG-resident CD4 and CD8 Trm cells requires a continuous recruitment of CD8 and CD4 Tem cells from circulation (74). Interestingly, the formation and maintenance of the SG-resident Trm cells is independent of TGF-β, IL-33 or TNF (74), which are the cytokines essential for Trm cell formation during other virus infections (76, 77). Unexpectedly, these SG-resident CD8 Trm cells sufficient antiviral function to against the SG-localized MCMV challenge (71, 75). This observation indicates a previously under-appreciated anti-MCMV function of SG-resident CD8 T cells. Alternatively, persistent viral replication in SGs following CD4 cell-depletion may be due to a defect in CD8 Trm development, given that CD4 T cells are important for supporting the development of CD8 Trm (78). Further studies are needed to understand the mechanism of Trm cell formation as well as the cell function in different organs.

## 1.2 NK cell responses following MCMV infection.

NK cells belong to the group of type I innate lymphoid cells (ILCs) (8). These innate immune cells control virus infections and provide tumor immunosurveillance through a rapid production of cytokines as well as cytotoxic activity (79). NK cell activation is determined by the balance between germline-encoded activating receptors and inhibitory receptors. The activating receptors are stimulated by stress-induced ligands along with the down-regulation of MHC class molecules (i.e., "missing self"). The inhibitory receptors recognize MHC class molecules (i.e., "self"). This dual sensing system allows NK cells to recognize and kill infected or transformed cells that down-regulate MHC molecules to evade cytotoxic T cell surveillance. While NK cells are classically described as a member of the innate immune compartment, increasing evidence has emerged suggesting that these innate immune cells also possess adaptive immune cell features. This session summarizes the factors that regulate the innate and adaptive immune responses of NK cells.

### *1.2.1 NK cell activation is determined by the balance between activating and inhibitory receptor signals*

NK cells express a large repertoire of inhibitory receptors on the cell surface that recognize MHC class and some non-MHC class I ligands (80). The inhibitory receptors belong to different superfamilies based on their structure. Killer cell immunoglobulin-like receptors (KIRs) and leukocyte immunoglobulin-like receptors (LILRs) are classified as type I glycoproteins which are part of the immunoglobulin superfamily, and Ly49 and CD94/NKG2A receptors are type II glycoproteins belonging to C-type lectin-like domain superfamily. Despite differences in extracellular structures, these receptors all possess a common signaling motif, immunoreceptor tyrosine-based inhibitory motif (ITIM), at their cytosolic tails (80). Receptor ligation results in

phosphorylation of ITIM at the tyrosine residue and subsequent recruitment of phosphatases that suppress NK cell activation.

NK cell activating receptors recognize a wide array of ligands that are either constitutively (eg. HLA-E) or transiently (eg. stress-induced ligands) expressed on target cells. NK cell activation occurs when activating signals override inhibitory signals (79). NK cell activating receptors typically have short cytosolic tails that associate with a signaling subunit for transducing activation signals. DAP-12 is a transmembrane-anchored signaling subunit that contains immunoreceptor tyrosine-based activation motifs (ITAMs). DAP-12 associates with activating receptors, such as NKG2C/CD94, Ly49H and Ly49D, NK1.1 and CD16 (79). Mouse Ly49 receptor family members contain both inhibitory and activating receptors that recognize H-2D, H-2K as well as the MCMV m157 viral protein. The inhibitory Ly49 receptors contain an ITIM in their cytosolic tail that transduces a suppressive signal. The two activating Ly49H and Ly49D receptors that lack ITIMs associate with the ITAM-containing DAP12 for NK cell activation (81). The ligation of the activating receptor triggers ITAM phosphorylation, which recruits ZAP-70 and Syk to the plasma membrane, leading to subsequent activation of PLC-γ ultimately triggering NFAT, NF-κB and MAP kinase activation (80). Similar to T cells, NK cell activating receptor-induced ITAM phosphorylation can also lead to the subsequent formation of CARMA-MALT1-BCL10 complex (82, 83). The cytokine production triggered by NK1.1 and Ly49H stimulation is compromised from *Bcl10*$^{-/-}$, *Malt1*$^{-/-}$, *Carma*$^{-/-}$, and *Card9*$^{-/-}$ NK cells (82), indicating the important role of the CARMA-MALT1-BCL10 complex for signal transduction in NK cells. Thus, despite being categorized as innate immune cells, NK cells activation induce highly similar signaling cascades to T cells.

### *1.2.2 Adaptive immune features of NK cells*

Although NK cells have been defined as innate immune cells, increasing evidence has shown that they possess some adaptive immune features, including education during development, antigen-specific clonal expansion in response to virus infection, and immunological memory formation. T cells development in thymus requires positive and negative selection in thymus through the interactions between TCR and autoantigens present by MHC class molecules on thymic epithelial cells. These processes select T cells that recognize host MHC class molecules but not self-react (80). NK cells develop primarily in bone marrow (79), with a small portion of cells that arises from the liver (84). Similar to T cell development, NK cell development also requires the positive and negative selections. Immature NK cells express a vast repertoire of inhibitory receptors that recognize host MHC class ligands (80). Ligation of these receptors educates NK cells how to recognize "missing self", an important mechanism for triggering NK cell-mediated cytotoxicity function when they recognize host cells that have lost MHC molecule expression on cell surface (85-87). Those NK cells expressing the inhibitory receptors that lack the cognate MHC class molecules or cells lacking inhibitory receptors will become hypo-responsive or anergic (88). Further, the strength of NK cell responses has a positive correlation with the number of inhibitory receptors that recognize self MHCs (89, 90). Notably, NK cell developmental programming is not fixed (91); indeed, those impaired cells can be re-educated in periphery to become functional again (92, 93).

The adaptive immune features of NK cells during virus infection has been best characterized following MCMV infection. The activating receptor Ly49H recognizes the MCMV m157 glycoprotein expressed on the surface of the infected cells, triggering this NK cell subset to undergo robust activation, a clonal expansion-like response and memory formation in C57BL/6

strain (94, 95). Although infected WT mice exhibit only three- to ten-fold increase in Ly49H$^+$ cell numbers by day 7 post infection (96), Ly49H$^+$ NK cells have been shown to expand 100- to 1000-fold when adoptively transferred into a Ly49H-eliminated mouse (95), suggesting a clonal expansion-like accumulation triggered by this activating receptor. This response is antigen-specific and only occurs during m157-competent virus infection (97) or upon encountering m157-expressing tumor cells (98). The signaling pathway downstream of the Ly49H receptor is highly analogous to TCR, given that both triggers the phosphorylation of ITAM at cytosolic tail of the accessary protein to drive the formation of the CARMA-MALT1-BCL10 complex to signal through ZAP-70 to activate the transcription factors NFAT and NF-κB, as well as MAPK signaling (83). However, it is unclear why other ITAM-bearing NK cell activating receptors cannot trigger a similar adaptive NK cell response. Adaptive immune features of NK cells have been reported in HCMV seropositive humans. CD94$^+$NKG2C$^+$ NK cells typically constitute around 1% of the total NK cell population in HCMV serological negative human; this percentage increases to 5% to 50% in the seropositive group (99, 100). Longevity studies have shown a clonal expansion-like response of CD94$^+$NKG2C$^+$ NK cells in immunocompromised patients who received solid organ transplantation (101) and in a B and T cell-deficient newborn who had an HCMV infection (102). However, whether this adaptive immune-like response is antigen-specific remains to be determined.

Co-stimulation and cytokines both contribute to the NK cell adaptive immune responses. Stimulation of CD80 (103), 4-1BB or GITR (104) enhances NK cell cytotoxicity. The co-inhibitory receptor PD-1 is upregulated on NK cells localized in tumor microenvironment. Additionally, the disruption of PD-1/PD-L1 interaction enhances NK killing function against tumor cells (105). CD28 stimulation enhances NK cell proliferation but has no contribution to the

cytotoxic function of cells in culture (106). Some NK cell receptors also confer co-stimulatory functions. Signaling through NKG2D enhances Ly49H$^+$ NK expansion, even though triggering this receptor by itself is not sufficient for driving NK cell proliferation (107). Moreover, proinflammatory and pro-survival cytokines have a profound impact on NK cell responses. IL-12 and type I IFN improve NK cell cytotoxicity and IFNγ production (5, 108) and drive Ly49H$^+$ NK cell expansion (109). Type I IFNs regulate NK cell activation by upregulating transcriptional factors including STAT1, STAT2, IRF8, IRF9 (110, 111). In addition, cytokines IL-18- and IL-33-driven MyD88 activation enhances Ly49H$^+$ NK cell proliferation (112, 113). Taken together, similar to other adaptive immune cells, NK cell function and response are affected by co-stimulatory molecule signaling and cytokine milieu.

## 1.3 Cell death pathways

### *1.3.1 Intrinsic cell death pathway*

The key process of intrinsic cell apoptosis is mitochondria outer membrane permeabilization (MOMP), which leads to the release of mitochondrial intermembrane space (IMS) proteins that trigger subsequent effector caspase activation (114). This process is tightly regulated by Bcl-2 family proteins, through a balance or pro-apoptotic and anti-apoptotic members (115). The pro-apoptotic members include those that initiate apoptosis (i.e., Bim, Bid, Noxa, Puma) and those that function on mitochondria member (i.e., Bax, Bak and Bok) to result in MOMP. In addition, there are the anti-apoptotic members (i.e., Bcl-2, Bcl-XL, Mcl-1) that inhibit apoptosis (116, 117). Anti-apoptotic members normally bind the apoptosis initiators to sequester them from the effector proteins (118, 119). Expression of pro-apoptotic proteins can be induced by mitochondrial damage, cell stress, DNA damage, or hypoxia. Growth factor deprivation leads to FOXO3-driven Bim expression (120). In addition, DNA damage induces p56-dependent Noxa and Puma upregulation (121). Insertion of Bax and Bak onto mitochondria membrane induces MOMP activation (122), releasing IMS proteins, such as cytochrome *c*, Apaf 1 and Casp9, to the cytosol where they form a complex termed apoptosome (123). Activated Casp9 further cleaves and activates the two apoptosis executioners Casp3 and Casp7 (123) which then initiate a cascade of events, including phosphatidylserine externalization, DNA degradation and cytoplasmic condensation, and the release of apoptotic bodies that are taken up by phagocytes (114).

### *1.3.2 Extrinsic apoptotic pathway.*

Extrinsic apoptosis pathway is best characterized following the activation of the cell surface TNF superfamily death receptor (DR), such as TNFR-1, Fas, TNF- related apoptosis-inducing ligand (TRAIL) receptor-1 and -2 (TRAIL-R1 and TRAIL-R2), DR2 and DR6 in mice.

This family of receptors contains a death domain (DD) at the cytosolic tail that is essential for activating the death pathway (124). As the key adaptor, Fas-associated protein with death domain (FADD) consists of a carboxyl-terminal DD and an amino-terminal death effector domain (DED) (Figure 1.2.). Following DR trimerization, the DDs at DR cytosolic tails recruit FADD through the DD domain interactions, leading to the formation of a death-inducing signaling complex (DISC) (or ripoptosome). The conformational changes of FADD allowing for the DED to be exposed and recruit Casp8 (125).

Casp8 is the central initiator of extrinsic apoptosis. Procaspase-8 is expressed as a zymogen, which consists of amino-terminal pro-domain comprising two DED domains, followed by one large proteolytic subunit (p20/p18), a short linker region and one small proteolytic subunit (p12/p10) (Figure. 1.2.). Once a procaspase-8 is recruited to FADD through DED interactions, additional recruitment of this procaspase leads to the formation an oligomerized structure (126). Procaspase-8 oligomerization allows the proteolytic domains to dimerize, which triggers auto-cleavage (127) to release the large and small subunits resulting in full Casp8 activation (125). The specific isoform of cellular Fas-associated death domain-like interleukin-1-β-converting enzyme-inhibitory protein (cFLIP) association with Caps8 in the cytosolic complex determines cell death fate. cFLIP is expressed in long form ($cFLIP_L$) or short form ($cFLIP_s$) depending on mRNA splicing (Figure. 1.2.). $cFLIP_s$ comprises the two DEDs and acts as a Casp8 inhibitor by blocking the formation of procaspase-8 dimerizers (128). $cFLIP_L$ is an inactive procaspase-8 homologue. Low levels of $cFLIP_L$ favor Casp8-initiated apoptosis, whereas high levels of the protein inhibit this pathway (129). Interestingly, Casp8 auto-processing mutation (D387A) only delays rather than preventing Casp3 activation upon Fas stimulation (130). This suggests that Casp8 self-cleavage contributes but is not essential for initiating extrinsic apoptosis. Once activated, Casp8 may cleaves

Casp3 directly, the step where intrinsic and extrinsic death pathways converge. In addition, when is present at lower levels Casp8 may cleave Bid to activate Bax and Bak (124), a process similar to the intrinsic pathway that has been called mitochondrial amplification. The fact that *Bak*$^{-/-}$*Bax*$^{-/-}$ (131) or *Bid*$^{-/-}$ (132) mice resist Fas-induced hepatitis is consistent with Bid-dependent crosstalk between extrinsic and intrinsic pathways.

Ligation of DRs can trigger death or promote cell survival. Receptor interacting protein kinase (RIPK)1 is the key regulator that determines which of the two possible outcomes will be fulfilled (133). RIPK1 comprises an N-terminal kinase domain (KD) followed by the central region that includes a RIP homotypic interaction motif (RHIM), and a carboxyl-terminal DD (Figure 1.2.). Upon TNFR-1 activation, RIPK1 is recruited by TRADD to form a membrane-associated complex, where RIPK1 is heavily ubiquitinated by the E3 ligase cIAP (134-136). RIPK1 polyubiquitination builds a platform for NEMO, TAK1 and TAB2 interactions, which lead to NF-κB and MAPK activation. NF-κB induces the expression of $cFLIP_L$ and cIAP which further promotes cell survival. Cell stress, inhibition of cIAP, or activation of deubiquitinases (such as A20 or CYLD) results in RIPK1 deubiquitination (137) and the formation of the cytosolic DISC platform that switches the fate of the cell in favor of apoptosis (138).

### *1.3.3 Necroptosis*

Necrosis is conventionally viewed as unprogrammed cell death induced by chemical toxicity or physical stress, resulting from swelling organelles and plasma membrane rupture. However, necrosis may be programmed and concisely regulated (139). DR-triggered necroptosis requires RIPK1-RIPK3 interactions through RHIM, which leads to the formation of a cytosolic amyloid structure. RIPK3 or/and RIPK1 in this complex undergo activation and subsequent recruitment of mixed lineage kinase domain-like pseudokinase (MLKL) (140) (Figure 1.2.). Once

activated by RIPK3, MLKL translocates to plasma membrane, where this effector protein oligomerizes to create membrane nanopores that eventually lead to osmotic force-induced membrane rupture (141, 142).

Necroptosis is normally inhibited by Casp8. Following DR activation, lack of survival signals favors the cytosolic DISC formation. When Casp8 function is intact, evidence suggests that this protease cleaves RIPK1 (143) and RIPK3 (144) to prevent necroptosis. Notably, unprocessed procaspases-8-cFLIP$_L$ heterodimers are also enzymatically active and are capable of suppressing necroptosis (145). Elimination of Casp8 or mutation that compromises its catalytic activities (*Casp8*$^{C362A}$ in mouse or *Casp8*$^{R248W}$ in human) ((145, 146), Newton et al. poster 2018) unleashes necroptosis (Figure 1.2.). This unleashing of necroptosis can be inhibited by mutations (147, 148) or pharmacological inhibitors (146, 148) that compromise RIPK kinases activities responsible for MLKL activation, or by MLKL elimination (149). Morever, RIPK1 or RIPK3 inhibition can favor Casp8-mediated apoptosis activation. RIPK1-elimination leads to prenatal lethality, which is fully rescued by knocking out RIPK3 together with Casp8 (or FADD) (150-153); whereas catalytically inactive mutation of RIPK1 (D138N) has no impact on the mouse development (147). These suggest that the scaffolding function of RIPK1 suppresses apoptosis and necroptosis during development. A kinase inactive RIPK3 D161N mutant strain exhibits embryonic lethality, which is rescued by Casp8 elimination (147), suggesting a vital RIPK3 kinase function in the suppression of Casp8-dependent apoptosis. However, *Ripk3*$^{-/-}$ mice develop with no evident abnormality. These confounding results were later clarified by work from Mocarski lab showing that cells obstaaining K51A, D161G, and D143N RIPK3 kinase inactive mutants retain viability (148), challenging the notion that RIPK3 kinase activities naturally promote survival (147). Instead, a kinase activity-independent, conformation-dependent role of RIPK3 drives

Casp8-cFLIP$_L$-RIPK1 death complex activation (148). In line with these observations, inducible dimerization of RIPK1 or RIPK3 triggers Casp8-dependent apoptosis when of MLKL is absent (154, 155). Combined, although a precise spatial and temporal mechanism remains to be explored, it is clear that a balance between extrinsic apoptosis and necroptosis is critical for development and appropriate responses to danger signals.

Extrinsic necroptosis and apoptosis can also be initiated independently of DRs, through pathogen recognition receptors such as Toll-like receptor (TLR)3, TLR4, Z-form nucleic acid binding protein (ZBP)1 (also called as DAI or DLM1). TLR3 and TLR4 recruit RIPK1 and RIPK3 through the adaptor of the RHIM containing protein TRIF (156), while ZBP1 is a RHIM containing protein and can directly recruit both kinases (157, 158). RHIM interaction-triggered necroptosis is potent host defense mechanism used to eliminate infected cells, such that these interactions are naturally targeted by virus-encoded inhibitors such that progeny can be produced (159). Surprisingly, the RIPK1 RHIM mutation-induced perinatal lethality is delayed by knocking out RIPK3 or MLKL and fully rescued by knocking out ZBP1 (160, 161). These data suggest that the RHIM of RIPK1 functions as a brake to prevent ZBP1 initiated, RIPK3/MLKL-dependent necroptosis during development. In addition, a DISC-like structure forms associations with RIG-I, an innate immune sensor for RNA viruses. Casp8-dependent cleavage of RIPK1 restricts IRF3 activation (162). RIG-I can also trigger necroptosis when Casp8 is inhibited (163). Furthermore, stimulation of T cell receptor and certain NK cell activating receptors (e.g., CD16 and 2B4) (164-167) initiates necroptosis when Casp8 function is compromised. Taken together, this core platform regulating extrinsic apoptosis and necroptosis has a very broad distribution in different cell types and can be activated in multiple ways for the regulation of development, immune cell homeostasis, and cell-autonomous host defense.

### *1.3.4 Extrinsic cell death and host defense*

[2]Considerable experimental evidence supports physiological interplay between alternate Casp8-mediated apoptosis and RIPK3-mediated necroptosis in host defense against multiple virus infection. As a natural mouse viral pathogen, MCMV has provided unambiguous evidence showing that interactions of Casp8 (168) and RIPK3 (157, 158, 169) build the first line of host defense (170). In return, the MCMV encode viral proteins function to inhibit cell death signaling for sustaining infection, dissemination, and persistence. The viral gene M36-encoded vICA inhibits basal activity as well as auto-cleavage activation of Casp8 (171, 172). The viral gene M45-encoded vIRA (169) acts as a natural RHIM competitor to suppress RIPK3 being recruited by ZBP1 (157). Viruses with single mutation on M36 or M45, or with double mutations are susceptible to premature death of infected cells through Casp8- and RIPK3-dependent pathways and fail to sustain infection in the host (169, 170, 173). Importantly, attenuation of these viruses is reversed in Casp8 and RIPK3 are eliminated in the host (170), reinforcing the critical role of these two pathways in host defense to virus infection. Overall, Casp8 and RIPK3 sustain potent cell-autonomous innate host defense to stop the spread of virus infection such that both pathways are inhibited by virus-encoded cell death suppressors.

### *1.3.5 Death-independent function of Casp8*

As the central mediator of extrinsic pathway, Casp8 has been shown to support host development and lymphocyte and activation. Elimination of Casp8 or FADD in mice results in embryonic lethality. Genetic defects in human that result in catalytic activity-mutated Casp8 are immunocompromised, due to a sever lymphocyte activation defect (164, 165). NK, B and T cells

[2] This paragraph is adapted from a publish paper "Remarkably Robust Antiviral Immune Response despite Combined Deficiency in Caspase-8 and RIPK3" (Feng et. al. 2018).

from these patients are resistant to Fas-triggered death but exhibit impaired NF-κB activation following stimulation. In line with this observation, mice with Casp8 or FADD eliminated specifically in T cells fail to mount antiviral T cell responses needed in the control of virus infections (166). However, this pro-survival function during development and lymphocyte activation has been confounded by its role of restricting necroptosis. Combined RIPK3 or MLKL elimination rescues these developmental and T cell activation defects (145, 147-149, 174, 175). This implicates necroptosis suppression as an essential death-regulating function of Casp8 beyond driving apoptosis (166, 167, 176).

Numerous publications in the last few years have demonstrated the death-independent function of Casp8 in innate immune signaling transduction. RIG-I activation assembles a complex that comprises Casp8, FADD, RIPK1 and RIPK3 (162). Casp8 catalytic activity keeps RIPK1 functions in check by cleaving the kinase to restrict the duration of IRF-3 activation. Another study has shown that Casp8 can directly cleave IRF-3 and result in its degradation by proteasome (177). Mice with Casp8 knocked out in the myeloid compartment (*LysMCre-Casp8*$^{flox/flox}$ or *CD11cCre-Casp8*$^{flox/flox}$) develop splenomegaly, autoantibody deposition, and lymphocyte infiltration into multiple organs (178, 179). While RIPK3 elimination can rescue the dysregulation in *LysMCre-Casp8*$^{flox/flox}$ mice, abnormality in *CD11cCre-Casp8*$^{flox/flox}$ mice is reversed by knocking out MyD88, suggesting death-independent function of Casp8 in suppressing the MyD88-dependent signaling pathways (178). Some studies have shown the supportive role of Casp8 in signal transduction downstream of ZBP1, TLR3, and TLR4 (125). *Casp8*$^{-/-}$*Ripk3*$^{-/-}$ mice exhibit a severe defect in pro-inflammatory cytokine production in response to infectious insult including *Citrobacter rodentium*, *Yersinia*, and influenza A infection (180-185). Notably, this defect is independent of Casp8-autoprocessing, given that Casp8-autoprocessing mutant bone marrow-derived

macrophages (BMDM) produce WT levels of proinflammatory cytokines (182). Whether the scaffolding function or catalytic function of Casp8 regulates innate immune signal transduction requires future study.

Casp8 function also impacts inflammasome regulation. Pathogen sensed by cell surface or cytosolic receptors induces the expression of inflammasome components, a step named "priming". Subsequent processing of pro-IL-1β and pro-IL-18 by Casp1 or Casp11 generates the active form of these proinflammatory cytokines, another step named "trigger" (186). When both Casp1 and Casp11 are eliminated in bone marrow-derived DC (BMDC), the NLRP3-ASC inflammasome recruits Casp8 to process IL-1β (187). Interestingly, this inflammasome platform triggers Casp8-dependent apoptosis in mouse tubular epithelial cells (188). These data suggest that these two pathways are regulated by crosstalk in different cell types. Casp8-dependent processing of IL-1β also occurs downstream of Dectin-1, also known as CLEC7A (189). Dectin-1 ligation triggers assembly of the CARD9-MALT1-BCL10 complex that induces pro-IL-1β expression. This complex subsequently recruits Casp8 through ASC for processing pro-IL-1β to its active form (189). In addition to Dectin-1, Casp8 is also involved in the priming stage downstream of TLR3 and TLR4 (181, 190). Following recruitment to inflammasome, Casp1 and Casp11 activate gasdermin (GSDM) D to induce pore formation in the plasma membrane. This highly inflammatory cell death is termed pyroptosis (186). A recent study shows that Casp8 can directly cleave GSDMD in response to Yersinia infection, leading to a pyroptosis-like cell death (191).

### 1.4 Casp8 and extrinsic death pathway in the regulation of T cells and NK cells

T cells and NK cells are the two critical immune cell types for combating virus infection. While these cells perform robust cytotoxic function to clear infection and develop immune

memory, uncontrolled responses cause immunoproliferative diseases. Therefore, the balance between proliferation and death is required for maintaining a healthy immune system.

### *1.4.1 Intrinsic death regulates T cell and NK cell during homeostasis and infection.*

Intrinsic apoptosis is critical during various development processes such that disruption of the death may lead to severe developmental disorders during development. *Casp3*$^{-/-}$ mice born at lower frequencies and often die before 3 week old (192), while *Casp3*$^{-/-}$*Casp7*$^{-/-}$ mice die rapidly within 10 days of birth (193). These data suggest an additive effect of multiple cell death effectors, even though eliminating Casp7 by itself in mice has no evident impact during development (193). In line with these observations, Bax-deficiency results in lymphoid hyperplasia and reproductive abnormality (194), while most *Bak*$^{-/-}$*Bax*$^{-/-}$ mice die perinatally, with less than 10% survival into adulthood (195). Surviving adults develop multiple disorders of the central nervous, hematopoietic compartment, and reproductive systems (195). Mice lacking Bim survive to adulthood but progressively accumulate lymphoid and myeloid cells with age, and have severe autoimmune kidney diseases (196). It is clear that intrinsic apoptosis removes undesired cells to maintain a balance during development.

Intrinsic apoptosis plays the dominant role in controlling T cell numbers following pathogen infection. The importance of this form of death in eliminating activated T cells was first shown by using superantigen to treat Bim-deficient mice (197). Later studies have demonstrated the importance of Bim (198-200), Puma (200), Bax and Bak (201) in driving both KLRG1$^{hi}$ and KLRG1$^{lo}$ antigen-specific T cell contraction. Pro-survival cytokine IL-7 supports naïve and effector T cell survival, through promoting STAT5 signaling-mediated Bcl-2 expression (202). CD8 T cell contraction is thought to be induced by a decrease in pro-survival signals. While Bcl-2 or Bcl-XL over-expression prolongs activated T cell survival (203), neutralizing IL-7 or IL-15

accelerates the contraction of both KLRG1$^{hi}$CD127$^{lo}$ and KLRG1$^{lo}$CD127$^{hi}$ CD8 T cell subsets (204). However, treatment of IL-15, but not IL-7, delays antigen-specific CD8 T cell contraction (205), suggesting a more important role of IL-15 in supporting CD8 T cell survival during virus infection. Further, STAT5 elimination impairs antiviral T cells responses (204), in line with the known role of the STAT-Bcl-2 pathway in supporting T cell survival.

IL-15 is the critical pro-survival cytokine for NK cell development and response of the Ly49H$^{+}$ subset to MCMV m157 (206). IL-15 maintains Mcl-1 expression and suppresses Bim expression. Deprivation of IL-15 leads to NK cell death, which is rescued by eliminating Bim (206). Elimination of Bim results in slower contraction of Ly49H$^{+}$ NK cells and impaired memory development (207).

### *1.4.2 Casp8 and extrinsic death pathway in the regulation of T cell homeostasis.*

The importance of Fas-mediated extrinsic T cell death, also termed as activation-induced cell death (AICD), was initially reported *in vitro* culture (208-210). Anti-CD3/CD28 stimulation results in T cell undergoing apoptosis, which can be rescued by preventing Fas-FasL interactions. In accordance to these observations, *lpr* or *gld* mice that have mutations in Fas or FasL, respectively, progressively accumulate the abnormal CD3$^{+}$B220$^{+}$CD4$^{-}$CD8$^{-}$ T cells, as well as conventional CD4 and CD8 T cells in peripheral lymphoid organs with age (211-214). These abnormal T cells are thought to be derived from previously activated CD4 and CD8 T cells, a hypothesis based on their high expression levels of activation markers (215). In contrast to Bim, Fas signaling has no impact on T cell development in the thymus. Autoimmune lymphoproliferative syndrome (ALPS) patients with Fas mutation develop similar symptoms as observed in *lpr* and *gld* mice, with enlarged lymph nodes, spleen, thymus, and liver attributable to immune cell infiltration and accumulation (216). The peripheral lymphoid organs and the

circulating cell population contain an unusually high number of the abnormal T cells. Although elimination of TNFR1 or TRAIL dose not confer any significant phenotype, knocking out TNFR1 together Fas exacerbates the homeostatic abnormality (217). These observations together point to the critical role of Fas-mediated cell death in eliminating activated T cells during homeostasis.

Based on the findings described above, restriction of abnormal T cell accumulation and lymphoid hyperplasia is dependent on extrinsic cell death. Notably, Fas death domain-deficient mice exhibit accelerated development of lymphadenopathy (218) in comparison with *lpr* mice with a DD mutation on Fas (213), demonstrating the importance of adaptor function of Fas in restricting ALPS development. Moreover, palmitoylation-defective Fas is defective in inducing apoptosis, but does not progress to lymphoid hyperplasia and abnormal T cell accumulation that develops in *lpr* mice (219). These observations suggest a death-independent function of Fas in suppressing ALPS.

Casp8 is the critical apoptosis initiator downstream of Fas; however, Casp8 (or FADD) elimination in mice leads to embryonic lethality, an outcome completely different from the phenotype in *lpr* mice (220). This suggests that the most important role of Casp8 during development is to suppress necroptosis. However, evaluation of this pro-survival role of Casp8 is confounded by the unleashing of necroptosis; Casp8-eliminated mice survive into fertile adult once on a necroptosis removed background (e.g. $Casp8^{-/-}Ripk3^{-/-}$ or $Casp8^{-/-}Mlkl^{-/-}$) (145, 147-149, 166, 167, 174, 221, 222). These genotypes with combined deficiency of extrinsic apoptosis and necroptosis all develop lymphoid hyperplasia and exhibit the abnormal T cell accumulation with age, in line with the crucial role of Casp8 functions directly downstream of Fas. Elimination of Casp8 (or FADD) within T cells along with germline loss of RIPK3 is sufficient to cause the abnormal T cell accumulation (166, 222); whereas disrupting only Casp8 (or FADD) in T cells

confers no evident phenotype (223-225). This implicates the RIPK3-mediated pathway in the removal of the abnormal T cells when extrinsic apoptosis is disrupted. Interestingly, *Casp8*$^{-/-}$*Mlkl*$^{-/-}$ mice exhibit accelerated lymphadenopathy and abnormal T cell accumulation above what is seen in *Casp8*$^{-/-}$*Ripk3*$^{-/-}$ (149). Further, this abnormality is less severe once RIPK1 is eliminated along with Casp8 (or FADD) and RIPK3 (150, 151, 153). It is possible that certain death-independent roles of these extrinsic pathway members regulate the development of this *lpr*-related diseases.

### *1.4.3 Casp8 and extrinsic death pathway in the regulation of virus-specific T cell responses.*

Although extrinsic cell death was initially implicated in T cell contraction, numerous studies have now shown that the intrinsic apoptosis pathway plays the dominant role during this process (226). The first *in vivo* study using Bim-deficient mice shows a defect in CD8 T cell contraction in response to staphylococcal enterotoxin B, contrasting to the competent T cell contraction in *lpr*, *lprTnfr1*$^{-/-}$ and *lprTnfr2*$^{-/-}$ mice (197). These findings were extended with studies that compared antiviral CD8 T cell responses in *lpr* and Bim-deficient mice, as well as the mice with the combined deficiency of both pathways following infection of herpesviruses. Interestingly, virus-specific CD8 T cell contraction during HSV-1 infection solely depends on Bim, whereas contraction following murine γ-herpesvirus-68 (MHV-68) infection requires the collaboration between Bim- and Fas-dependent death (116, 227). Notably, elimination of Bid also leads to a slower antiviral CD8 T cell contraction in response to MHV-68 infection (228). *lprTnfr1*$^{-/-}$ mice exhibit slower clearance of MCMV in multiple organs; whether this is due to a defect in T cell antiviral function or a failure of the infected cell clearance remains to be clarified (229). These data together indicate that the Bim-mediated pathway is critical for T cell contraction during acute infection, such as HSV-1 infection, whereas eliminating the expanded T cells following persistent

virus infection (such as MHV-68) depends on a collaboration between Fas-and Bim-mediated pathways, probably through the connection by Bid.

One shortcoming of the previous studies using DR knockout mice is that multiple DRs can trigger the same downstream pathway used in the initiation of apoptosis. Thus, mutation of a common downstream key member, like Casp8 or FADD, helps to eliminate the entire death pathway without having to eliminate each of the DRs capable of triggering extrinsic death (176). One major difficulty of studying Casp8 and FADD in T cell is that compromising the function of either molecule leads to defective T cell activation (164, 165, 223-225). This defect was initially attributed to a pro-survival role of Casp8 and FADD by supporting NF-κB activation. Multiple papers have shown that TCR stimulation leads to the recruitment of Casp8 by the CARMA-MALT1-BCL10 complex (230, 231). TCR activation triggers the downstream formation of the CARMA-MALT1-BCL10 signaling complex, which creates a polyubiquitin scaffold used to recruit and phosphorylate the IκB kinases (IKK) for activating NF-κB. CARMA-MALT1-BCL10 can recruit FADD and Casp8 (231), possibly through the DD homotypic interactions between FADD and MALT1 (83, 165, 232). A study shows that the paracaspase domain of MALT1 directly suppresses the Casp8 pro-apoptotic function during T cell activation (230). Although a wealth of studies focused on the death-independent function of Casp8 in activated T cells, most of these previous experiments were performed in Casp8-deficient T cells, and were confounded by the unleashed necroptotic death following TCR activation. Careful analysis indicates that there is intact NF-κB activation despite the Casp8 or FADD deficiency (167, 232). Later studies show that removing RIPK3 completely rescue this proliferation defect, given that $Cd4^{Cre}Casp8^{-/-}Ripk3^{-/-}$ and $Lck^{Cre}Fadd^{dd}Ripk3^{-/-}$ mice mount robust antigen-specific T cell expansion following virus infection (166, 222). Similar to the mice with Casp8 specifically disrupted in T cell, $Casp8^{-/-}Ripk3^{-}$

$^{-/-}$ mice exhibited robust and functional CD8 T cell immunity following MCMV infection (150, 174, 233). These results strongly support the conclusion that a critical function of Casp8 in activated T cells is to restrict the induction of necroptosis. Importantly, now we have these T cells lacking the confounding necroptosis dysregulation, which can be used to ask more definitive questions about the roles of Casp8 in T cell regulation.

Little evidence has shown the Casp8 contributes a specific function within NK cells. Mutation within the catalytic site of Casp8 leads to an activation defect within NK cells following 2B4 or CD16 stimulation, similar to that observed in activated T cells (164, 165). This suggests that Casp8 keeps necroptotic death in check in NK cells. It is introduced above that stimulation of NK cell activating receptors induces a signaling cascade similar to that following TCR activation, including the CARMA-MALT1-BCL10 complex formation that subsequently triggers NF-κB activation (83). Whether Casp8 can be recruited to this plasma membrane-associated complex in NK cells remains to be explored.

### *1.4.4 Casp8 and extrinsic death pathway in proliferation.*

The death-independent role of the extrinsic apoptosis pathway in regulating T cell proliferation has primarily been studies downstream of Fas (234). Fas can act as a co-stimulation receptor to regulate T cell proliferation. Low dose Fas agonist improves T cell proliferation, along with enhanced IL-2, IFNγ, TNF secretion (235). While low doses of Fas agonist improves T cell proliferation, high doses inhibit proliferation through interfering the recruitment of protein kinase C-Θ to TCR (236). This defect in proliferation can be rescued by PMA/inomycin treatment which can circumvent TCR-associated signaling complex and directly trigger T cell activation. These data indicate that the regulation of Fas on T cell proliferation engages the signaling platform proximal to TCR.

Recent studies used cells lacking Casp8 (or FADD) on a necroptosis-deficient background to investigate the death-independent role of Casp8. A few publications have shown that elimination of both Casp8 and RIPK3 enhances the accumulation of live, divided CD8 T cells following stimulation in culture (151, 152, 222, 233). However, whether this is due to a decrease in T cell death or enhanced proliferation remains to be determined. Mice with Casp8 specifically deleted in hepatocytes have improved liver regenerative capacity, which has been attributed to an enhanced NF-κB activation that induces the earlier expression of cell cycle progression proteins (237). Compromising Casp8 catalytic activities also leads to sustained NF-κB and Erk activation depending on RIPK1 and RIPK3 kinase functions in myeloid cells, resulting in enhanced cytokine production following TLR3 and TLR4 stimulation (238, 239). Together such observations suggest that Casp8 may function to keep RIPKs-mediated activation in check in certain cell types, such that elimination of this protease may result in prolonged NF-κB activation in these cells.

Cell death pathways have been shown to crosstalk with proliferation pathways. Two cell cycle regulators p21 and p27 are natural substrates of Casp3 and Casp8 (240, 241). Previous studies have shown that Casp3 suppresses B cell proliferation through a p21-dependent mechanism (242). Notably, the abnormalities of T cell in *lpr* mice are reversed upon p21 overexpression (243), further suggesting crosstalk between proliferation and extrinsic death. In addition, a supportive role of Casp3 in proliferation has also been observed in hair follicle sebocytes (244). Anastasis is a process during which cells recover from apoptosis. These anastatic cells are widespread in the intestine, visceral muscle, eyes, antenna, central brain, nerve cords and reproductive system (245). For those cells that are difficult to regenerate, such as neurons or cardiomyocytes, this process helps to preserve them if they are not irreversibly damaged (246). Interestingly, a study using HeLa

cells showing that recovering cells exhibited enhanced proliferation capacity, indicated by the increase in cell numbers and upregulation of transcripts related to cell cycle progression (247).

Studies in the last few years have revealed that extrinsic apoptotic and necroptotic pathways are regulated by shared core machinery, where Casp8 activities dictate the outcomes. A wealth of experiments have been conducted to explore how the pro-survival function of Casp8 supports lymphocyte activation and proliferation. However, these studies have been confounded by the role of Casp8 in suppressing necroptosis, leaving many phenomena previously attributed to Casp8 needing reexamination. Mice with combined deficiency of Casp8 and RIPK3 lack this gross dysregulation and provide opportunities to more accurately determine the contribution of Casp8 in lymphocytes following virus infection. Moreover, a series of publications have highlighted the crosstalk between Casp8-bearing DISC and innate immune signaling pathways, mostly shown in myeloid cells. This crosstalk involving Casp8 can lead to supportive or suppressive effect on innate immune signaling, depending on the receptor and complex engaged. Whether this function in myeloid cells regulates virus-specific lymphocyte responses remains to be explored. Previous studies from our lab have shown that *Casp8*$^{-/-}$*Ripk3*$^{-/-}$ (DKO) mice are immunocompetent and capable of controlling MCMV infection. In this dissertation, I undertook a detailed characterization of the innate and adaptive immune response parameters in these mice. Immune responses were evaluated following MCMV infection to explore the importance of Casp8 in different arms of host defense to this natural mouse pathogen. Further, I investigated the CD8 T cell- and NK cell-autonomous function of Casp8 in regulating proliferation or death in response to viral infection.

## 1.5 Figures and Figure Legends.

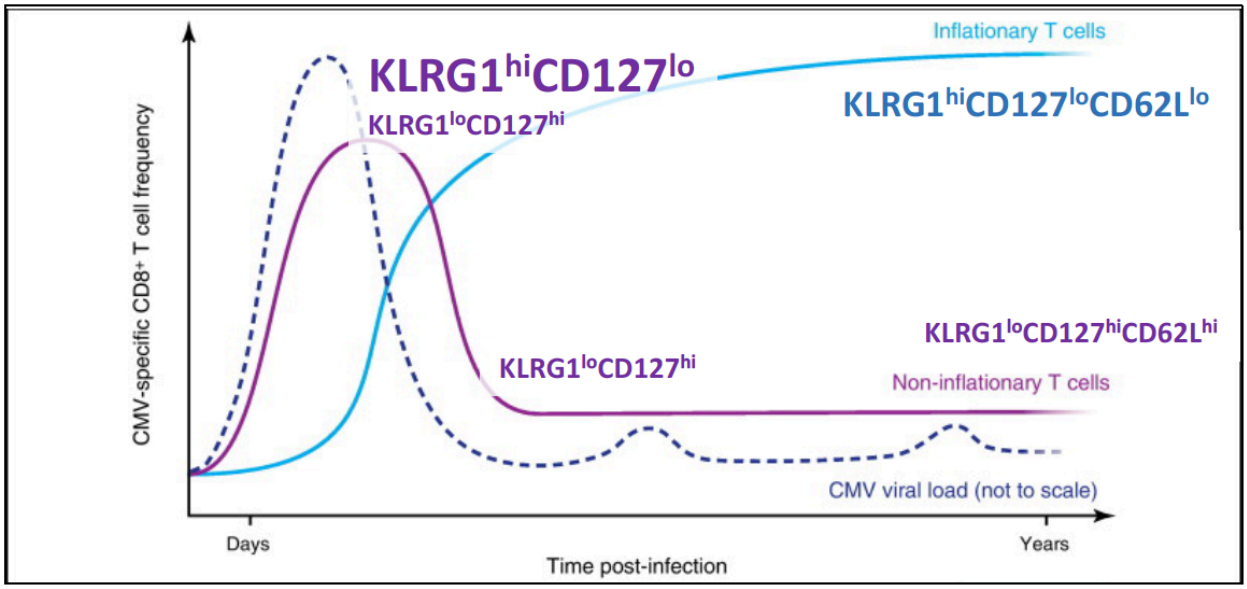


**Figure 1.1[3] Overview of conventional and inflationary CD8 T cell kinetics during the acute and latent phases of MCMV infection.**

Conventional CD8 T cells follow classical kinetics of expansion, contraction and stable memory. Following the peak of the acute phase, the majority of the KLRG1$^{hi}$CD127$^{lo}$ SLECs contract, leaving the KLRG1$^{lo}$CD127$^{hi}$ MPECs that differentiate into memory subsets. Conventional CD8 T cells mostly exhibit CD62L$^{hi}$KLRG1$^{lo}$CD127$^{hi}$ Tcm phenotype during long-term infection. In contrast, inflationary CD8 T cells gradually accumulate in frequency over time even when no active virus replication is detectable in any organ. Inflationary CD8 cells mostly exhibit CD62L$^{lo}$KLRG1$^{hi}$CD127$^{lo}$ Tem phenotype.

[3] This figure is adapted from a published paper "Memory T cell inflation: understanding cause and effect" (O'Hara et. al. 2012).

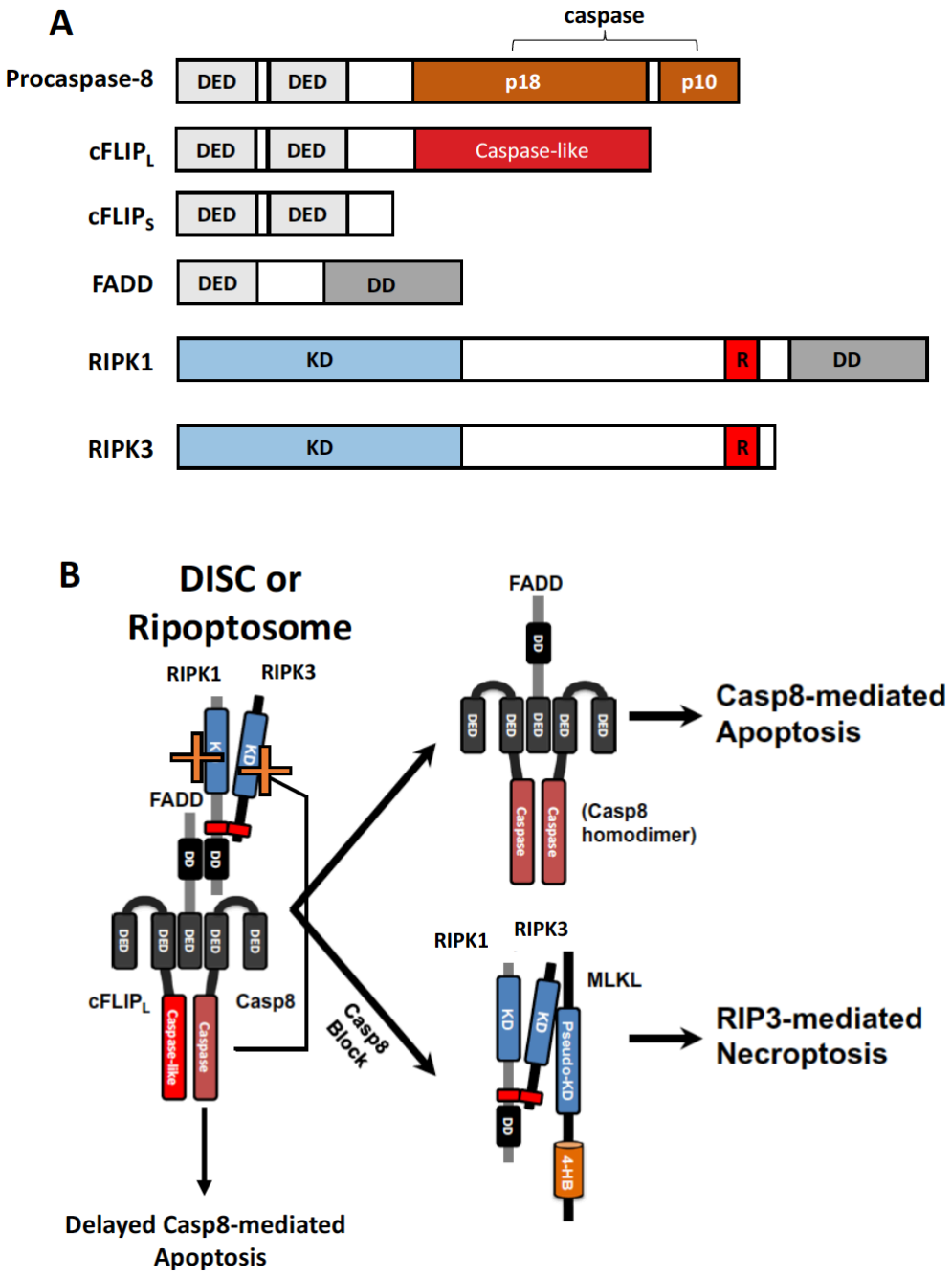


**Figure 1.2 Casp8 determines the outcomes of extrinsic pathway**.

(**A**) Schematic diagram of proteins in DISC. (**B**)[4] Following extrinsic pathway activation, FADD recruits Casp8, cFLIP$_L$, RIPK1, and RIPK3 to form a DISC (or ripoptosome). Procaspase-8

[4] Panel B derives from a published paper "Manipulation of apoptosis and necroptosis signaling by herpesviruses" (Guo et. al. 2015).

dimerization leads to auto-cleavage that releases both large and small subunits for full Casp8 activation, and subsequent apoptosis initiation. Association with $cFLIP_L$ blocks procaspase-8 auto-cleavage, which delays but not impairs apoptosis activation upon DR stimulation. $cFLIP_L$-Casp8 associatiation maintains Casp8 basal catalytic activities sufficient for suppressing RIP kinases-dependent necroptosis. Casp8 catalytic activity inhibition initiates necroptosis. Activation of RIPK1 and RIPK3 by phosphorylation leads to the recruitment and activation of MLKL, which triggers necroptosis.

# Chapter 2.

Remarkably Robust Antiviral Immune Response

Despite Combined Deficiency in Caspase-8 and RIPK3

The data presented in this chapter was published in the Journal of Immunology as:

Yanjun Feng, Devon Livingston-Rosanoff, Linda Roback, Aarthi Sundararajan, Samuel H. Speck, Edward S. Mocarski, Lisa P. Daley-Bauer (2018). "Remarkably Robust Antiviral Immune Response Despite Combined Deficiency in Caspase-8 and RIPK3." *J Immunol.* 2018 Oct 15;201(8):2244-2255. http://www.jimmunol.org/content/201/8/2244.long.

 Data not generated by the Ph.D. candidate is indicated in the figure legends.

## 2.1 Abstract

Caspase-8 (Casp8)-mediated signaling triggers extrinsic apoptosis while suppressing receptor interacting protein kinase (RIPK)3-dependent necroptosis. Even though Casp8 is dispensable for the development of innate and adaptive immune compartments in mice, the importance of this proapoptotic protease in the orchestration of immune response to pathogens remains to be fully explored. Here, *Casp8*$^{-/-}$*Ripk3*$^{-/-}$ C57BL/6 mice show robust innate and adaptive immune responses to the natural mouse pathogen, murine cytomegalovirus. When young, these mice lack *lpr*-like lymphoid hyperplasia and accumulation of either B220$^{+}$CD3$^{+}$ or B220$^{-}$CD3$^{+}$ CD4$^{+}$ and CD8$^{+}$ T cells with increased numbers of immature myeloid cells that are evident in older mice. Dendritic cell activation and cytokine production drive both NK and T cell responses to control viral infection in these mice, suggesting that Casp8 is dispensable to the generation of antiviral host defense. Curiously, NK and T cell expansion is amplified, with greater numbers observed by 7 days post infection compared to either *Casp8*$^{+/-}$*Ripk3*$^{-/-}$ or wild type (*Casp8*$^{+/+}$*Ripk3*$^{+/+}$) littermate controls. Casp8 and RIPK3 are natural targets of virus-encoded cell death suppressors that prevent infected cell apoptosis and necroptosis, respectively. It is clear from the current studies that the initiation of innate immunity and the execution of cytotoxic lymphocyte functions are all preserved despite the absence of Casp8 in responding cells. Thus, Casp8 and RIPK3 signaling is completely dispensable to the generation of immunity against this natural herpesvirus infection even though the pathways driven by these initiators serve as a crucial first line for host defense within virus-infected cells.

## 2.2 Introduction

The self-activating protease Casp8 is an important cell signaling protease that controls alternate apoptotic and necroptotic cell death pathways (248) in host defense (249, 250). Casp8 also influences the activation of cytokines and differentiation of myelomonocytic lineage cells (125, 186). Best characterized following TNF superfamily (TNFR1, TRAIL and Fas) DR activation (125, 251), soluble Casp8 has been shown to form a death-inducing signaling complex (also called complex II or ripoptosome) with FADD, $cFLIP_L$, RIPK1 and RIPK3 (125) in the cytosol. In addition to DR activation, this complex controls signaling following either the activation of TLR3, TLR4 (156, 252, 253) or TCR (166, 167), or the induction of genotoxic stress (254). Several different outcomes may occur following complex formation: (i) cytokine activation via NF-κB, JNK and p38 signaling pathways, (ii) extrinsic apoptosis following autocleavage activation of Casp8, and, (iii) alternate RIPK3-dependent, MLKL-mediated necroptosis when Casp8 is compromised (125). Taken together, Casp8 is now recognized for its importance in integrating divergent cell death and inflammatory signals.

Considerable experimental evidence supports the physiological interplay between alternate Casp8-mediated apoptosis and RIPK3-mediated necroptosis in host defense against HCMV (173, 255) and MCMV (157, 158, 169-172), vaccinia virus (256-258), Sendai virus (163) as well as human influenza A virus (184, 185, 259, 260) and HSV (159, 261). Studies in a natural mouse pathogen MCMV have provided unambiguous evidence revealing the importance of Casp8 (168) and RIPK3 (157, 158, 169) interactions in anti-viral host defenses (170). These anti-viral host defenses are countered by the MCMV M36 and M45 gene-encoded that function to inhibit cell death signaling and sustain infection, dissemination, and persistence. MCMV M36 gene-encoded viral inhibitor of caspase 8 activation (vICA) blocks basal activity as well as auto-cleavage

activation of this protease (171, 172). The M45-encoded viral inhibitor of RIP activation (vIRA) (169) is a RIP homotypic interaction motif (RHIM) competitor that naturally suppresses recruitment of RIPK3 by ZBP1 (157) and blocks subsequent phosphorylation of MLKL (156). ΔM36, M45mutRHIM and combined ΔM36/M45mutRHIM mutant viruses fail to sustain infection in the host due to premature death of infected cells and certain non-death antiviral mechanism driven by Casp8 and RIPK3 (169, 170, 173). Importantly, the attenuation of these mutant viruses in wild type (WT) mice is reversed in $Casp8^{-/-}Ripk3^{-/-}$ mice (170), reinforcing the importance of both pathways in restricting virus infection *in vivo*. HCMV and MCMV encode evolutionarily-conserved Casp8 inhibitors (171, 172); although, these betaherpesviruses block different points in the necroptotic pathway (159, 255). The mechanism of cell death suppression by MCMV has remarkable similarity to HSV, an alphaherpesvirus (261, 262). Overall, Casp8 and RIPK3 potentiate a potent cell-autonomous innate host defense to stop the spread of virus infection and so both pathways are targeted by virus-encoded cell death suppressors.

Despite the importance in host defense, Casp8 function appears dispensable in the activation of immune cells that control MCMV infection (150, 174). Initially, Casp8 was thought to be critical for the activation of NF-kB in immune cells given that lymphocytes from either mice or patients with a disruption in Casp8 display defective translocation of this transcription factor into the nucleus (164, 231). These observations were later clarified in mouse studies revealing the important role of Casp8 as a suppressor of RIPK3-mediated necroptosis following TCR activation as, once on a RIPK3-eliminated background, Casp8-deficient cells become activated and exhibit intact functionality (166). $Cd4^{Cre}Casp8^{flox/flox}$ and $Lck^{Cre}FADD^{dd}$ mice with intact RIPK3-mediated necroptotic function exhibit compromised antiviral responses (166, 222) aligning with the observed immune defect in controlling herpesvirus infection in human patients carrying a

destabilizing Casp8 mutation (*Casp8*$^{C248T}$) (164). In contrast, the overall antiviral immunity is preserved in DKO and *Ripk1*$^{-/-}$*Casp8*$^{-/-}$*Ripk3*$^{-/-}$ mice despite the combined absence of Casp8 and RIPK3 (148, 150, 174). Further, *Cd4*$^{Cre}$*Casp8*$^{flox/flox}$*Ripk3*$^{-/-}$ (166) and *Lck*$^{Cre}$*FADD*$^{dd}$*Ripk3*$^{-/-}$ (222) mice that have T cell-specific genetic disruptions in Casp8 (or FADD) on a RIPK3-eliminated background mount effective antiviral immunity suggesting that pathways driven by these molecules are dispensable to T cell expansion, contraction and cytotoxicity. In fact, like the *lpr* mice that have a disruption in the DR Fas that is upstream of Casp8, patients with ALPS are indeed immunocompetent (215). Neither *lpr* mice nor ALPS patients develop any opportunistic infection or other clinical signs of immunodeficiency (263) arguing strongly that anti-microbial immunity is intact when both Casp8 and RIPK3 signaling pathways are compromised. The combined evidence suggest that, in mice as well as humans, the pathways controlled by Casp8 are dispensable for the generation of antiviral immunity once RIPK3-mediated necroptosis is eliminated in parallel. Thus, DKO animals lack the confounding impact of unleashed necroptosis and therefore permit studies in a setting where Casp8 contribution to immune regulation may be assessed independent of necroptosis.

Even with the strong immune activation, DKO mice exhibit higher MCMV titers at 7 dpi compared to WT mice (150, 174), reminiscent of the increased viral titers seen in animals lacking both Fas and TNFR1 signaling (229). In contrast, *Ripk3*$^{-/-}$ mice exhibit similar viral titers, infection-induced inflammation (157, 169) and antiviral T cell responses (150) compared to WT mice, suggesting that RIPK3 is dispensable for control of WT MCMV. Comparative assessment of *Ripk3*$^{-/-}$ and *Casp8*$^{+/-}$*Ripk3*$^{-/-}$ (HET) mice did not reveal any additional impact on MCMV titers or antiviral immunity when one allele of Casp8 was deleted (unpublished data). Together, these studies suggest that increased WT MCMV titers in DKO mice (150) is attributable to the

elimination of both Casp8 alleles and raise the question of whether DKO mice mount effective immune responses at different stages of MCMV infection.

In this study, we take advantage of viable Casp8-deficient DKO mice along with HET and WT controls to investigate Casp8-mediated regulation of antiviral immunity. We focused on young (6- to 8-week old) mice to circumvent confounding contributions of the lymphoid hyperplasia and accumulating abnormal $B220^{+}CD3^{+}$ T cells that develop as DKO mice age (145, 174), first reported in Fas signaling-deficient *lpr* mice (264). We report that DKO mice develop antiviral immune responses sufficient to control acute MCMV infection. Our investigation reveals the capacity of these mice to generate elevated dendritic cell (DC), NK cell as well as T cell numbers against MCMV even though control of acute MCMV infection appears comparable to WT mice. Thus, despite the contribution of Casp8 and RIPK3-mediated pathways to host defense within virus-infected cells, these signaling components are completely dispensable for the generation of anti-viral immunity.

## 2.3 Results

*Myeloid cell homeostasis in naïve DKO mice*

Prior to evaluating the response to MCMV infection, we set out to determine whether viable Casp8-deficient mice develop myeloid and lymphoid compartments sufficient to support antiviral immunity. DKO mice showed the expected lymphadenopathy that developed with age (145, 174). The immune compartments of 8-week-old naïve DKO mice were characterized, because this was a time when lymphoid organs appeared more normal (149). We compared these younger mice to older (16-week-old) adult mice as well as to age-matched WT and HET controls.

Although young WT and DKO mouse spleens comprised similar frequencies (Fig. 2.1*A*, top panels) and numbers (Fig. 2.1*B*) of $CD45^+CD3^-CD11c^+MHC\text{-}II^{lo}$ pre-cDCs (265, 266), DKO cells expanded dramatically by 16 weeks of age to numbers six-fold greater than WT mice (Fig. 2.1*A*, bottom panels and 2.1*B*). In contrast, the frequencies and numbers of more mature $CD45^+CD3^-CD11c^+MHC\text{-}II^{hi}$ cDCs in DKO mice were sustained at these ages; however, cell numbers were approximately twice that of WT controls regardless of age (Fig. 2.1*C*) due to increased numbers of $CD8\alpha^+$ cDC1 and $CD11b^+$ cDC2 subsets (Fig. 2.1*D* - *F*). $CD45^+B220^+SiglecH^+$ pDCs accumulated faster with age in DKO mice to levels greater than 2.5-fold that of WT controls (Fig. 2.1*G*). Curiously, in HET mice, numbers of both cDCs and pDCs decreased with age to levels lower than observed in 16-week-old WT mice (Fig. 2.1*C* - *G*), suggesting that RIPK3 impacts DC numbers when Casp8 is present. Given the higher levels of DCs in DKO mice compared to HET mice, elimination of Casp8 appeared to reverse the reduced DC numbers in RIPK3-deficient mice. Thus, our data show that DKO mice develop the more mature DC subsets known to contribute to the antiviral immune response in WT mice, even though

the contribution of Casp8 to pre-cDCs and cDCs homeostasis appears similar to that shown in mice with CD11c-specific disruption of Casp8 (178, 267).

Next, we investigated the impact of Casp8 and RIPK3 deficiency on the development of splenic monocyte subsets and $CD45^+CD11b^+F4/80^+CD11c^-$ Macs. By 16 weeks of age, both $CD45^+CD115^+CD11b^+$ $Ly6C^+Gr\text{-}1^-F4/80^+CD11c^-CD62L^-$ IMs (Fig. 2.1*H*) and $CD45^+CD115^+CD11b^+Ly6C^-$ $Gr\text{-}1^-$ $F4/80^+CD11c^+CD62L^+$ PMs (Fig. 2.1*I*) in DKO mice expanded to numbers that were 8-fold greater than WT controls. Importantly, this pattern was comparable to that observed with LysM-specific disruption of Casp8 or Fas (179, 220, 268), implicating the Fas-Casp8 axis in maintaining homeostasis of less mature myeloid cells. Mac numbers in younger DKO mice were greater than WT controls and expanded faster as animals aged (Fig. 2.1*J*). Interestingly, although Mac numbers were also greater in 8-week-old HET mice, the levels dropped over time to match the increase in WT animals by 16 weeks of age, indicating that RIPK3 impacts numbers of more mature myeloid cell. These data suggest that the myeloid compartment of DKO mice is relatively complete and may be expected to support MCMV infection and antiviral response even though Casp8 appears to contribute to the homeostatic equilibrium of less mature myeloid cells and Macs.

*T cells in naïve DKO mice accumulate and acquire activation markers with age*

Next, we sought to characterize T cells in naïve DKO mice. Consistent with previous observations (149), aberrant $CD45^+CD3^+B220^+$ T cells are detectable by six weeks of age and continue to elevation in numbers over time (Fig. 2.2*A*). As expected (174), conventional $CD45^+B220^-CD3^+$ $CD4^+$ and $CD8^+$ T cells accumulated to significantly greater numbers by 16 weeks of age in DKO mice compared to controls. T cells in *lpr* mice express high levels of CD44 ascribed to defective turnover in response to self-antigens or cytokines (264). Increasing

proportions of T cells from DKO mice expressed CD44 over time such that frequencies of $CD44^{hi}$ CD4 and $CD44^{hi}$ CD8 T cells reached 60% and 70%, respectively, by 12 weeks of age compared to the 30% levels in WT and HET controls (Fig. 2.2*B*). Notably, the increase in frequencies in DKO mice was less dramatic at 6 weeks of age compared to controls. Altogether, these data confirm that Casp8 is dispensable for T cell development (174) but may contribute to the suppression of T cell accumulation and homeostatic activation state in aging mice (269).

Given the observed increase in activation state during homeostasis, we sought to investigate the capacity of T cells from DKO mice to respond to TCR engagement. Purified splenic conventional T cells from 6 and 12-week-old mice were labeled with CFSE, stimulated with CD3 and CD28 Abs then analyzed at 72 h by flow cytometry for extent of proliferation. In contrast to observations made using young T cell-specific $Cd4^{Cre}Casp8^{flox/flox}Ripk3^{-/-}$ mice (166), proliferating CD8 T cells accumulated to greater levels in DKO mice compared to WT controls regardless of age (Fig. 2.2*C*), consistent with the high proportion of $CD44^{hi}$ cells in DKO mice (Fig. 2.2*B*).

To better understand how Casp8 and RIPK3 regulate cell death in CD8 T cells following TCR stimulation, we quantified 7-$AAD^{+}$ events in cultures of CFSE-labelled cells purified from spleens of 6-week-old mice. Cells from WT mice had the highest proportion (Fig. 2.2*D*) and numbers (Fig. 2.2*E*) of dead, undivided (7-$AAD^{+}CFSE^{hi}$) CD8 T cells at 72 h post-stimulation whereas 20% of the population had remained alive and had divided (7-$AAD^{-}CFSE^{lo}$). In contrast, the levels of dead, undivided cells in cultures from both HET and DKO mice were significantly reduced (Fig. 2.2*D* and *E*), suggesting a RIPK3-dependent but Casp8-independent contribution to cell death following TCR stimulation. of CD8 T cells. Upon entering the cell cycle, $CFSE^{lo}$ DKO cells underwent extensive proliferation and, compared to controls, a smaller proportion of dead (7-

$AAD^+CFSE^{lo}$) cells was observed (Fig. 2.2*D*). Notably, similar numbers of these dead, divided 7-$AAD^+CFSE^{lo}$ cells were recovered from all cultures (Fig. 2.2*E*). Thus, notwithstanding the heightened activation state, DKO CD8 T cells respond to TCR stimulation *in vitro* and undergo more extensive proliferation with dampened putative Casp8-dependent activation-induced-cell-death (264).

*Virus-induced DC activation is robust in DKO mice*

Previously, DKO mice, similar to $Cd4^{Cre}Casp8^{flox/flox}Ripk3^{-/-}$ and $Ripk1^{-/-}Casp8^{-/-}Ripk3^{-/-}$ mice, were found to be immunocompetent and capable of controlling viral infections (150, 166, 174); however, detailed characterization of innate and adaptive immune response parameters have not been reported. We characterized the antiviral response to MCMV in young (6 to 8-week-old) DKO mice because they retained intact leukocyte populations without exhibiting the gross myeloid and lymphoid abnormalities that became apparent with age. Given their important role in activating NK cells and in being the predominant APCs responsible for priming adaptive immunity (15), we characterized the DC response in spleens of WT, HET and DKO mice at 1.5 dpi. Even though the cDC frequency was lower in infected DKO mice (Fig. 2.3*A*), the total numbers of cDC1 and cDC2 subsets were greater in these mice than in littermate controls (Fig. 2.3*B*). WT and HET mice exhibited comparable numbers of both subsets, revealing that RIPK3 is dispensable for the cDC response to infection despite an apparent contribution to homeostasis (Fig. 2.1*C-F*). Importantly, cDC maturation following infection was evident in all three genotypes where CD80 and CD86 were upregulated (Fig. 2.3*C-D*), indicating cDC activation in response to virus despite Casp8 and/or RIPK3 deficiency.

IL-12 produced by DCs early after MCMV infection is critical for promoting cytotoxic NK and CD8 T effector cell activation (5, 15). Given that DCs are the major source of IL-12 (7), we

assessed concentrations in spleen and serum at 1.5 dpi to understand whether Casp8 and RIPK3 influenced the production of this cytokine. Infection increased IL-12 levels in spleens regardless of genotype; although, levels in DKO mice were notably lower than controls even following infection (Fig. 2.3*E*). Thus, Casp8 contributes to the optimal production of this cytokine in splenocytes. As expected (5), systemic IL-12 production was undetectable in mock-treated WT mice but increased at 1.5 dpi (Fig. 2.3*F*) in a pattern that was independent of Casp8 and RIPK3. Even though splenic levels were lower in DKO mice, serum IL-12 levels were similar to controls. Thus, despite the absence of Casp8 and RIPK3, higher numbers of cDC appeared to be accompanied by sufficient systemic IL-12 production in response to MCMV infection.

*Antiviral NK cell response is robust in DKO mice*

Activated DCs collaborate with Ly49H activation by viral m157 to promote NK cell proliferation and maturation (94, 270), contributing to early control of MCMV infection in C57BL/6 mice. Here, $CD45^{+}B220^{-}CD3^{-}NK1.1^{+}Ly49H^{+}$ NK cells responded more robustly between 1.5 and 7 dpi in the absence of Casp8 and RIPK3 than in controls (Fig. 2.4*A* and *B*). The percentages of $Ly49H^{+}$ NK cells at 1.5 dpi appeared substantially lower in DKO mice than in infected WT or HET mice or mock-treated controls (Fig. 2.4*A*). Nevertheless, all three genotypes of mice showed increased percentages over mock by 7 dpi, indicating $Ly49H^{+}$ NK cells respond to MCMV independent of Casp8. Consistent with the proportional assessment, the numbers of $Ly49H^{+}$ NK cells expanded between 1.5 and 7 dpi in all three genotypes, with a more dramatic expansion in DKO mice (Fig. 2.4*B* and *C*). Despite differences in expansion, $Ly49H^{+}$ NK cells exhibited comparable elevation of IFNγ and CD69 at 1.5 dpi in all mice (Fig. 2.4*D*), indicating that Casp8 deficiency did not impair NK cell activation. Virulence of MCMV depends on the source as well as preparation of virus stock (271, 272). Importantly, NK cells in DKO mice

exhibited both enhanced cell expansion (Fig. 2.4*C*) and robust activation (Fig. 2.4*D*) in response to either tissue culture-propagated strain K181-BAC or the more virulent SG-propagated strain V70. Thus, the patterns of NK cell response in DKO mice occurred independent of virus strain and preparation.

Next, to assess the antiviral function of NK cells, we compared K181-BAC to Δm157 mutant derivative that was unable to activate Ly49H$^+$ NK cells (97). At 5 dpi, when NK cell-mediated antiviral immunity is dominant, WT and DKO mice exhibited similar 10-fold lower virus titers with K181-BAC compared to Δm157 (Fig 2.4*E*). Thus, competent NK cell function developed despite Casp8 and RIPK3 deficiency. The difference in titer was less pronounced at 7 dpi, a time point when CD8 T cells contribute to control of this virus (97). Thus, DKO mice mount a robust NK cell response that controls MCMV early during infection; however, the pattern suggests that Casp8 may normally dampen NK cell expansion without impacting overall antiviral function.

*Antiviral T cell response is robust in DKO mice*

We sought to characterize the T cell response against MCMV given its importance in the ultimate control of virus replication and maintenance of latency (40). We compared the splenic CD8 T cell response in infected WT, HET and DKO mice by evaluating the virus-specific response to M45, the dominant epitope during acute infection, as well as the response to inflationary epitope IE3 (17), employing stimulation with specific peptides. CD8 T cells responded robustly to infection independent of Casp8 and/or RIPK3 deficiency (Fig. 2.5*A* and *B*). The three genotypes of mice exhibited similar frequencies of M45-specific CD8 T cells at either 5 or 14 dpi (Fig. 2.5*A*); however, at 7 dpi when the acute response peaked, significantly greater frequencies of Ag-specific T cell populations were present in DKO mice. Thus, Casp8 appears to restrict initial T cell

expansion without any apparent impact on contraction. Instead of an acute response, IE3-specific CD8 T cells are not detectable until at least three weeks post infection. Whereas WT and HET mice exhibited the expected low percentages of this subset by 14 dpi, DKO mice developed faster expansion of IE3-specific CD8 cells between 7 and 14 dpi (Fig. 2.5*B*). Similar patterns of CD8 T cell expansion were observed in DKO mice infected with MCMV K181-BAC (Fig. 2.5*C* and *D*). In summary, DKO mice mount a robust CD8 T cell response to MCMV infection, although the unexpected pattern suggests a role for Casp8 in restricting CD8 T cell expansion without affecting contraction.

To evaluate CD8 T cell cytotoxic function, we injected $2 \times 10^7$ WT M45 peptide-pulsed and CFSE-labeled splenocytes into mice at 7 dpi. A comparable level of killing was observed over an 18 h time frame in all genotypes (Fig. 2.5*E*). Specific killing of Ag-pulsed cells was nearly complete in all mice regardless of whether infected with V70 or K181-BAC (Fig. 2.5*F*), indicating CD8 T cell cytotoxicity was preserved in DKO mice. The antiviral function of CD8 T cells in DKO mice was evaluated with Δm157 virus to circumvent the contribution of NK cells. DKO mice controlled MCMV infection by 14 dpi independent of NK cell activation by m157 (Fig. 2.4*E*). WT and DKO mice exhibited similar patterns of Δm157 virus clearance, demonstrating intact T cell function in DKO mice. In addition, the sharper drop in titer between 5 and 7 dpi in all Δm157 virus-infected mice is consistent with enhanced T cell effector function in the absence of activated NK cells (97, 273). Taken together, mice mount cytotoxic CD8 T cell responses with full antiviral capacity independent of Casp8.

Whereas acute MCMV infection is controlled via overlapping NK and CD8 T cell responses, CD4 T cells contribute to viral clearance from SGs, as well as the Ab response and establishment of latency (274). We evaluated the splenic CD4 T cell response at 14 dpi following

expression of CD11a and CD49d (67). Total CD4 T cells showed modest elevation in WT and HET mice (Fig. 2.5*G*); whereas, this population of cells started out higher in mock-treated DKO mice and increased significantly in response to infection. Ag-experienced $CD49d^{+}CD11a^{+}$ CD4 T cell frequencies increased significantly in WT and HET mice by 14 dpi; whereas, in DKO mice, this population again started three-fold higher and increased during infection, although with high animal-to-animal variability (Fig. 2.5*H*). When evaluated further, these Ag-experienced CD4 T cells showed proportionally increased intracellular cytokine staining for $IFN\gamma^{+}$ as well as for $IFN\gamma^{+}TNF^{+}$ and $IFN\gamma^{+}TNF^{+}IL\text{-}2^{+}$ (Fig. 2.5*I*). Consistent with this assessment, DKO mice developed significantly greater numbers of CD4 T cells producing single (Fig. 2.5*J* - *L*) and multiple cytokines (Fig. 2.5*M*), indicating the presence of high numbers of terminally differentiated CD4 T cells. The elevated cytokine production may be a phenotype already present in naïve cells, given that CD4 T cells in mock-treated DKO mice displayed increased activation markers and cytokine production. Thus, Casp8 appears to dampen the expansion of Ag-experienced CD4 T cells but is dispensable for mounting a response to virus infection.

*Ab response patterns in DKO mice*

Although dispensable for limiting initial MCMV replication, Abs play a crucial role in preventing reinfection (275). We assessed the serum Ab response, comparing naïve to virus-infected mice at 14 dpi. Consistent with previous observations (149), naïve 8-week-old DKO mice had had detectable levels of anti-dsDNA Abs (Fig. 2.6*A*) compared to HET and WT mice; however, these levels did not significantly increase after infection in either DKO or control mice, regardless of Ab isotype examined. We also observed higher levels of total Ig (IgM, IgG1, IgG2b and IgG2c) in DKO mice compared to WT or HET controls (Fig. 2.6*B*), correlating with enhanced anti-dsDNA Ab levels. Despite these differences in homeostasis, all genotypes exhibited an increase in total

IgG2c during infection. DKO and WT mice developed comparable MCMV-specific IgG2c titers (Fig. 2.6*C*); whereas HET mice had unexpectedly higher levels than WT controls. These data demonstrate that mice mount Ab in response to MCMV infection independent of Casp8 function.

## 2.4 Discussion

Our study demonstrates that Casp8-deficient mice mount a robust and functional innate and adaptive immune response to natural virus infection so long as pro-necroptotic RIPK3 signaling has been eliminated. This is remarkable because both Casp8 and RIPK3 execute potent antiviral activities in the WT mouse that eliminate virus-infected cells if not blocked by virus-encoded cell death suppressors (249, 250). DKO mice survive MCMV infection and higher splenic titers are detected at 7 dpi (150) but are nevertheless controlled by 14 dpi (170), demonstrating that viral control is complete despite the absence of Casp8 and RIPK3 host defense pathways. Innate and adaptive immune control of this viral pathogen proceeds in even when both pathways are eliminated from the natural mammalian host. The cell-autonomous role of Casp8 and RIPK3 in extrinsic cell death and innate immune host defense (125), together with the contribution of these pathways to inflammatory consequences of infection (170) remain clear evidences supporting our long-standing hypothesis that Casp8 and RIPK3 evolved to eliminate pathogens rather to regulate the immune response (249, 250). It is not yet clear whether this hypothesis applies to infections with other viruses or bacteria, but such studies are clearly warranted (125, 186). Innate DC activation along with the crucial antiviral cytotoxic function of NK and T cells proceeds independent of Casp8 and RIPK3 signaling pathways, with a pattern of faster and enhanced NK and T cell expansion. Given the strong immune response in these animals, the slower viral clearance showed in the previous literature (150) may in fact be the result of a deficiency in components necessary to control virus infection in target cells when Casp8 is lacking.

Hyper-accumulation of virus-specific T cells in DKO mice was not observed in T cell-specific $Cd4^{Cre}Casp8^{flox/flox}Ripk3^{-/-}$ mice (166), suggesting that the influence of Casp8 is not T cell-autonomous. A previous study indicates that DCs from $Cd11c^{Cre}Casp8^{flox/flox}Ripk3^{-/-}$ mice

exhibit improved ability to induce T cell proliferation *in vitro* (178). Separate studies demonstrate the resistance of Fas-deficient DCs to CTL killing *in vivo*, resulting in prolonged DC survival and enhanced antiviral T cell numbers (276, 277). These data suggest that disruption of the Fas-Casp8 signaling axis may extend DC lifespan and promote T cell expansion. Furthermore, increased proportion of T cells in unchallenged DKO mice upregulate CD44, CD11a and CD49d, and produce cytokines, indicating that cells acquire an activation phenotype and are more prone to proliferation when stimulated by Ag (278). It was shown that Casp8 deficiency in DCs or Macs results in T cell hyperactivation in naive mice (178, 179), a dysregulation that is reversed by eliminating Myd88 instead of RIPK3 in these myeloid cells. The data indicate a TLR-dependent dysregulation in APCs contributing to T cell hyperactivation when Casp8 is absent. Similarly, hyperaccumulation of DKO NK cells in response to viral infection may be due to their enhanced activation during homeostasis, though a marker to confirm this is yet to be identified. Taken together, Casp8 is predicted to control APC survival and innate immune signaling, thereby contributing to homeostatic T cell activation as well as cell expansion in response to viral infection.

DCs and Macs are among the most important host cell targets of MCMV infection, contributing to Ag presentation, virus dissemination and establishment of latency (15). It has become very clear that the success of infection in these virus-susceptible myeloid cell populations is dependent on virus-encoded Casp8 and RIPK3 inhibitors, vICA (171, 172, 279) and vIRA (157, 158), responsible for suppression of cell death pathways to prolong infection enough to support pathogenesis. In other words, MCMV-mediated suppression of cell death pathways in WT Macs and DCs reflects the virus-host relationship in DKO DCs where apoptosis and necroptosis are absent. Nevertheless, infected DCs constitute only a small portion of total splenic DCs *in vivo* and are functionally paralyzed by additional viral suppressors of Ag presentation as well as cytokine

secretion (15). Indeed, activation of MCMV-specific CD8 T cells has been attributed to the role of uninfected DCs (>95% of total DCs *in vivo*) and Ag cross-presentation. Despite the Casp8 and RIPK3 deficiencies, both DC1s and DC2s undergo robust activation by 1.5 day after MCMV infection as indicated by the upregulation of co-stimulatory molecules that are critical for T cell activation (6, 15). Taken together, our data suggest that DCs retain their function in response to MCMV infection despite the absence of death-dependent and -independent functions of Casp8 and/or RIPK3.

Proinflammatory cytokines are produced through signal transduction downstream of innate pathogen sensors, playing a crucial role in DC maturation as well as cytotoxic effector cell activation. Cytokine production defects result in a compromised immune response that fails to protect hosts from pathogen invasion (3). The death-independent role of Casp8 contributes to innate immune signaling transduction directly downstream of TLR3, TLR4 and ZBP1, or indirectly through the engagement of DRs (125). Recently, this protease has been shown to regulate the priming process of inflammasome as well as to directly interact with the components in the complex (125, 280). Casp8-deficient mice exhibit low systematic cytokine levels in response to *Citrobacter rodentium*, Yersinia or influenza A infection (180, 181, 183, 184, 260), correlated with a defect in producing proinflammatory cytokines. Furthermore, a study of Yersinia reveals the consequence of low cytokine levels driving poor lymphocyte responses (183), especially Th1 cells that are necessary for ultimate control of the invading bacteria (281). The manifestation of immune hypoactivation to bacterial infection in Casp8-deficient mice is likely an indication of the unique role that CD4 T cells play in such settings. Surprisingly, Casp8-deficient mice exhibited normal systemic IL-12 production sufficient to promote NK and CD8 T cell responses necessary for controlling acute MCMV infection. Thus, the contributions of Casp8 to anti-microbial immune

control may not be as clear cut as initially perceived as it is now evident that Casp8-dependent and independent functions in the host are likely dictated by the nature of the infecting pathogen.

The discrepancy between current natural herpesvirus pathogen and previous cross-species bacterial and influenza studies in mice may be attributed to species-specific regulation of Casp8 depending on the pathogen sensor(s) engaged. This hypothesis is supported by the defective cytokine secretion of DKO bone marrow-derived Macs in response to TLR3 and TLR4 stimulation but not to TLR2 stimulation or Sendai virus infection, which is TLR7-dependent (163, 183). Furthermore, multiple cell surface and cytosolic receptors sensing MCMV infection (282) coordinate a balanced outcome of cell survival, cell death and innate cytokine production to control infection. It is possible these sensors compensate for each other to overcome any signaling transduction defect that is a consequence of Casp8 deficiency, ensuring the induction of antiviral immunity that brings infection under control. Taken together, instead of a ubiquitous influence on innate immune signaling, Casp8 appears dispensable downstream of the innate sensors triggered by MCMV infection.

Our study shows that RIPK3-deficient mice mount robust antiviral immunity despite dysregulated homeostasis. A previous study reports that both *Ripk3*$^{-/-}$ and *Ripk3*$^{K51A/K51A}$ (148) mice retain intact antiviral immunity, questioning whether adaptor function or kinase activity of RIPK3 is generally important for the anti-MCMV immune response. By using WT and RIPK3-deficient HET mice as controls to compare with DKO mice, we have confirmed the requirement of Casp8 for suppressing the hyperaccumulation phenotype. However, the adaptor function of RIPK3 may certainly influence antiviral immunity in Casp8-deficient mice. Future studies comparing *Casp8*$^{-/-}$*Ripk3*$^{K51A/K51A}$ or *Casp8*$^{-/-}$*MLKL*$^{-/-}$ mice to *Casp8*$^{-/-}$*Ripk3*$^{-/-}$ mice will help

dissect the necroptosis-independent contribution of RIPK3 to Casp8-deficient animal during infection.

Although Casp8 function is critical for cell-autonomous host defense and innate signaling transduction, mice lacking Casp8 and/or RIPK3 trigger robust innate and adaptive immune response to MCMV infection. Importantly, the cytotoxic NK and CD8 T cells in DKO mice retain the full capacity to recognize and control virus, reinforcing long-standing principles in the immune control of herpesvirus infection. MCMV-infected mice develop enhanced NK and T cell expansion, possibly due to the Casp8-deficient APCs that elevate the activation state of these lymphocytes prior to the spread of infection.

## 2.5 Materials and Methods

*Mice, viruses and experimental infection*

DKO mice were derived as described previously (174) and backcrossed to >97% on the C57BL/6 background as indicated by single nucleotide polymorphism scanning (Jackson Laboratories). DKO, HET and *Casp8*$^{+/+}$*Ripk3*$^{+/+}$ (WT) littermates were generated from mating *Casp8*$^{+/-}$*Ripk3*$^{+/-}$ mice. C57BL/6 WT mice (Jackson Laboratories) used as controls for K181-BAC infection were bred and maintained in house. Mice were maintained at the Emory University Division of Animal Resources and experimental procedures were conducted in accordance with the National Institutes of Health and Emory University Institutional Animal Care and Use Committee guidelines. MCMV strain V70 (kindly provided by C. Biron, Brown University) (5) and was propagated in SGs as described (272). Briefly, BALB/c mice were inoculated intraperitoneally (i.p.) with $1 \times 10^3$ PFU V70 and SG were collected at 14 days post infection (dpi). Clarified supernatant (2700 × g at 4°C, 10 min) was collected from sonicated SG (10% weight/volume in Dulbecco's Modified Eagle Medium; DMEM with 10% FBS/1% penicillin/streptomycin). Strain K181-BAC (283) and K181-BAC-derived Δm157 (kindly provided by W. Brune; Heinrich Pette Institute, Hamburg) (284) were propagated in NIH 3T3 murine fibroblasts (American Type Culture Collection CRL-1658) (169) and purified from clarified tissue culture medium. Aliquots of virus were stored at -80°C until use. Experimental mice were inoculated i.p. with either medium (mock control), $1 \times 10^5$ PFU V70, or $1 \times 10^6$ PFU tissue culture-propagated viruses.

*Plaque assay*

Tissues were homogenized in DMEM and overlaid onto 3T3 Swiss Albino murine fibroblasts (ATCC CCL-92). Virus titers were calculated at 4 days when cells were fixed with methanol and stained with Giemsa for plaque visualization (285).

*Antibodies*

For flow cytometry, Abs to CD16/CD32 (FcγRII/III; Clone 2.4G2), Ly6C (Clone AL-21), CD80 (Clone 16-10A1), IL-2 (Clone JES6-5H4), CD4 (Clone RM4-5), TNF (Clone MP6-XT22), CD62L (Clone MEL-14), NK1.1 (Clone PK136), B220 (Clone RA3-6B2), CD11b (Clone M1/70) and CD3ε (Clone 17A2) were purchased from BD PharMingen; IFNγ (Clone XMG1.2), CD49d (Clone R1-2), CD3ε (Clone 145-2C11), CD115, CD44 (Clone 1M7), CD86 (Clone GL-1) and I-A/I-E (Clone M5/114.15.2) were purchased from BioLegend; and CD11c (Clone N418), CD69 (Clone H1.2F3), CD3ε (Clone 145-2C11), Siglec H (Clone eBio440c), CD3ε (Clone 17A2), CD11b (Clone M1/70), Ly49H (Clone 3D10), Ly6C/6G (Gr-1; Clone RB6-8C5), CD11a (Clone M17/4) and CD28 (Clone 37.51) were purchased from eBioscience. The following Abs were purchased from Invitrogen: CD8α (Clone 5H10), F4/80 (Clone BM8) and CD45 (Clone 30-F11). For ELISA, purified mouse IgM, IgG1, IgG2b and IgG2c, and polyclonal nonconjugated and alkaline phosphatase (AP)-conjugated goat anti-mouse Ig isotypes were purchased from Southern Biotech.

*ELISA*

Total serum IgM and IgG isotypes were measured by ELISA (286). Well volumes were 50 µl, incubations were overnight at 4°C unless otherwise specified and plates were washed after each incubation. Polystyrene 96-well microtiter plates (Nunc ImmunoMaxisorp plates; Fisher Scientific) were coated with 10µg/ml goat anti-mouse Ig isotypes (Southern Biotech), blocked, then incubated 4 h at room temperature (RT) with three-fold serial dilutions of sera. Wells were then incubated with alkaline phosphatase -conjugated goat anti-mouse Ig isotypes. Binding was detected with p-nitrophenyl phosphate (Sigma) in diethanolamine buffer. Optical density readings were taken at 405 nm using a microplate reader (Biotek Synergy HT) and the associated Gen5

software. Concentrations were calculated from standard curves constructed with purified mouse Ig isotypes (Southern Biotech).

MCMV-specific IgGs were detected using a modified version of the protocol described above. Microtiter plates were incubated with 0.5 μg/ml virion protein purified on a sucrose gradient and endpoint titers for bound IgG2c and IgG1 were determined as the reciprocal of the highest serum dilution from infected mice with greater than twice the optical density of the corresponding dilution from naïve mice.

Serum dsDNA-specific Abs were assayed using a modified protocol described previously (150). Briefly, Immulon 1B plates (Fisher Scientific) were exposed to UV light overnight. Well volumes were 50 μl. Wells were incubated 1h at RT with 2 μg/ml calf-thymus DNA (Sigma), washed, blocked then incubated 4 h with three-fold serial dilutions of sera. Bound IgG was detected overnight at 4 °C using alkaline phosphatase-conjugated goat anti-mouse isotype-specific Ab and the assay was developed as above.

IL12(p70) production in mice was evaluated at 40 hpi with MCMV. For spleens, tissues were disrupted by sonification in 1 ml DMEM and clarified supernatants were assayed. Sera were prepared from blood collected by cardiac puncture. ELISA was conducted by using the Mouse IL-12 (p70) ELISA Set (BD OptEIA; BD Biosciences) following manufacturer's instructions. Briefly, 96-well microtiter polystyrene plates (Costar) were coated overnight at 4 °C with capture Ab. Incubations were conducted at RT and followed by a washing step unless otherwise stated. Plates were blocked, incubated with samples and IL-12(p70) standard followed by the detection Ab-HRP-SAv mixture then developed using the 3,3′,5,5′-tetramethylbenzidine substrate reagent set.

1M $H_3PO_4$ was added directly wells to stop the enzymatic reaction and optical density readings were taken at 450 nm with λ correction 570 nm.

*Flow cytometry*

Spleens were harvested from euthanized mice, disrupted by mashing through a metal sieve, incubated with erythrocyte lysis buffer then passed through a filter (100 mm mesh). Viable cell counts were performed on a hemocytometer using trypan blue dye exclusion. Cell surface FcγRII/III were blocked prior to incubating with surface Ag-specific Abs for multiparametric flow cytometric analyses. $CD45^+$ leukocytes were gated to identify $CD3^-CD11c^+MHC\text{-}II^{lo}$ pre-cDCs and more mature $CD3^-CD11c^+MHC\text{-}II^{hi}$ cDCs that were further separated into $CD8\alpha^+$ cDC1 and $CD11b^+$ cDC2 subsets. Leukocytes were also identified as $B220^+Siglec\text{-}H^+$ pDCs, $CD115^+CD11b^+Ly6C^+Gr1^-F4/80^+CD11c^-CD62L^-$ IMs, $CD115^+CD11b^+Ly6C^-Gr1^-F4/80^+CD11c^+CD62L^+$ PMs and $CD11b^+F4/80^+CD11c^-$ Macs. $CD45^+$ leukocytes were also gated to identify $B220^-CD3^-NK1.1^+$ NK cells and the $Ly49H^+$ subset, $B220^+CD3^+$ aberrant T cells, and conventional $B220^-CD3^+CD8^-CD4^+$ (CD4) and $B220^-CD3^+CD4^-CD8^+$ (CD8) T cell subsets. For intracellular cytokine staining (ICCS), cells were either evaluated directly *ex vivo*, as in the case of NK cells, or stimulated 5 h with anti-CD3/CD28 or with M45, M38 or IE3 peptides (17) in the presence of brefeldin A, as was done for T cell analyses, using the Cytofix/Cytoperm kit (BD Biosciences). Data were acquired by flow cytometry (BD LSRII cytometer and FACSDiva Software; BD Biosciences), analyzed with FlowJo (TreeStar), and graphed with Prism 7 (GraphPad).

*T cell proliferation*

$B220^-CD3^+$ T cells were isolated by EasySep Mouse T Cell Isolation Kit (Stem Cell), labeled with 0.5 μM CFSE in 0.1% BSA/PBS for 10 min at 37 °C then stimulated with plate-bound anti-CD3

and anti-CD28 for 3 days in a 37 °C incubator. Isolated T cells ($2 \times 10^5$) were resuspended in 200 µl RPMI 1640 with 10% FBS/1% penicillin/streptomycin (complete RPMI) as well as 50µM 2-mercaptoethanol in 96-well plate. Cells were stained with 7-AAD for dead cell exclusion as well as Abs specific for surface markers. All samples were resuspended in an equal volume of FACS staining buffer and collected for the same amount of time on the flow cytometer (222).

*In vivo CTL killing assay*

CTL killing in spleens of MCMV-infected WT, HET and DKO mice was assessed at 7 dpi. To generate target cells, splenocytes from naïve C57BL/6 WT mice were pulsed with M45 peptide by one hour incubation at 37 °C in RPMI complete medium with 2-mercaptoethanol. The M45-pulsed/unpulsed cells were labeled with 0.5µM/5µM CFSE, respectively, at 2 x $10^7$ cells/ml concentration in PBS supplemented with 0.1% BSA. The $CFSE^{hi}$ and $CFSE^{lo}$ cells were mixed at a 1:1 ratio to obtain $2 \times 10^7$ cells in 250 µl medium, and injected into tail vein. Spleens were harvested at 4 or 18 hour post transfer from recipient mice and frequencies of $CFSE^+$ splenocytes were analyzed by flow cytometry (287). The specific killing was defined as 100 x [1 – Ratio (naïve) / Ratio (infected)], with Ratio representing $CFSE^{hi}$ / $CFSE^{lo}$.

*Statistical analysis*

Statistical analysis was performed by unpaired one-way or two-way ANOVA with Tukey analysis, using GraphPad Prism 7. $P \leq 0.05$ was considered significant.

## 2.6 Figures and Figure Legends

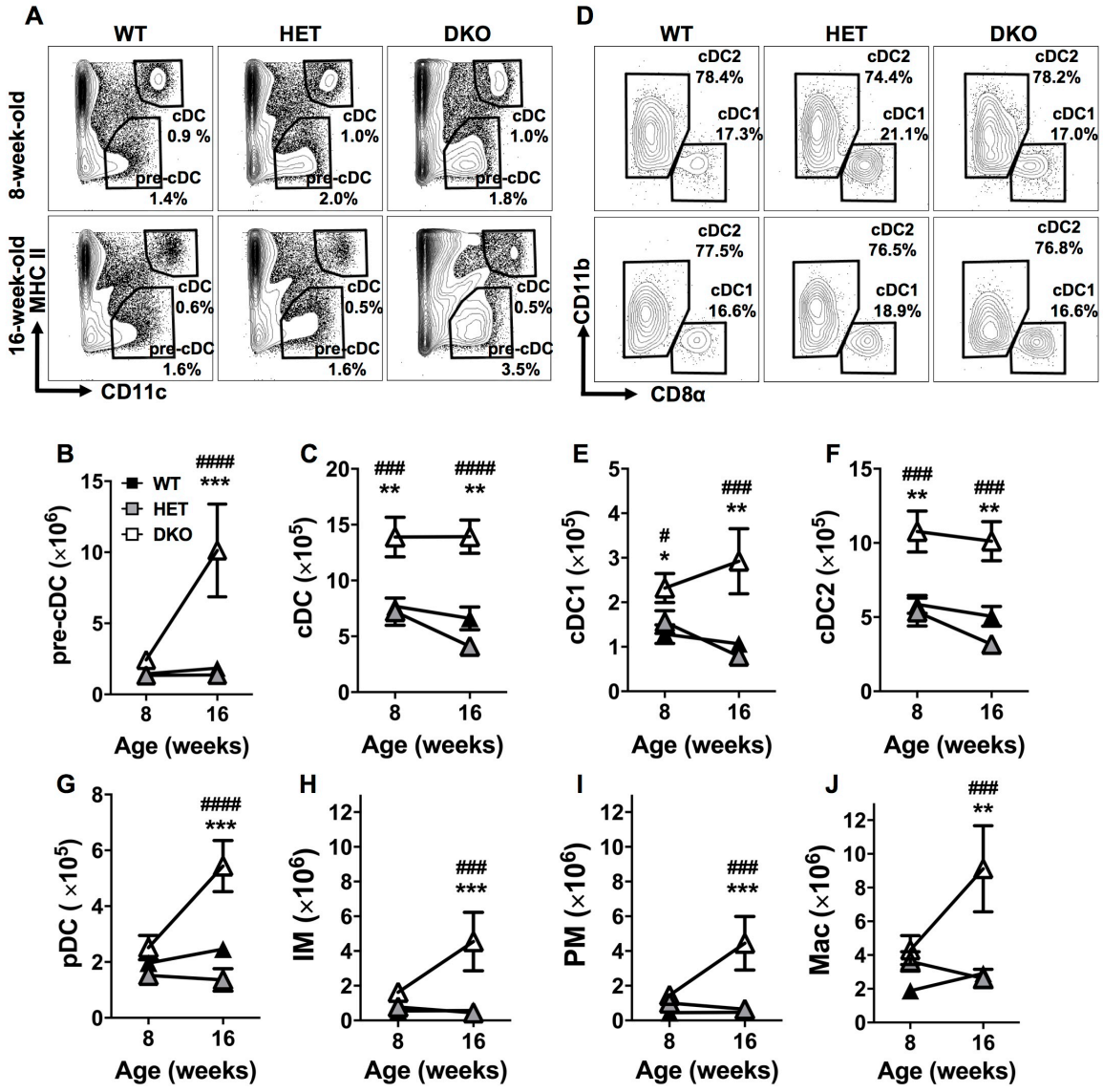


**Figure 0.1 Age-dependent impact of Casp8 and RIPK3 deficiency on myeloid cell homeostasis.**

(**A** - **F**) Analysis of developmentally (**A** - **C**) and functionally (**D** - **F**) distinct DCs in spleens of WT, HET and DKO mice at the indicated weeks of age. Splenic $CD45^{+}B220^{-}CD3^{-}$leukocytes from 8 (top panels) and 16 (bottom panels) weeks-of-age were displayed to identify $CD11c^{+}MHCII^{lo}$ pre-cDCs and $CD11c^{+}MHC\text{-}II^{hi}$ cDCs. Representative flow cytometry plots

comparing frequencies of pre-cDCs and cDCs (**A**), and graphs showing the total numbers of the subsets represented as the mean ± S.E.M. (**B** and **C**). cDCs were then separated to identify $CD8\alpha^+$ cDC1 and $CD11b^+$ cDC2 subsets. Representative plots comparing frequencies of cDC1s and cDC2s (**D**), and graphs showing the total mean numbers ± S.E.M. of the subsets (**E** and **F**). (**G** – **J**) Graphs showing total numbers of myeloid cell subsets represented as the mean ± S.E.M. $CD45^+$ leukocytes were gated to identify $B220^+$Siglec-$H^+$ pDCs (**G**), $CD115^+CD11b^+$ $Ly6C^+$Gr-$1^-F4/80^+CD11c^-CD62L^-$ IMs (**H**), $CD115^+CD11b^+Ly6C^-$ Gr-$1^-$ $F4/80^+CD11c^+CD62L^+$ PMs (**I**) and $CD11b^+F4/80^+CD11c^-$Macs (**J**). Combined data of n = 11 mice from up to three independent experiments are shown. Significant differences between DKO and WT (*) or HET (#) mice are indicated as * or #, $p < 0.05$; ** or ##, $p < 0.01$; *** or ###, $p < 0.001$, **** or ####, $p < 0.0001$. Data in this figure were generated by Y. Feng and L. Daley-Bauer.

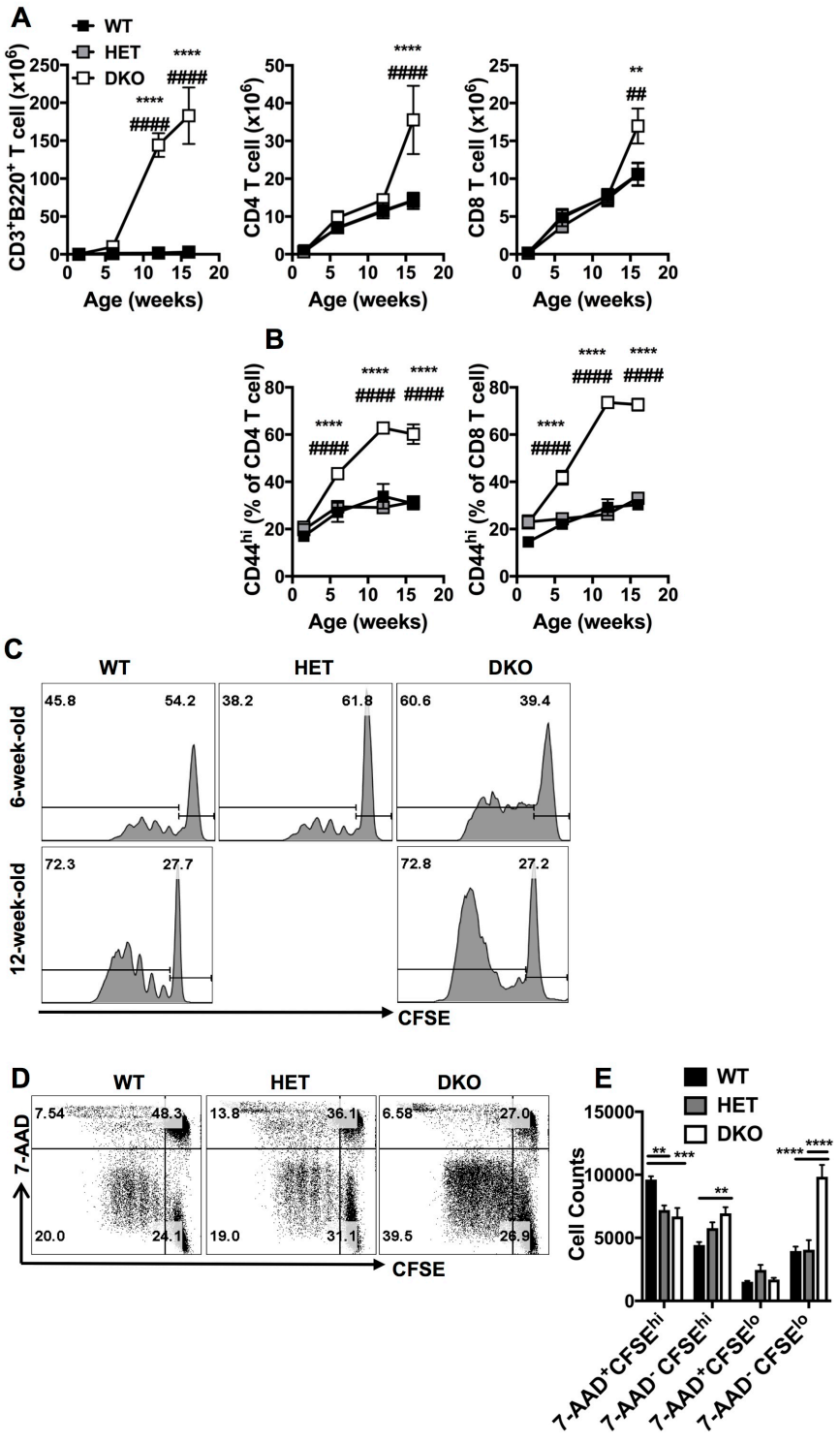


**Figure 0.2 Impact of Casp8 and RIPK3 deficiency on T cell homeostasis at different ages.**

(**A** and **B**) Graphs showing levels of T cell subsets represented as the mean ± S.E.M. in spleens of WT, HET and DKO mice at the indicated weeks of ages. Splenic $CD45^+$ leukocytes were gated to

identify $B220^{+}CD3^{+}$ T cells, $B220^{-}CD3^{+}CD8^{-}CD4^{+}$ (CD4) and $B220^{-}CD3^{+}CD4^{-}CD8^{+}$ (CD8) T cells. Graphs showing the total numbers of the T cell subsets (**A**) and the frequencies of $CD44^{hi}$ CD4 and $CD44^{hi}$ CD8 T cells (**B**). Significant differences between DKO and WT (*) or HET (#) mice are indicated as * or #, respectively, * or #, $p < 0.05$; ** or ##, $p < 0.01$; *** or ###, $p < 0.001$; **** or ####, $p < 0.0001$.

(**C** - **E**) Flow cytometry plots showing CD8 T cell proliferation and death. CFSE dilution analyses of purified splenic T cells after stimulation with anti-CD3 and anti-CD28 for 72 hr. Representative histograms comparing CFSE distribution of $7\text{-}AAD^{-}$ CD8 T cells from mice at the indicated ages (**C**). Representative plots showing CFSE vs. 7-AAD of cells from 6-week-old mice (**D**) and bar graphs showing the numbers of different cell population recovered in culture following stimulation, represented as the mean ± S.E.M. Combined data of n = 11 mice from up to three independent experiments are shown. **, $p < 0.01$; ***, $p < 0.001$; ****, $p < 0.0001$.

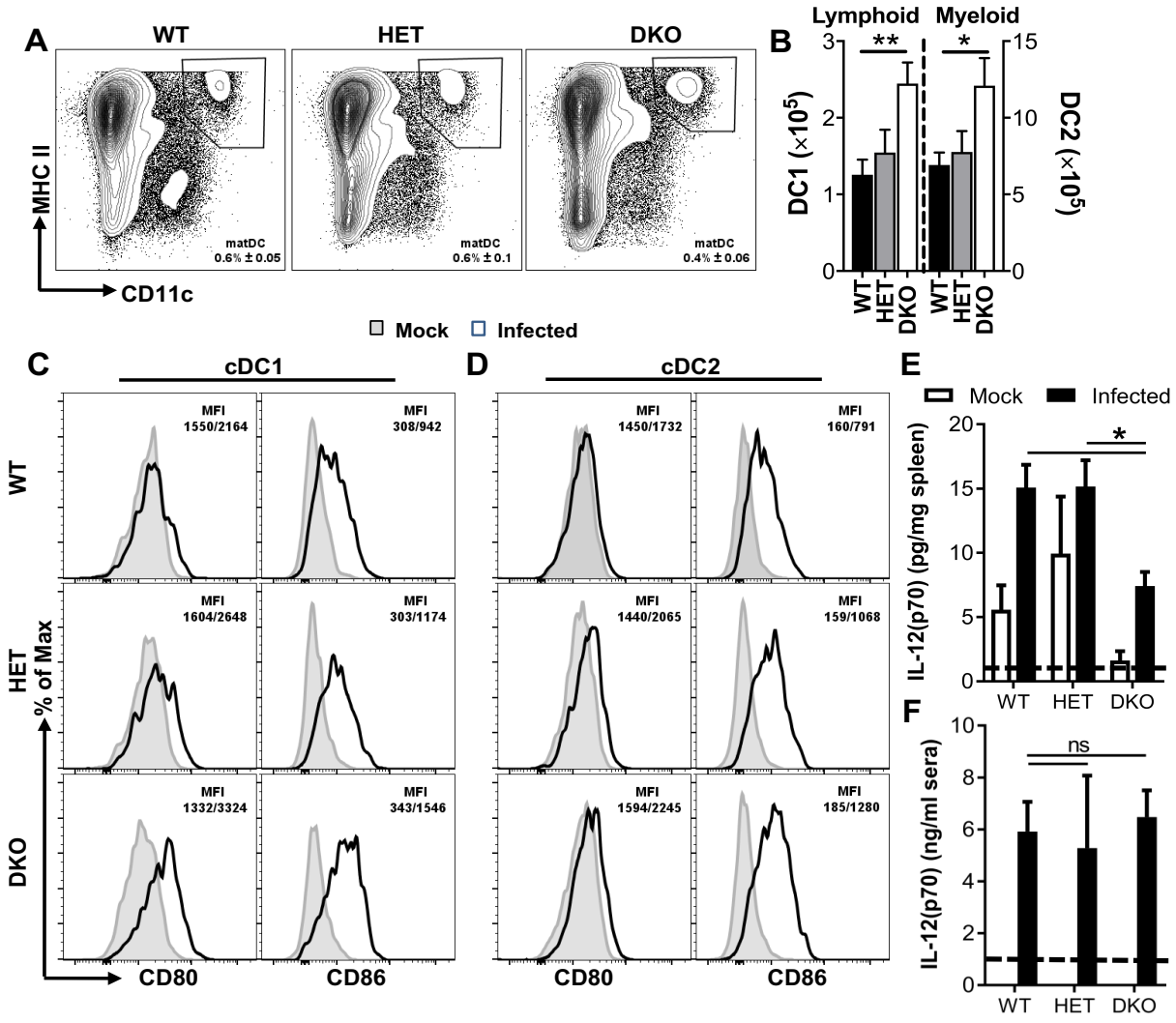


**Figure 0.3 Impact of Casp8 and RIPK3 deficiency on DC activation following MCMV infection.**

(**A** and **B**) Representative contour plots showing frequencies of mature cDCs (**A**) and bar graphs showing total mean numbers ± S.E.M. of cDC1s and cDC2s (**B**) in spleens of infected mice. (**C** and **D**) Representative histograms showing CD80 and CD86 expression on cDC1s (**C**) and cDC2s (**D**) from either mock or infected mice. (**E** and **F**) Bar graphs showing concentrations ± S.E.M. of IL-12(p70) in spleen homogenate (**E**) and serum (**F**) as quantified by ELISA. Dash lines indicate limit of detection. Eight-week-old WT, HET and DKO mice were inoculated intraperitoneally

(i.p.) with $10^5$ PFU MCMV (V70 strain) per mouse. Splenocytes were analyzed at 1.5 dpi by flow cytometry, as described in Figure 1. Spleen homogenates or sera were analyzed by ELISA. Combined data of n = 11 mice from up to three independent experiments are shown. *, $p < 0.05$; **, $p < 0.01$; ***, $p < 0.001$. Data in this figure were generated by Y. Feng and L. Daley-Bauer.

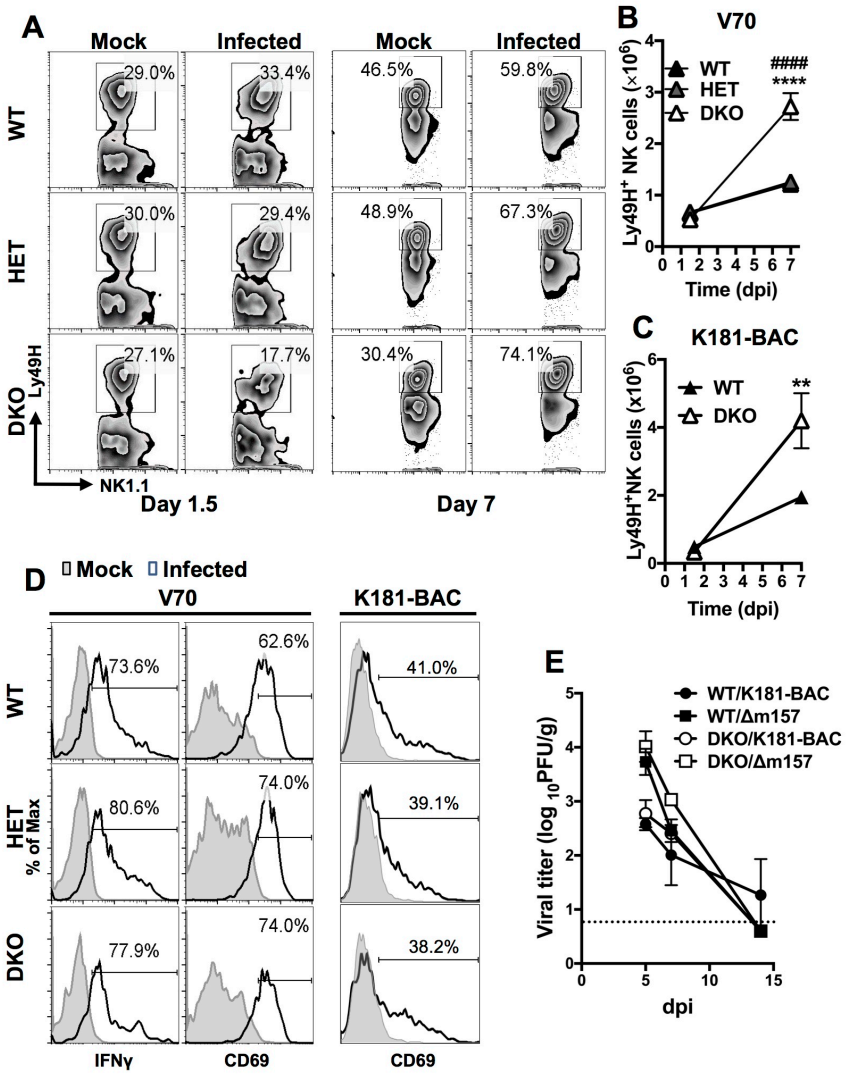


**Figure 0.4 Impact of Casp8 and RIPK3 deficiency on NK cell responses following MCMV infection.**

(**A** – **D**) Graphs showing the levels and phenotype of Ly49H$^+$ NK cells responding to MCMV infection. Splenic total CD45$^+$CD3$^-$B220$^-$NK1.1$^+$ (NK) cells gated to identify Ly49H$^+$ NK cells from 8-week-old WT, HET and DKO mice infected for 1.5 or 7 days with MCMV as described in Figure 3. Representative flow cytometry contour plots comparing Ly49H$^+$ NK cell frequencies (**A**) and graph showing mean total numbers ± S.E.M (**B**) in mock or MCMV V70-infected mice. Graph showing mean numbers ± S.E.M. of Ly49H$^+$ NK cells in K181-BAC-infected mice (**C**).

Representative histograms showing frequencies of $Ly49H^+$ NK cells expressing IFNγ or CD69 at day 1.5 post infection with strain V70 or K181-BAC (**D**).

(**E**) Graph showing viral titers in spleens. WT and DKO mice were i.p.-inoculated with $10^6$ PFU MCMV K181-BAC or Δm157. Tissues were harvested on day 5, 7 and 14 post infection and homogenates were analyzed by plaque assay. Dash line indicates limit of detection. * and # denote the significantly differences of DKO cells relative to WT and HET cells, respectively. ** or ##, $p < 0.01$; *** or ###, $p < 0.001$. Data represent two to three independent experiments using $n = 4 – 5$ mice per group. Data in panels B and D were generated by L. Daley-Bauer.

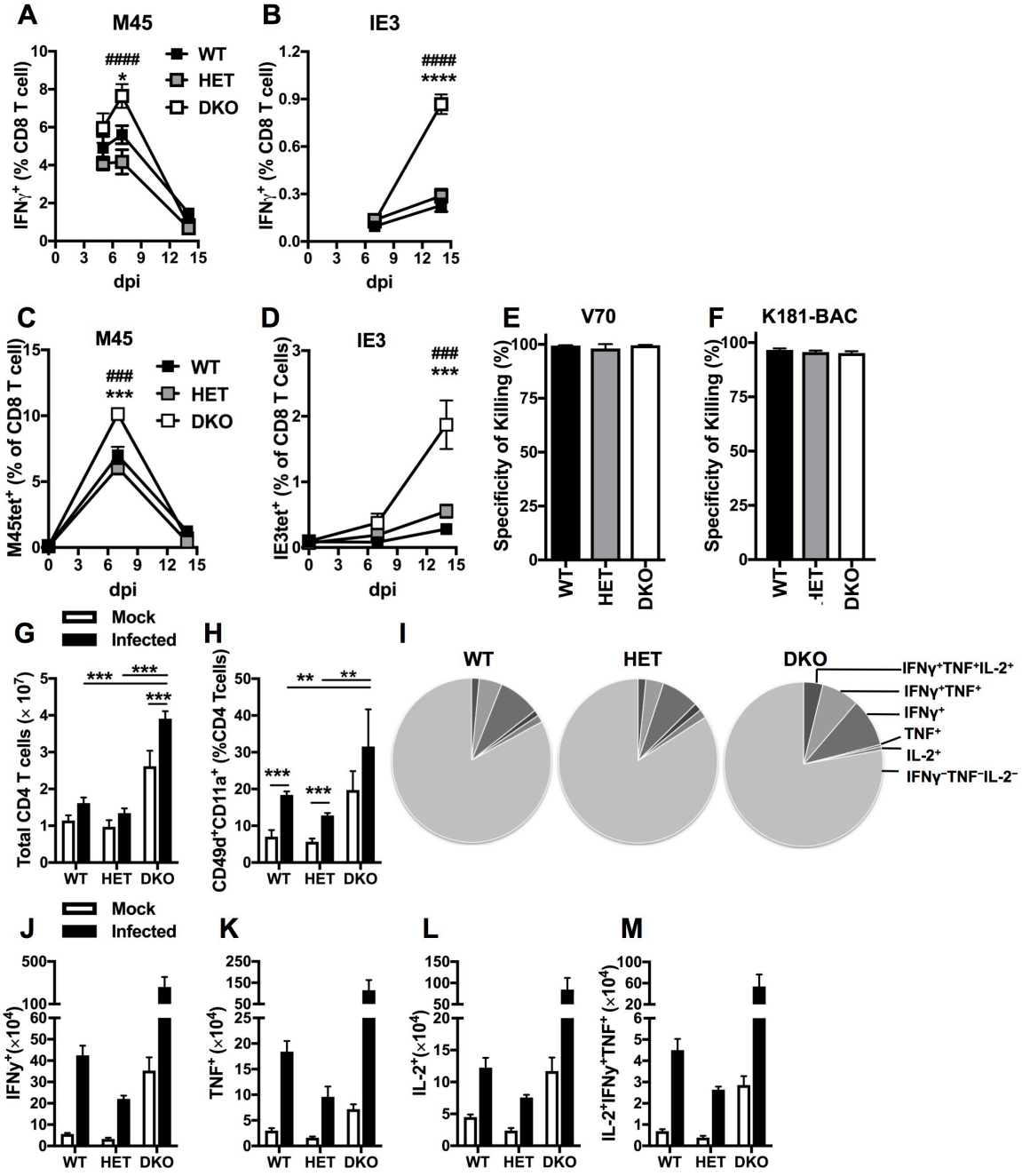


**Figure 0.5 Impact of Casp8 and RIPK3 deficiency on T cell antiviral responses.**

(**A** – **D**) Graphs comparing mean ± S.E.M. frequencies of MCMV-specific CD8 T cell subsets in spleens from 8-week-old WT, HET and DKO mice infected with MCMV. Frequencies of $IFN\gamma^+$ CD8 T cells following *ex vivo* M45 (**A**) or IE3 (**B**) peptide stimulation at 5, 7 and 14 dpi with V70 as described in Figure 3. Frequencies of M45 (**C**) or IE3 (**D**) tetramer-positive CD8 T cells in

K181-BAC-infected mice at 0, 7 or 14 dpi. Significant differences between DKO and WT (*) or HET (#) mice are indicated as * or #, $p < 0.05$; ** or ##, $p < 0.01$; *** or ###, $p < 0.001$; **** or ####, $p < 0.0001$.

(**E** and **F**) Bar graphs comparing mean ± S.D. CD8 T cell-specific killing. Non-pulsed $CFSE^{lo}$ and M45 peptide-pulsed $CFSE^{hi}$ splenocytes were adoptively transferred into naïve or infected recipients by V70 (**E**) or K181BAC strain (**F**) at 7 dpi, and spleens were harvested at 18 (**E**) or 4 (**F**) hour post transfer from recipient mice and frequencies of $CFSE^{+}$ splenocytes were analyzed by flow cytometry.

(**G** – **M**) Flow cytometric analyses of CD4 T cells in spleens at 14 dpi. Bar graphs showing the numbers of total (**G**) and $CD11a^{+}CD49d^{+}$ (**H**) CD4 T cells represented as the mean ± S.E.M.. Pie charts depicting mean percentages of indicated CD4 T cell subsets following stimulation of anti-CD3/CD28 for 5h (**I**). Bar graphs showing mean ± S.E.M. total numbers of CD4 T cells that were $IFN\gamma^{+}$(**J**), $TNF^{+}$ (**K**), IL-$2^{+}$ (**L**), or $IFN\gamma^{+}TNF^{+}$IL-$2^{+}$ (**M**). Data represent two to three independent experiments using $n = 5$ mice per group.

Data in panels A, B and D were generated by D. Livingston-Rosanoff. Data in panels G to M were generated by L. Daley-Bauer.

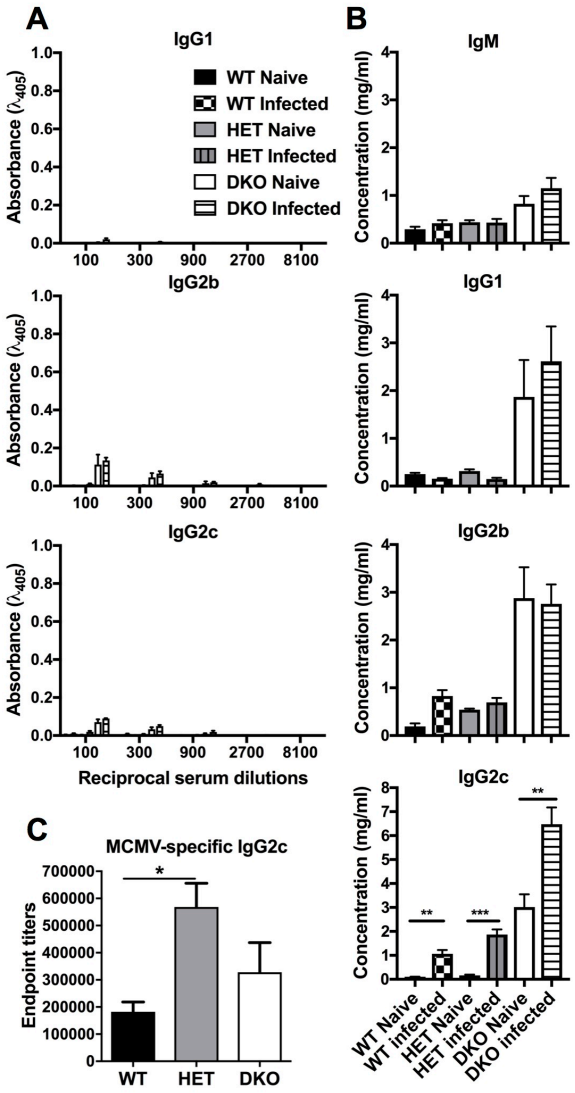


**Figure 0.6 Impact of Casp8 and RIPK3 deficiency on Ab levels following MCMV infection.**

Mean ± S.E.M. concentrations of different Ig isotypes in sera from mice infected as described in Fig. 5H – N. Bars graph depict relative dsDNA-reactive IgG levels (**A**), total Ab concentrations (**B**) and MCMV-specific IgG2c endpoint titers (**C**) as derived by ELISA. *, $p < 0.05$; **, $p < 0.01$; ***, $p < 0.001$. Data represent one experiment using $n = 5$ mice per group. Data in this figure were generated by A. Sundararajan and L. Daley-Bauer.

# Chapter 3

Caspase-8 Restricts Natural Killer Cell-triggered Antiviral CD8 T Cell Hyperaccumulation

A version of this chapter has been submitted to *Proc. Natl. Acad. Sci*. as Yanjun Feng, Lisa P. Daley-Bauer, Linda Roback, Heather S. Koehler, Hongyan Guo, Marc Potempa, Lewis L. Lanier, Edward S. Mocarski, "Caspase-8 Restricts Natural Killer Cell-triggered Antiviral CD8 T Cell Hyperaccmulation".

## 3.1 Abstract

The magnitude of a CD8 T cell response against different viruses is checked by the balance of proliferation and death. This response is influenced by caspase-8 (Casp8) following T cell receptor (TCR) engagement – through apoptosis initiation, necroptosis suppression, and cell death-independent modulation of signal transduction. The understanding of Casp8 function during T cell activation is confounded by unleashed RIPK3-mediated necroptosis. *Casp8*$^{-/-}$*Ripk3*$^{-/-}$ (DKO) mice lack this confounding dysregulation and open the way to understand the contribution of Casp8 to antiviral CD8 T cell responses. Here, we show that these mice develop higher antiviral CD8 T cell numbers than *Casp8*$^{+/-}$*Ripk3*$^{-/-}$ littermates or WT C57BL/6 mice during the acute phase of murine cytomegalovirus or herpes simplex virus-1 infection. This increase is ascribed to KLRG1$^{hi}$ effector subsets. DKO CD8 T cells hyperaccumulate even when transferred into WT recipients, attributable to an increase in proliferation. These data demonstrate a CD8 T cell-autonomous impact of Casp8 on restricting proliferation upon stimulation. Notably, the m157-driven Ly49H$^{+}$ natural killer (NK) cell response drives hyperaccumulation by promoting T cell survival in DKO mice. Interestingly, early inflationary DKO T cell responses are not sustained during long-term infection. Despite the absence of memory inflation, these mice are immune to secondary challenge. Combined, this study highlights a non-death role of Casp8 in restricting CD8 T cell proliferation. In the infected host, an aggressive antiviral NK cell response triggers effector T cell expansion that is kept in check by T cell-autonomous Casp8 activities.

## 3.2 Introduction

In response to virus infection, naïve CD8 T cells expand dramatically and differentiate into heterogeneous subsets with different memory potential and effector function (22, 36). One important subset during the acute phase expresses high levels of KLRG1 and low levels of IL-7Rα (CD127), indicating that the population is terminally differentiated and short-lived. While these $KLRG1^{hi}CD127^{lo}$ terminal effector cells perform robust cytotoxic killing to clear infection, their responses are effectively turned off through rapid cell contraction once the pathogen is controlled (202). In contrast, $KLRG1^{lo}CD127^{hi}$ memory precursor effector cells survive and differentiate into memory cell subsets. Further, $KLRG1^{hi}CD127^{hi}$ effector cells downregulate KLRG1 during the contraction phase and retain plasticity of memory differentiation (33). Most of these features can be applied to the conventional epitope-specific CD8 T cells in response to MCMV, a natural mouse herpesvirus (39). The conventional T cell responses follow classical antiviral T cell kinetics, including phases of expansion, contraction and memory formation (37). Most of these cells exhibit Tcm phenotype ($CD62L^{hi}KLRG1^{lo}CD127^{hi}$) in latently infected mice. Meanwhile, another subset of MCMV-specific CD8 T cells shows sustained expansion during over the course of lifelong infection with patterns that largely exhibit Tem phenotype ($CD62L^{lo}KLRG1^{hi}CD127^{lo}$). This phenomenon termed “memory inflation” is a hallmark of CMV infection (39), and is thought to be driven by low level antigens through sporadic viral reactivation from latency in infected non-hematopoietic cells (37, 288). The magnitude and phenotypes of these conventional and inflationary T cell subsets are dictated by antigen load, co-stimulatory molecule signaling and cytokine milieu (2). These factors together balance cell proliferation, death and differentiation to ensure an optimal antiviral T cell immunity.

T cell numbers are tightly regulated by two death pathways: intrinsic (or mitochondrial) and extrinsic pathways (115). Intrinsic death, regulated by Bcl-2 family members, predominates in the control of CD8 T cell numbers during the expansion and contraction phases (197, 201, 202). Elimination of pro-death Bcl-2 family member Bim, or Bax and Bak increases overall antiviral T cell numbers (197, 201). In contrast, extrinsic death plays subtle roles in T cell contraction, despite a key role in post-thymic homeostasis (124). Extrinsic death is triggered by ligation of cell surface TNF superfamily death receptor (DR), including TNFR1, TRAIL and Fas, which results in recruitment of Casp8 by the adaptor Fas-associated death domain protein (FADD) to form the DISC together with $cFLIP_L$, RIPK1 and RIPK3 (125). A similar complex forms downstream of TLR3, TLR4 or TCR (125). In the DISC, auto-proteolytic cleavage following homodimerization activates Casp8 to trigger Casp3-mediated apoptosis. Casp8 function also keeps RIPK3-dependent, MLKL-mediated necroptosis in check because elimination of Casp8 or inhibition of its basal enzymatic activities sensitizes cells to necroptotic death (133, 145, 174). Besides the roles in cell death regulation, Casp8 function influences cytokine production via NF-κB and MAP kinase signaling pathways (125). Casp8 was determined to support T cell proliferation (289), because cells with the enzyme eliminated or catalytic activity mutated show defective TCR-driven division (165, 290). A similar defect is observed in T cells with impaired FADD, the critical adaptor of Casp8 (223, 291). All of these studies are confounded by the crucial role of Casp8 in suppressing necroptosis, because the proliferation defect is restored in the absence of the pro-necroptotic kinase (166, 167, 222). Curiously, virus-specific CD8 T cell numbers trend higher in $Lck^{Cre}Fadd^{dd}Ripk3^{-/-}$ mice infected with murine hepatitis virus (222); however, no differences have been observed in $CD4^{Cre}Casp8^{flox/flox}Ripk3^{-/-}$ mice following lymphocytic choriomeningitis virus (LCMV) Armstrong infection (166). These results suggest that Casp8 may dampen T cell responses during

certain viral infections in addition to its function in initiating apoptosis and suppressing necroptosis.

MCMV is a natural mouse pathogen where CD8 T cell immunity controls acute infection and prevents reactivation (39). To prolong virus persistence in the infected cells, MCMV encodes viral proteins that inhibit Casp8 and RIPK3 functions (133, 249). Disruption of either or both inhibitors attenuates virus replication and dissemination in the host, due to the pre-mature death of the infected cells and death-independent antiviral mechanisms (157, 169, 170). Despite the importance for first-line host defense, Casp8 appears dispensable for triggering immune cell activation following MCMV infection (150, 174, 233). Indeed, previous studies have showed that young adult DKO mice mount enhanced responses of conventional and inflationary CD8 T cells compared to HET littermate controls or WT C57BL/6 mice (174, 233), suggesting that Casp8 normally dampens the magnitude of MCMV-specific CD8 T cell responses. Notably, DC numbers are also higher in DKO mice than controls when assessed during the acute phase of infection (233). Upon MCMV infection, uninfected cDC1s cross-present virus antigens to prime virus-specific CD8 T cells (6, 15). Greater cDC1 numbers may lead to enhanced CD8 T cell numbers during infection. In addition, Casp8 elimination in the myeloid compartment influences cytokine milieu during homeostasis and infection (178, 179, 184, 292, 293), a dysregulation that may influence the magnitude of T cell responses. Further, DKO mice exhibit enhanced response of the $Ly49H^+$ NK cell (233), an NK cell subset known to regulate T cell numbers and function (294). Thus, it is unclear whether the T cell-autonomous dysregulation or extrinsic environmental factor alteration contributes to DKO CD8 T cell hyperaccumulation in response to MCMV infection.

In the current study, we show that DKO CD8 T cells hyperaccumulate independently of the environmental milieu of DKO mice following MCMV infection, attributable to an increase in

proliferation rather than death deficit. DKO mice exhibit enhanced levels of conventional and inflationary epitope-specific CD8 T cells during the acute phase of MCMV infection, due to the hyperaccumulation of KLRG1$^{lo}$CD127$^{hi}$ terminal effector subsets rather than memory precursors. While Casp8-elimination enhances CD8 T cell proliferation, the increase in cell numbers also requires m157-driven Ly49H$^{+}$ NK cells that support DKO T cell survival. Paradoxically, the enhancement of inflationary T cell subset fails to sustain during long-term infection. Together, our data show a death-independent role of Casp8 in restricting cell proliferation during the expansion phase following virus infection. This T cell-autonomous mechanism of Casp8 together with the T cell-extrinsic regulation of NK cells oversee the proper antiviral effector T cell accumulation.

## 3.3 Results

*Antiviral CD8 T cells in DKO mice hyperaccumulate during the acute phase of viral infection*

We have shown that DKO mice mount enhanced antiviral CD8 T cell responses during the acute phase of MCMV infection (233). To further investigate the contribution of Casp8 to CD8 T cell response kinetics, splenocytes from MCMV K181-BAC strain-infected WT, HET and DKO mice were analyzed on days 5, 7, 9 and 14 post infection. CD8 T cell numbers were comparable on day 5 (Fig. 3.1*A*), expanded to peak levels on day 7 that were higher in DKO mice than controls, as expected (233), and contracted through days 9 and 14 post infection. In contrast, CD4 T cell numbers as were generally comparable independent of genotype (Fig. 3.1*B*). The higher cell numbers in DKO mice at 9 days-post infection (dpi) eventually contracted to control levels by day 14. This pattern reinforces the fact that Casp8 is dispensable for T cell contraction (115). Instead, Casp8 appears to restrain CD8 T cell expansion (233).

To investigate the MCMV-specific CD8 T cell response, we used MHC-I tetramer-staining to measure the conventional M45-specific CD8 T cells that predominate in acute phase, as well as inflationary M38- and IE3-specific cells (17, 37). All epitope-specific subsets accumulated to significantly higher numbers and percentages during acute phase in DKO mice compared to WT or HET controls (Fig. 3.1*C* – *E*), suggesting an overall enhanced antiviral CD8 T cell response when mice lack Casp8 and RIPK3. The numbers (Fig. 3.1*C*, top panel) and percentages (Fig. 3.1*C*, bottom panel) of DKO M45-specific CD8 T cells peaked higher than controls at 7 dpi and contracted dramatically, reinforcing that Casp8 restrains conventional epitope-specific CD8 T cell expansion without contributing to contraction as reported (233). The M38- and IE3-specific CD8 T cell numbers decreased from a peak at day 7 through days 9 and 14 post infection (Fig. 3.1*D* – *E*). The percentages of DKO IE3-specific cells continued to rise to higher levels than controls

throughout the observation period, attributable to the faster contraction of other epitopes-specific subsets. Taken together, these observations indicate that Casp8 plays a role in restraining hyperaccumulation of both conventional and inflationary epitope-specific T cells during the acute phase.

Effector CD8 T cells exhibit heterogeneity in expression of surface markers, including KLRG1 and CD127 that have conventionally been used to define subsets with distinct differentiation potential (22, 202). Next, we sought to identify the subsets of virus-specific CD8 T cells that hyperaccumulate when Casp8 is absent. When M45-specific CD8 T cells were evaluated, DKO mice exhibited significantly greater numbers of the KLRG1$^{hi}$ subsets, especially the KLRG1$^{hi}$CD127$^{lo}$ terminally differentiated effectors at 7 dpi (Fig. 3.1*F*); whereas, no impact was observed on the KLRG1$^{lo}$ subsets (KLRG1$^{lo}$CD127$^{hi}$ and KLRG1$^{lo}$CD127$^{lo}$). Following the peak of the response, all populations contracted to numbers comparable to controls by 14 dpi independent of genotype. Consistent with this assessment of cell numbers, enhanced proportions of DKO M45-specific CD8 T cells were KLRG1$^{hi}$CD127$^{lo}$ at 7 dpi (Fig. 3.1*G*) in comparison with WT or HET controls. Similar enhancement of KLRG1$^{hi}$ subsets was observed with the inflationary epitopes M38 (Fig. S3.1 *A – B*) and IE3 (Fig. S3.1 *C – D*) and this phenomenon was independent of IL-2 production from CD4 T cells (Fig. S3.1 *E*). Thus, the hyperaccumulation that occurs in DKO mice is mainly due to substantially elevated short-lived effector cell numbers. Taken together, Casp8 restrains the accumulation of terminally differentiated antiviral CD8 T cells in response to virus infection.

To investigate whether Casp8-dependent antiviral CD8 T cell hyperaccumulation occurs with another Casp8-deficient strain, we assessed *Casp8*$^{-/-}$*Ripk3*$^{K51A/K51A}$ (C8$^{-/-}$R3$^{K51A}$) mice (148) together with *Ripk3*$^{K51A/K51A}$ (R3$^{K51A}$), DKO and *Ripk3*$^{-/-}$ mice. By 7 dpi, DKO and C8$^{-/-}$R3$^{K51A}$

mice showed increased numbers and proportions of M45-specific CD8 T cells in comparison with all control *Ripk3*$^{-/-}$ and R3$^{K51A}$ and WT mice (Fig. 3.1*H* – *I*). Thus, Casp8 in general restricts antiviral T cell number once RIPK3 function is compromised.

To assess whether Casp8 regulates CD8 T cell immunity to infection with another herpesvirus, C8$^{-/-}$Ripk3$^{K51A}$ mice were inoculated with HSV-1. A similar enhanced pattern of total (Fig. 3.1*J*) as well as gB-specific CD8 T cells (Fig. 3.1*K* – *L*) was observed in the C8$^{-/-}$R3$^{K51A}$ mice compared to R3$^{K51A}$ or WT controls. Thus, Casp8-dependent regulation of virus-specific CD8 T cells is not restricted to MCMV infection.

*The early enhanced response of inflationary DKO CD8 T cells was not sustained during long-term infection*

The enhanced responses observed in DKO mice during acute phase infection prompted us to investigate whether similar patterns were sustained during long-term infection. Following contraction, the percentages (Fig. 3.2*A*) and numbers (Fig. 3.2*B*) of M45-specific CD8 T cells in spleens remained low in all genotypes. The population was largely KLRG1$^{lo}$CD127$^{hi}$ at 25 weeks post infection (wpi) (Fig. 3.2*C*), and exhibited the expected Tcm phenotype of conventional CD8 T cells responding to long-term infection (37). IE3-specific CD8 T cells in WT and HET mice reached high frequencies (Fig. 3.2*D*) and numbers (Fig. 3.2*E*) by 25 wpi with the majority exhibiting the expected KLRG1$^{hi}$CD127$^{lo}$ Tem phenotype (Fig. 3.2*F*). This inflationary T cell phenomenon is indicative of continuous replenishment by new effector cells that differentiate from naïve or central memory pools (37, 39). Strikingly, despite the enhanced response during acute phase, the IE3-specific subset in DKO mice showed a low percentage and number in spleens at 25 wpi. In addition, lower proportions (Fig. 3.2*F*, left panel) and numbers (Fig. 3.2*F*, right panel) of these cells exhibited Tem phenotype when compared with controls, suggesting a failure to recruit

or sustain these recently differentiated effector cells during long-term infection (37, 39), even though DKO mice displayed enhanced KLRG1$^{hi}$ cell differentiation during acute phase (see Fig. S3.1 *C – D*). Furthermore, the patterns of the M45-, IE3- and M38-specific CD8 T cells in blood of DKO and C8$^{-/-}$R3$^{K51A}$ mice (Fig. S3.2 *A – C*) reflected the patterns in spleens, indicating that Casp8-deficient mice have a global rather than organ-specific defect in memory inflation once RIPK3 function is compromised. DKO mice accumulate B220$^{+}$CD3$^{+}$ abnormal T cells during homeostasis (145, 150, 174, 233), reminiscent of mice lacking Fas death domain (DD) signaling (124, 213). These abnormal splenic T cell numbers would be expected to occupy space in the lymphoid organs, leading to the observed hypo-inflationary response. However, the numbers of these cells decreased from 400 million at 8 wpi to less than 10 million by 25 wpi (Fig. 3.2*G*). Thus, abnormal T cells did not crowd out the inflationary response. At 25 wpi, virus was consistently detected in the SGs (Fig. 3.2*H*) and sporadically in other organs of DKO mice, while control mice did not have detectable virus in any organ. Curiously, high virus titers in the SG occurred despite the enhanced IFN$\gamma^{+}$ CD4 T cells (66) in spleen and blood of DKO mice (Fig. S3.2 *D*). Given a recent study showing the contribution of inflationary CD8 T cells to SG virus control (71), high virus titers in these mice is correlated with the hypo-memory inflation. It is also possible that active persistent virus replication dampened inflationary responses, which are driven by low level antigen presentation in latently infected mice (1). Whether MCMV infection actually dampens the abnormal T cell accumulation remains to be fully understood. Overall, Casp8 function helps sustain T cell inflation during long-term infection. Persistent infection may undermine splenic hyperplasia and accumulation of abnormal T cells.

CD8 T cells, and particularly, inflationary subsets contribute to host protection against primary infection and reactivation (68, 295, 296). We sought to investigate whether long-term

infected DKO mice were protective from secondary challenge, even though inflationary responses were compromised. Mice at 20 wpi with K181-BAC (or mock treated) were challenged with V70, a more virulent strain of MCMV (Fig. 3.2*J*). Four days later, challenged mice had no detectable virus replication in spleen (Fig. 3.2*K*) or liver (Fig. 3.2*L*), in contrast to the high virus titers in organs of mice undergoing primary infection. Similar to DKO mice and $C8^{+/-}Ripk3^{K51A}$ littermate controls, challenged $C8^{-/-}R3^{K51A}$ mice had no detectable virus in either organ. Secondary infection did not alter persistent SG titers (Fig. 3.2*M*). Taken together, DKO mice developed immunological memory sufficient to combat secondary infection, despite a reduced inflationary response.

*The pattern of enhanced CD8 T cell accumulation is independent of viral replication levels*

Next, we sought to determine the mechanism that causes DKO CD8 T cell hyperaccumulation during acute phase of virus infection. Viral antigen load is a critical factor that determines the magnitude of antiviral CD8 T cell response (202). To reduce antigen load, mice were treated daily with the antiviral drug cidofovir (CDV) starting three days prior to MCMV infection through day 7 (Fig. 3.3*A*) (17, 297). PBS-treated mice showed the expected similar peak titers at 3 dpi (97) that became more variable at 7 dpi as virus was brought under control by CD8 T cells (Fig. 3.3*B*, left panel). Following CDV treatment, virus was not detected in spleen (Fig. 3.3*B*, right panel) or other organs (data not shown) regardless of genotype. CD8 T cells specific to the dominant epitope M45 were assessed at 7 dpi. Even with a compromised antigen load, the pattern of the enhanced total (Fig. 3.3*C*) and M45-specific (Fig. 3.3*D* and *F*) CD8 T cell responses in DKO mice was sustained. Taken together, the antiviral CD8 T cell hyperaccumulation in DKO mice occurs independently of viral antigen load.

*DKO CD8 T cell proliferative response*

The enhanced accumulation of DKO CD8 T cells occurred between day 5 and 7 post infection, the period of clonal expansion. We sought to determine whether the enhancement was attributable to cell death or cell proliferation. Casp8 triggers apoptosis and also impedes T cell proliferation following TCR engagement, although this latter function has been ascribed to induction of necroptosis in the absence of Casp8 function (125, 166, 167). CD8 T cell proliferation was assessed using Ki67 (298). The percentages of $Ki67^+$ (Fig. 3.4*A*) CD8 T cells in DKO mice were normal on days 0 and 3, but increased to significantly higher levels than WT controls on days 5 and 7 post infection. These data indicate the enhanced proliferation of DKO cells during the expansion phase. Cell death was assessed using fixable viability staining (FVS), a cell-impermeable dye that stains late stage dead cells. Upon infection, a similar increase in frequencies of $FVS^+$ events were detected in WT and DKO spleens by 5 dpi (Fig. 3.4*B*). While the frequencies in WT mice dropped by 7dpi, the levels sustained in DKO spleens, suggesting that lacking Casp8 and RIPK3 confers no cell survival benefit in general during virus infection. Casp8-initiated apoptosis depends on activation of Casp3 (125), an executioner caspase that is also associated with proliferating T cells (289). We used fluorescent-labeled inhibitor of caspases (FLICA) for active Casp3 measurement. The percentages of $FLICA^+$ CD8 T cells in DKO mice were similar on days 0 and 3, increased to peak levels at 5 dpi that were higher in DKO mice than WT controls, and decreased by 7 dpi (Fig. 3.4*C*). This increased dying cell events despite the lack of Casp8 and RIPK3 is most likely a consequence of Bim-dependent intrinsic death (124). Together, our data demonstrate that enhanced proliferation rather than cell death deficit confers the pattern of T cell hyperaccumulation during the expansion phase in DKO mice.

MCMV-infected DKO mice mount enhanced T cell response, accompanied by increased DC and NK cell numbers (233) that may influence T cell response magnitude. To determine

whether CD8 T cell hyperaccumulation occurs independently of the DKO environment following virus infection, CFSE-labeled total splenocytes containing $1 \times 10^6$ CD8 T cells from CD45.2$^+$ WT or DKO mice were transferred into CD45.1$^+$ WT recipients, followed by MCMV infection 24 h later (Fig. 3.4*D*). CFSE dilution was assessed on days 5 and 6 post infection. Recipient WT T cell numbers were comparable at 6 dpi, indicating that the genotype of donor cells did not alter the endogenous response (Fig. 3.4*E*). Even in this WT-like environment, donor DKO CD8 T cells exhibited enhanced accumulation in comparison with WT donors. Furthermore, higher proportions of CFSE$^{lo}$ DKO CD8 T cells on days 5 and 6 post infection (Fig. 3.4*F*), indicating increased cell divisions compared to WT. During infection, the enhanced proliferation of DKO CD8 T cells does not depend on the environmental milieu of DKO mice following virus infection.

In accordance with observations in virus-infected mice, increased cell division is observed with CD8 T cells purified from DKO or *Lck*$^{Cre}$*FADD*$^{dd}$*Ripk3*$^{-/-}$ mice upon TCR stimulation (222, 233). This suggests that T cell-specific disruption of Casp8 or FADD is sufficient to enhance cell proliferation. It is important to note that a greater proportion of CD8 T cells in these genotypes upregulates CD44 (233), indicating the cells already acquire activation state and may retain a greater proliferative potential. To determine whether CD44$^{lo}$ DKO CD8 T cells also proliferate better, purified splenic CD44$^{lo}$ CD8 T cells were labeled with CFSE, stimulated with anti-CD3 and anti-CD28 antibodies then subjected to flow cytometry analysis at 72 h. The purity of CD44$^{lo}$ CD8 T cells was higher than 99% (data not shown). Upon TCR stimulation, naïve DKO CD8 T cells proliferated more vigorously than WT controls, correlating with a higher proportion of CFSE$^{lo}$ cells (Fig. 3.4*F*) as well as numbers of CFSE$^{lo}$7-AAD$^{lo}$ divided, live cells (Fig. 4*G*) in the culture. The data suggest that enhanced proliferation of DKO CD8 T cells is not dependent on their activation state prior to stimulation.

Upon recruitment to DISC, Casp8 undergoes dimerization and autoprocessing, which unleashes the full activities of the enzyme that results in apoptosis (133). Casp8 autoprocessing mutation (*Casp8*$^{DA/DA}$) still retains the basal catalytic activities sufficient for suppressing necroptosis, leading to the robust T cell proliferation upon TCR stimulation (145, 299). Recent studies using *Casp8*$^{DA/DA}$ myeloid cells implicate the scaffolding function of Casp8 in regulating NF-κB signaling (182, 183). *Casp8*$^{DA/DA}$ CD8 cells exhibited proliferation capacity indistinguishable from WT controls and significantly lower than the Casp8-deficient DKO cells (Fig. 3.4 *F* and *G*), demonstrating that Casp8 autoprocessing has no contribution to CD8 T cell proliferation. Thus, these data suggest a potential contribution of Casp8 scaffolding function or/and its basal catalytic activities in restricting CD8 T cell proliferation.

*Ly49H*$^{+}$ *NK cells driven by m157 are necessary for the DKO CD8 T cell hyperaccumulation*

After understanding the CD8 T cell-autonomous impact of Casp8, we sought to explore any extrinsic factors that support DKO CD8 T cell hyperaccumulation during the acute phase of virus infection. In C57BL/6 mice, NK cells expressing Ly49H receptor dominate the innate immune response and render early control of MCMV infection (1, 300). Ligation of this receptor to the MCMV-encoded MHC class I like glycoprotein m157 triggers activating signals that result in robust proliferation and cytotoxicity of Ly49H$^{+}$ NK cells (94). Given that m157 specifically binds to Ly49H, which is only expressed by this NK cell subset, Δm157 MCMV fails to trigger Ly49H$^{+}$ NK cell expansion (301). Using these mutants, previous reports have shown the impact of Ly49H$^{+}$ NK cells on antiviral CD8 T cell responses (97, 273, 302). We employed Δm157 MCMV infection and traced CD8 T cell responses. The mutant virus infection compromised splenic Ly49H$^{+}$ NK cell numbers to comparable levels in all genotypes (Fig. 3.5*A*), even though the subset in K181-BAC-infected DKO mice accumulated to significantly higher numbers than

WT and HET controls at 7 dpi, as shown previously (233). Strikingly, the total (Fig. 3.5*B*) and the M45-specific (Fig. 3.5*C – D*) CD8 T cell responses in DKO mice returned to control levels when Ly49H$^+$ NK cell numbers were compromised, and this was attributable to reduced numbers (Fig. 3.5*E*) of KLRG1$^{hi}$CD127$^{lo}$ and KLRG1$^{hi}$CD127$^{hi}$ subsets. Cell death analysis showed that Δm157 virus infection led to higher frequencies of FVS$^+$ dead cells in DKO spleens compared to K181-BAC infection at 7 dpi (Fig. 3.5*F*). Consistently, this mutant virus infected DKO mice exhibited higher percentages CD8 T cells positive for annexin V staining when compared with K181-BAC infection (Fig. 3.5*G*), indicating elevated dying CD8 T cell events. Thus, m157-driven Ly49H$^+$ NK cells is necessary for DKO T cell hyperaccumulation through supporting these T cells survival.

To further assess the NK cell-dependent regulation of the antiviral CD8 T cell response, depletion was performed by i.p. inoculation of anti-NK1.1 Ab two days before as well as on days 0 and 3 post infection with K181-BAC virus (Fig. S3.3 *A*) (303). All Ab-treated animals exhibited increased viral titers in liver and lungs at 7 dpi (Fig. S3.3 *B – D)*, consistent with the expected compromised antiviral NK cell responses (97). Although NK cells were effectively reduced by 5 dpi in all genotypes (Fig. S3.3 *E*), the numbers of total and Ly49H$^+$ NK cells in DKO mice bounced back by 7 dpi to levels comparable to non-treated WT and HET controls (Fig. S3.3 *F*). This was different from Δm157 infection which dampened Ly49H$^+$ NK cell quantities throughout the observed period (See Fig. 3.5*A*). The reduction by 5 dpi was not sufficient for reversing hyperaccumulation of total CD8, CD4 T cells or M45-specific CD8 T cells (Fig. S3.3 *G – J*). Taken together, our data suggest that the Ly49H$^+$ NK cell response between days 5 to 7 post infection is critical for enhancing DKO CD8 T cell accumulation.

To understand whether WT Ly49H$^+$ NK cells driven by m157 can also improve DKO CD8 T cell accumulation, CFSE-labeled total CD45.2$^+$ WT or DKO splenocytes that contained $1 \times 10^6$

CD8 T cells were transferred into congenic CD45.1$^+$ recipients, followed by infection with K181-BAC or Δm157 virus 24 h later (Fig. 3.6*A*). The numbers of endogenous CD45.1$^+$ Ly49H$^+$ NK cells were comparable in all K181-BAC-infected recipients and equally decreased to similar levels upon Δm157 infection (Fig. 3.6*B*). The data suggest that the numbers of responding Ly49H$^+$ NK cells were generated independently of the donor cell genotype. Strikingly, hyperaccumulation of total and M45-specific DKO CD8 T cells returned to control levels when the mice were infected with mutant virus (Fig. 3.6*C*), indicating that WT Ly49H$^+$ NK cells suffice to enhance DKO CD8 T cell accumulation. Cell proliferation assessment using CFSE dilution revealed that the m157-driven Ly49H$^+$ NK cell response did not alter DKO CD8 T cell proliferation (Fig. 3.6*D*), reinforcing the cell-intrinsic dysregulation due to Casp8 deficiency in the capacity for hyper-proliferation. Combined, Ly49H$^+$ NK cells, regardless of genotype, support DKO CD8 T cell hyperaccumulation upon MCMV infection. Further, this NK cell subset sustains survival of hyper-proliferated DKO CD8 T cells rather than affecting proliferation.

## 3.4 Discussion

This study demonstrates a vital death-independent role of Casp8 in suppression of CD8 T cell proliferation during the acute phase of virus infection. With the elimination of Casp8 (together with RIPK3), antiviral CD8 T cells, mainly the terminal effector subsets, accumulate to significantly higher levels due to an enhanced proliferation capacity. Although non-death functions of Casp8 has long been implicated in T cell activation (289), information drawn from Casp8-deficient T cells is suspect owing to the confounding impact of necroptosis. Here, we use a system that eliminates Casp8 together with RIPK3 function to show that Casp8 suppresses rather than supports CD8 T cell proliferation following TCR stimulation. Importantly, while hyper-proliferation a T cell-autonomous dysregulation due to Casp8-deficiency, the enhanced CD8 T cell numbers during MCMV infection requires a robust m157-driven Ly49H$^+$ NK cell response that supports T cell survival. Modulation of the Ly49H$^+$ NK cell response reverses DKO CD8 T cell hyperaccumulation through comprising the T cell survival. Here, we propose that the magnitude of this antiviral response is checked by T cell-autonomous Casp8 function along with T cell-extrinsic regulation of NK cells.

Upon infection, activated-naive CD8 T cells undergo 10,000- to 100,000-fold expansion and differentiation into different effector subsets (202). Following the elimination of virus, these expanded cells undergo an equally dramatic contraction, leaving a small percentage of memory precursors to survive and differentiate into memory subsets. This system ensures robust responses to combat pathogens as well as to avoid unnecessary cytotoxicity and inflammation that can harm the hosts. Antiviral CD8 T cell numbers are strictly controlled by cell death pathways. In contract to the dominant role of Bim-mediated intrinsic apoptosis, extrinsic pathway is less critical for the regulation of T cell death in response to virus infection (115). DKO CD8 T cells, which lack

extrinsic death pathway, retain the intrinsic death pathway that drives cells undergoing contraction. This observation reinforces two important points: i) the intrinsic pathway is sufficient for antiviral CD8 T cell elimination; and, ii) intrinsic and extrinsic death pathways proceed independently of each other in this infection setting.

The CD8 T cell hyper-accumulation phenotype in DKO mice was initially thought to be independent of T cell-autonomous function of Casp8, given the normal LCMV Armstrong-specific CD8 T cell expansion in $Cd4^{Cre}Casp8^{flox/flox}Ripk3^{-/-}$ mice (166). However, adoptive transfer analysis in the current study has shown that a similar enhancement pattern of DKO CD8 T cells occurs in WT environment following MCMV infection. Perhaps this discrepancy can be ascribed to certain environmental milieu triggered by MCMV infection distinct from LCMV Armstrong, such as the robust activation and proliferation of $Ly49H^+$ NK cells (96, 304). Previous studies have taken advantage of comparing WT and Δm157 virus to study the positive and negative impact of NK cells on CD8 T cell antiviral immunity (97, 273, 302). Utilizing the mutant virus, we have shown that a robust $Ly49H^+$ NK cell response supports the survival of the hyper-proliferated DKO CD8 T cells, resulting in the cell hyperaccumulation. This positive impact is dependent on the $Ly49H^+$ NK cell response between day 5 and 7 post infection. Previous studies show that NK cells promote MCMV-specific CD8 T cell responses through regulating type I IFN levels (302) or DC numbers (97, 270, 273, 302). In addition, NK cells can directly dampen antiviral T cell responses through a TRAIL- or Fas-dependent elimination (305, 306). Combined deficiency of Casp8 and RIPK3 may induces a switch to a prosurvival response in CD8 T cells. HSV-1 infection results in a similarly, though less significant, enhanced pattern of antiviral CD8 T cells. This middle ground phenotype may be due to an NK cell-dependent mechanism, given that a study shows the

supportive impact of NK cell on HSV-1-specific CD8 T cells (307). Certainly, analysis of T cell-specific knockout mice with different viruses will address this hypothesis in the future.

Our study shows that the enhanced proliferation and hyperaccumulation of virus-specific CD8 T cells in DKO mice is independent of the cell activation state prior to infection. DCs and T cells from unchallenged *CD11c*$^{Cre}$*Casp8*$^{flox/flox}$ mice are activated, a dysregulation rescued by the elimination of MyD88 but not by elimination of RIPK3 (178). A recent study has further shown that these mice mount an enhanced CD8 T cell response to infection with LCMV clone 13 (292), suggesting Casp8 in DC can dampen the magnitude of T cell response during virus infection. On the other hand, T cells from *Lck*$^{Cre}$*Fadd*$^{dd/dd}$*Ripk3*$^{-/-}$ mice also acquire enhanced activation phenotype during homeostasis and exhibit more robust proliferation upon TCR stimulation *in vitro* (222). These studies together point to a direction that elimination of Casp8 in T cells or APCs enhances CD8 T cell activation state during homeostasis, resulting in the amplified proliferation upon activation. Our current work, however, shows that CD44$^{lo}$ CD8 T cells from young DKO mice also proliferate more vigorously than WT controls, suggesting the hyper-proliferation capacity is independent of CD44 expression levels prior to stimulation. Certainly, CD44$^{lo}$ DKO CD8 T cell may have developed some abnormality that favors cell proliferation. A system that has Casp8-eliminated only in activated CD8 T cells will be useful to remove the confounding factors during development.

The signaling complex involving Casp8 forms downstream of TCR or DR in T cells (308). Upton TCR activation, CARMA-MALT1-BCL10 complex forms at the plasma membrane associated with the receptor, triggering NF-κB, MAPK and NFAT pathways (309). Biochemical analysis has shown that FADD interacts with MALT1 through DD interaction (125, 310) and recruit components including Casp8, cFLIP$_L$, RIPK1 and RIPK3 to the complex. TCR stimulation

triggers cleavage of Casp8 along with the subsequent activation of NF-κB and Casp3 (232). Whereas this signaling pathway occurs directly downstream of TCR stimulation, separate studies have shown that Fas acts as a co-stimulatory molecule receptor to enhance or suppress T cell proliferation depending on FasL concentration (234, 235). These data all point to the key role of Casp8 in T cell activation and align with known activation defects of Casp8-deficient T cells both in humans and mice (164, 165, 290). However, these conclusions were drawn prior to understanding the role of Casp8 in suppressing necroptosis and should be revisited. In the current study, the enhanced proliferation of DKO CD8 T cells suggests that Casp8 surprisingly plays a suppressive rather than supportive role following TCR activation. RIPK1 is a key molecule involved in cell activation, survival and necroptosis. Casp8-dependent cleavage of RIPK1 results in inhibition of these outcomes, depending on settings (143, 311). The increased proliferation of DKO cells may be due to the enhanced RIPK1-mediated NF-κB activation that is normally checked by Casp8. Interesting, *Ripk1*$^{-/-}$*Casp8*$^{-/-}$*Ripk3*$^{-/-}$ mice exhibited normal CD8 T cell response comparable WT mice in response to MCMV infection (150); however, no evidence has shown whether this is due to a T cell-autonomous impact or environmental alteration due to the lack of RIPK1. Studies have shown some cell cycle inhibitors, such as p21 and p27, are the substrate of Casp8 (240-242). It is possible that Casp8 restricts proliferation through inducing these inhibitors activation. Importantly, this enhancement does not occur in the Casp8-autoprocessing mutant cells, suggesting the key contribution of Casp8 scaffolding function or/and its basal catalytic activities (130, 299). Taken together, although the precise spatial and temporal relationships remain to be dissected, we show a novel role of Casp8 in restricting CD8 T cell proliferation besides its function in initiating apoptosis and suppressing necroptosis.

It is curious that the enhanced response of inflationary epitope-specific CD8 T cells is not sustained during long-term infection. Multiple factors are important for memory inflation. Previous studies have shown that *Cd4*$^{-/-}$ and *IL-2rα*$^{-/-}$ mice exhibit impaired inflationary CD8 T cell responses (312), suggesting the importance of IL-2 from CD4 T cells for memory inflation. However, in the current study, we observe no defect of IL-2 and CD4 T cell levels in DKO mice in different phases of infection. Further, as introduced earlier, a sustained response requires newly activated T effector cells differentiated from both naïve and Tcm pools, driven by sporadic viral reactivation. While inflationary epitope-specific CD8 T cells in *Cd4*$^{-/-}$ mice are largely Tem during long term infection, most of DKO inflationary CD8 T cells exhibited Tcm phenotype, a sign of reactivation defect independent of CD4 T cells. OX40 and 4-1BB, two co-stimulatory signaling TNF superfamily receptors, play important role for memory inflation. Interestingly, 4-1BB-deficient mice mount enhanced response of the inflationary subsets that contract overtime (56), a phenotype similar to DKO mice. Although this receptor cannot recruit Casp8/FADD due to the lack of DD domain at cytosolic tail (133), Casp8 may contribute to the signaling transduction through other mechanisms. Curiously, DKO mice exhibit persistent virus replication, a phenotype that may be the cause or the result of hypo-inflationary response. Although the virus control in SG only depends on CD4 T cells (65, 66), a more recent work shows the crucial function of SG-resident inflationary CD8 T cells to control re-infection (71). High antigen load during the early stage of infection improves inflationary T cell response (17); however, it is not yet clear whether persistent virus replication might suppress the inflationary response, as occurs with LCMV clone 13. Furthermore, the $B220^{+}CD3^{+}$ abnormal T cells that accumulate in naïve aging DKO mice (174, 233) surprisingly contract to low levels by 25 wpi, indicating an unexpected beneficial impact of MCMV on ameliorating autoimmunity. Together, our observation opens another very important

question for understanding Casp8-dependent mechanism that regulates inflationary response. Further, interruption of autoimmunity through persistent MCMV infection may offer some important therapeutic insight.

We show an unexpected role of Casp8, a crucial regulator of extrinsic death pathway, in dampening CD8 T cell proliferation following TCR stimulation. In addition, our work indicates the combined contribution of T cell-autonomous function of Casp8 and T cell-extrinsic regulation by $Ly49H^+$ NK cells to dampen antiviral CD8 T cell response magnitude. Further, our study points out the possible influence of persistent virus replication on compromising memory inflation and ameliorate abnormal autoimmunity marker accumulation; these will be critical topics for CMV-based vaccine study as well as therapeutic development.

## 3.5 Materials and Methods:

*Mice, viruses and experimental infection*

DKO (174) and $C8^{-/-}R3^{K51A}$ (148) were derived as described previously and backcrossed to > 98% on the C57BL/6 background, based on single nucleotide polymorphism scanning analysis (Jackson Laboratories). DKO and HET littermates were generated by mating DKO fathers and HET mothers and maintained in house. $C8^{+/-}R3^{K51A}$ and $C8^{-/-}R3^{K51A}$ used for long-term infection and memory challenge experiments were generated by mating $C8^{+/-}R3^{K51A}$ parents. $R3^{K51A}$ mice used for HSV1 infection were generated as described previously on C57BL/6 background (148). *Casp8*$^{DA/DA}$ mice were derived as described previously (280). C57BL/6 WT and B6.SJL-Ptprca Pepcb/BoyJ (CD45.1) mice were purchased from Jackson Laboratories and maitained at the Emory University Division of Animal Resources. Mouse experimental procedures were conducted in accordance with the National Institutes of Health and Emory University Institutional Animal Care and Use Committee guidelines.

*Flow cytometry, proliferation, and cell death assays*

Spleens were harvested and disrupted by mashing through metal sieves. Cell mixture were the incubated with red blood cell lysis buffer to lyse erythrocytes and pass through 100 μm strainer. Cells numbers were determined by counting cells on a hemocytometer using trypan blue exclusion. Cells were stained with FVS for dead cell exclusion, and then incubated with anti-CD16/CD32 plus 10% rat serum in FACS staining buffer for blocking Fc receptor as well as non-specific bindings. Cells were then stained with Abs specific for surface and intracellular antigens and prepared for multiparametric flow cytometric analysis. For intracellular cytokine staining, splenocytes were stimulated with peptides (M45, M38, IE3; JPT Peptide Technologies) or with anti-CD3 (10 μg/ml, Clone Clone 17A2, BD Pharmingen) and anti-CD28 (2 μg/ml, Clone 37.51,

eBioscience) for 5 hr in brefeldin A added RPMI 1640 with 10% FBS/1% penicillin/streptomycin (complete RPMI). Intracellular cytokines were stained with antibodies in the usage of the Cytofix/Cytoperm kit (BD Biosciences). Cells undergoing active proliferation were measured with intracellular staining for Ki67. For death assessment, splenocytes were stained with FVS for measurement of late stage dead cells. For FLICA or Annexin V positive event assessment, splenocytes were stained with FLICA or Annexin V for detecting dying cells. Data were acquired by flow cytometry (BD LSRII cytometer and FACSDiva Software; BD Biosciences), analyzed with FlowJo (TreeStar), and graphed with Prism 7 (GraphPad).

*Treatment of mice with CDV or depleting Ab*

CDV was dissolved in 1 × PBS and filtered through 0.2 μm to sterile. The solution was stored at -80°C until use. Mice were daily injected i.p. with 5 mg/kg CDV in PBS or PBS only (297), starting from 3 day prior to infection and sacrificed on days 3 and 7 post infection for viral titer and immune cell analysis.

For NK cell depletion experiment, mice were i.p. inoculated with anti-NK1.1 (Clone PK136, kindly provided by J. Sun; Sloan Kettering Institute, New York) on days -2, 0 and 3 post infection (303). Depletion of NK cells were confirmed by co-staining leukocytes with anti-CD49b, anti-NKp46 and anti-Ly49H mAbs.

*CD8 T cell adoptive transfer*

Total CD45.2$^+$ spenocytes from naïve WT or DKO mice were labeled with 0.5 μM CFSE (Invitrogen) in 1 × PBS for 10 min at 37 °C. CD45.2$^+$ Splenocytes that contained 1 × $10^6$ CD8 T cells were transferred intravenously into CD45.1$^+$ WT mice, followed with MCMV infection on recipient mice at one day post transfer.

*In vitro CD8 T cell proliferation*

$B220^{-}CD3^{+}CD4^{-}CD44^{lo}$ CD8 T cells were isolated by EasySep Mouse CD8 T Cell Isolation Kit (STEMCELL). Biotinylated anti-B220 (Clone RA3-6B2, STEMCELL) and anti-CD44 (Clone IM7, STEMCELL) Abs were spiked in to facilitate the removal of $B220^{+}CD3^{+}$ abnormal T cells and $CD44^{hi}$ cells. Purified cells were labeled with 0.5 μM CFSE in 1 × PBS for 10 min at 37 °C then stimulated with plate-bound anti-CD3 (10 μg/ml, Clone Clone 17A2, BD Pharmingen) and soluable anti-CD28 (2 μg/ml, Clone 37.51, eBioscience) for 72 hr in a 37 °C incubator. Cells were stained with Abs for specific surface markers as well as 7-AAD for dead cell detection. For comparing cell counts in the culture, all samples were suspended in an equal volume of FACS staining and collected for the same amount of time using flow cytometer.

*Virus infections*

K181-BAC (283) and K181-BAC-derived Δm157 (284) (kindly provided by W. Brune; Heinrich Pette Institute, Hamburg) were propagated in NIH 3T3 murine fibroblasts (American Type Culture Collection CRL-1658) in 10% weight/volume in Dulbecco's Modified Eagle Medium (DMEM) with 10% FBS/1% penicillin/streptomycin. Viruses were collected from clarified tissue culture medium and stored at -80°C until use (169). MCMV V70 strain was kindly provided by C. Biron, Brown University and propagated in SG as described previously (272). Mice were injected intraperitoneally (i.p.) with either DMEM (mock control), $1 \times 10^5$ PFU V70 or $1 \times 10^6$ PFU tissue culture-propagated MCMV. HSV-1 (KOS strain) was provided by Dr. Sandra Weller (University of Connecticut Health Center). Virus was propagated and tittered in Vero cells as previously described (313). Mice were inoculated via footpad injection with $2 \times 10^6$ PFU virus in DMEM. Tissues collected in DMEM were homogenized via sonication and added onto NIH 3T3 cells.

Virus plaques were counted on day 4 post infection. Infected cells were fixed with methanol and stained with Giemsa for plaque visualization.

*Antibodies*

For flow cytometry, antibodies (Abs) to CD16/CD32 (FcγRII/III; Clone 2.4G2), CD45 (Clone 30-F11), CD45.1 (Clone A20), CD45.2 (Clone 104), CD4 (Clone GK1.5), NK1.1 (Clone PK136), B220 (Clone RA3-6B2), CD3ε (Clone 17A2), CD3ε (Clone 145-2C11), CD8 (Clone 53-6.7), KLRG1 (Clone 2F1), CD127 (Clone SB/199), Ki67 (Clone SolA15), IFNγ (Clone XMG1.2), CD62L (MEL-14) were purchased from BD PharMingen; and CD3ε (Clone 17A2), CD44 (Clone IM7) were purchased from BioLegend; and Ly49H (Clone 3D10) was purchased from eBioscience.

*Statistical analysis*

Statistical analysis was performed by unpaired one-way or two-way ANOVA with Tukey analysis, using GraphPad Prism 7. $P \leq 0.05$ was considered significant.

## 3.6 Figures and Figures Legends

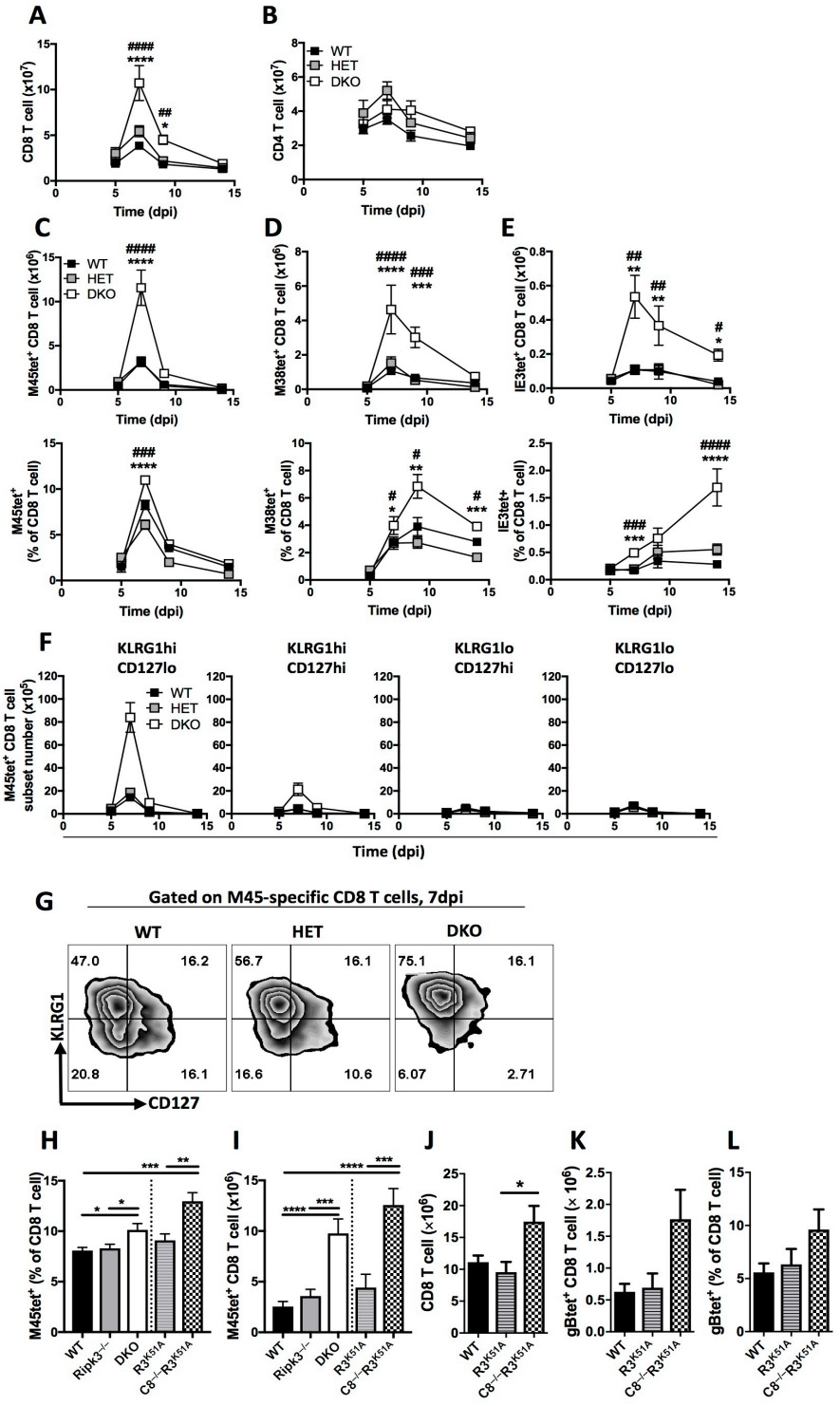


**Figure 0.1 Impact of Casp8 on antiviral T cell responses during the acute phase of virus infection.**

(**A – G**) Six- to eight-week-old WT, HET and DKO mice were inoculated intraperitoneally (i.p.) with $1 \times 10^6$ PFU/mouse MCMV K181-BAC strain per mouse. Spleens were processed on day 5, 7, 9 and 14 post infection and stained with tetramers and antibodies specific for the indicated cell-surface markers. Graphs comparing total mean numbers ± S.E.M. of CD8 (**A**) and CD4 (**B**) T cells. Levels of M45 (**C**), M38 (**D**) or IE3 (**E**) tetramer-positive CD8 T cells were shown as mean numbers ± S.E.M. (top panels) and frequencies ± S.E.M. (lower panels). (**F – G**) Graphs showing total mean numbers ± S.E.M. of different effector subsets following gating on M45tet$^+$ CD8 T cells on indicated days post infection (**F**). Representative zebra plots showing the percentages of indicated subsets following gating on M45tet$^+$ CD8 T cells at 7 dpi (**G**). Data represent at least two independent experiments using n = 5 mice per group. Significant differences between DKO and WT (*) or HET (#) mice are indicated as * or #, $p < 0.05$; ** or ##, $p < 0.01$; *** or ###, $p < 0.001$; **** or ####, $p < 0.0001$.

(**H – I**) WT, *Ripk3*$^{-/-}$, R3$^{K51A}$, DKO and C8$^{-/-}$R3$^{K51A}$ mice were infected as indicated in Fig. 1*A*. Splenocytes were analyzed at 7 dpi by flow cytometry. Bar graphs showing numbers (**H**) and percentages (**I**) of CD8 T cells specific to M45 tetramer. Data are present as mean numbers ± S.E.M., and represent two independent experiments using n = 5 mice per group.

(**J – L**) Mice were infected with $2 \times 10^6$ PFU/mouse HSV1 (KOS strain) via footpad inoculation route. Splenoctyes were analyzed at 7 dpi. Bar graphs showing total CD8 T cell numbers (**J**), as well as numbers (**K**) and percentages (**L**) of CD8 T cells specific to gB tetramer. Data are present as mean numbers ± S.E.M. and represent one experiment with n = 5 mice per group.

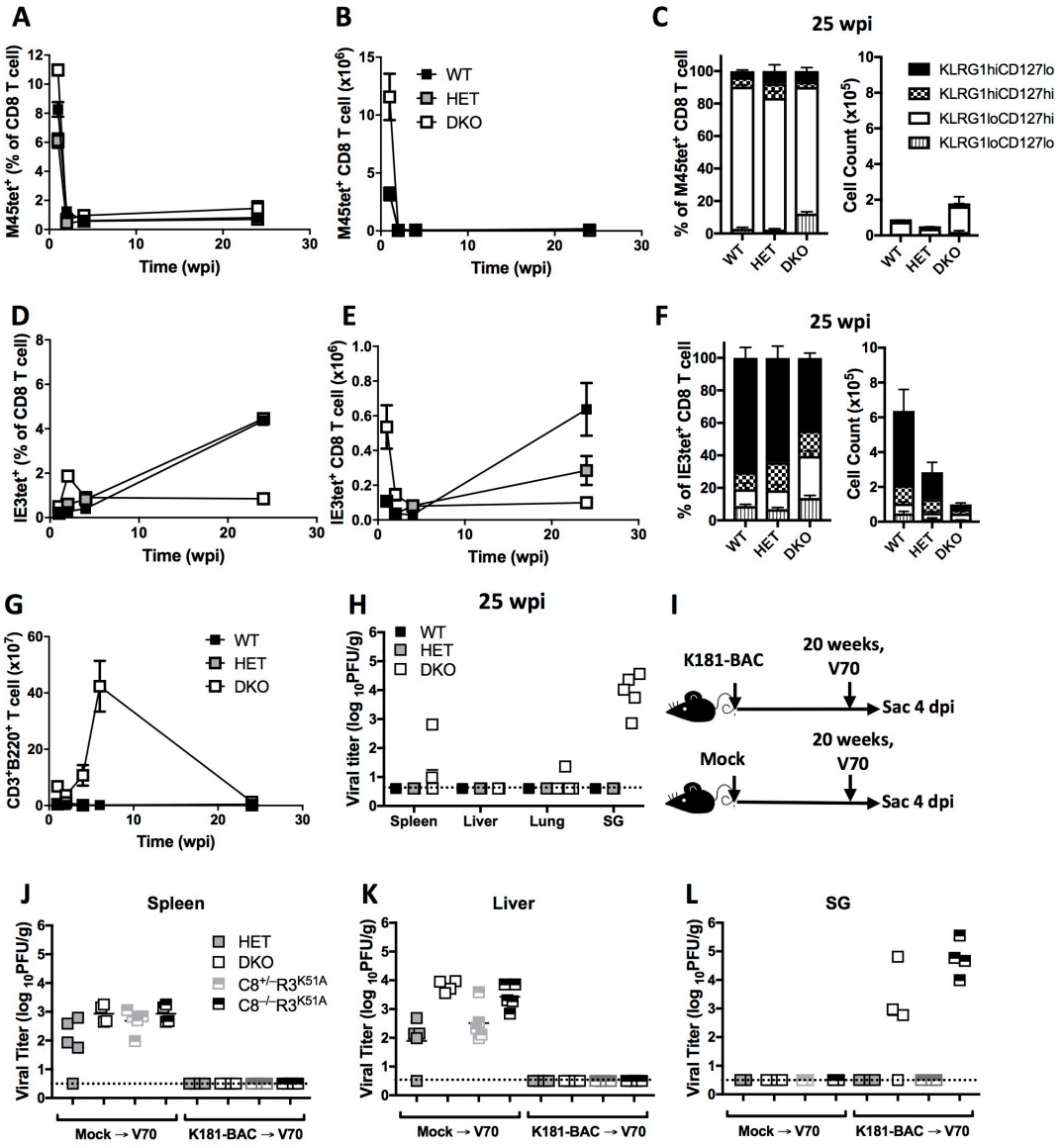


**Figure 0.2 Impact of Casp8 on antiviral T cell responses during long-term infection.**

(**A** – **H**) Comparing levels and phenotype of T cells from WT, HET and DKO mice infected with K181-BAC as described in Fig. 1. Graphs showing frequencies and numbers of splenic CD8 T cells positive for M45 (**A** and **B**) or IE3 (**D** and **E**) tetramer staining at 1, 2, 4 and 25 wpi. Bar graphs showing the proportions and numbers of KLRG1$^{hi}$CD127$^{lo}$, KLRG1$^{hi}$CD127$^{hi}$, KLRG1$^{lo}$CD127$^{hi}$ or KLRG1$^{lo}$CD127$^{hi}$ subsets within the M45- (**C**) or IE3- (**F**) specific CD8 T cells at 25 wpi. Horizontal dash line depicts limit of detection of the assay. Graph showing mean

numbers ± S.E.M of $B220^{+}CD3^{+}$ abnormal T cells in spleens on indicated wpi (**G**). Data were represented as means ± S.E.M. Spleen, liver, lung and SG titers at 25 wpi obtained by plaque assay (**H**). Data represent at least two independent experiments with n d SG titers at

(**I** – **L**) Mice at 20 wpi with K181-BAC or mocked treated were challenged with $1 \times 10^5$ V70 MCMV through i.p. inoculation route (**I**). Graphs showing spleen (**J**), liver (**K**) and SG (**L**) titers at 4 dpi. Dash line showing limit of detection of the plaque assay. Data represent one experiment with $n \geq 5$ per group.

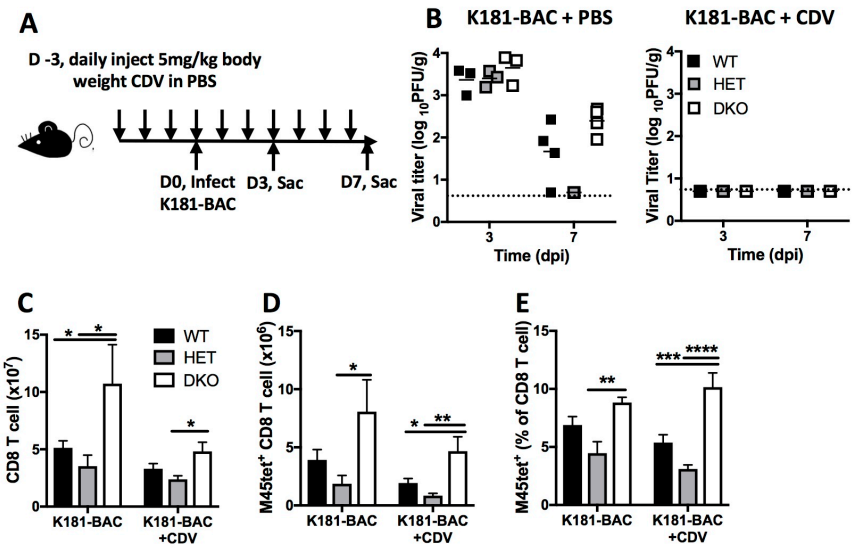


**Figure 0.3 Patterns of antiviral CD8 T cell responses when antigen levels are compromised.**

Mice were daily injected with 5 mg/kg CDV in PBS (or mock treated) via i.p. inoculation route, starting from 3 day prior to infection (**A**). Viral titers at 3 or 7 dpi in spleens of CDV or mock treated, K181-BAC infected mice obtained by plaque assay. Data represent two independent experiments with n ≥ 3 mice in each group. Dash line showing the limit of the detection (**B**).

(**C** – **E**) Bar graphs showing numbers of total CD8 T cells (**C**), as well as numbers (**D**) and percentages (**E**) of M45 tetramer-positive CD8 T cells at 7 dpi. Data are presents as mean ± S.E.M. and represent two independent experiments with n = 4 mice per group.

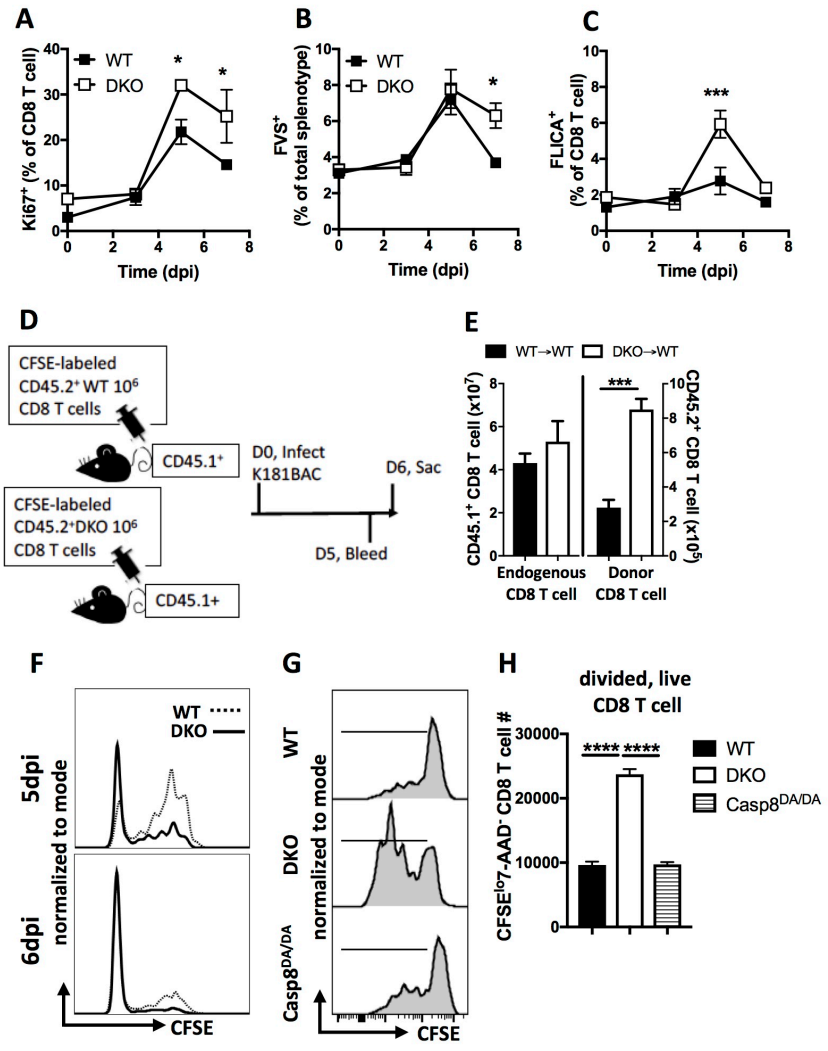


**Figure 0.4 Assessment of CD8 T cell proliferation and death.**

(**A – C**) Analysis of proliferation and death during the expansion phase following MCMV infection. Splenocytes from K181-BAC-infected WT and DKO mice at 0, 3, 5, 7 dpi were assessed. Graphs showing percentages ± S.E.M of $Ki67^+$ CD8 T cells (**A**). Frequencies ± S.E.M of $FVS^+$ dead cells in spleens of WT and DKO mice (**B**). Graphs showing percentages ± S.E.M of $FLICA^+$ CD8 T cells. $FVS^+$ dead cells were excluded from this analysis (**C**).

(**D – F**) Proliferation analysis using adoptive transfer. CFSE-labeled $CD45.2^+$ Splenocytes from WT or DKO mice that contained $1 \times 10^6$ total CD8 T cells were transferred into $CD45.1^+$ WT

recipients via i.v. inoculation route, followed with infected the next day (**D**). Bar graphs comparing numbers of $CD45.1^+$ endogenous CD8 T cells and $CD45.2^+$ donor CD8 T cells at 6 dpi (**E**). Representative histograms comparing CFSE distribution of transferred CD8 T cells on days 5 and 6 post infection (**F**). Data are present as mean ± S.E.M. and represent two independent experiments with n = 4 mice per group.

(**G – H**) Assessment of proliferation and signaling mechanism following TCR stimulation. CFSE dilution analysis of purified splenic $CD44^{lo}$CD8 T cells after stimulation of anti-CD3 and CD28 for 72 h. Representative plots comparing CFSE division of CD8 T cells from indicated genotypes (**G**). Bar graphs showing the mean numbers ± S.E.M. of $CFSE^{lo}$7-$AAD^-$ cells recovered in culture following stimulation (**H**).

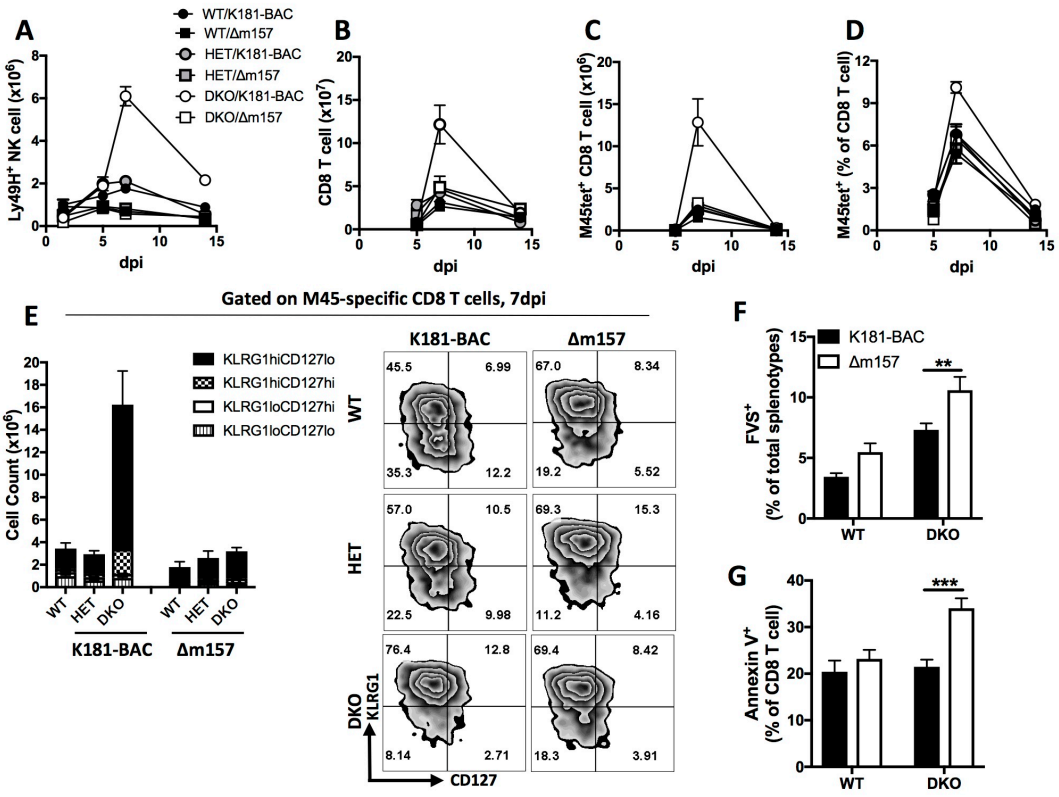


**Figure 0.5 Impact of m157-driven NK cells on antiviral CD8 T cell responses.**

WT, HET and DKO mice were i.p. inoculated with $1\times 10^6$ PFU/mouse K181-BAC or Δm157 virus. Graph showing the numbers of $Ly49H^+$ NK cells in spleens on days 1.5, 5, 7 and 14 post infection (**A**). (**B – E**) Expansion, contraction and phenotype of splenic CD8 T cell responding to infection. Graphs showing numbers of total CD8 T cells (**B**) as well as numbers (**C**) percentages (**D**) of M45-specific cells on day 5, 7 and 14 post infection. Data were presents as mean ± S.E.M.. Bar graphs comparing numbers ± S.E.M. of different effector subsets (**E**, left panel) and representative zebra plots showing KLRG1 and CD127 expression (**E**, right panel) following gating on M45-specific CD8 T cells at 7 dpi.

(**F – G**) Cell death analysis on day 7 post infection of K181-BAC or Δm157 virus. Bar graphs comparing frequencies of $FVS^+$ dead cells in spleens of WT and DKO mice (**F**). Bar graphs comparing percentages of Annexin $V^+$ cells within CD8 T cells. $FVS^+$ dead cells were excluded

from this analysis (**G**). Data are present as mean ± S.E.M. and represent two independent experiments with $n \geq 4$ mice per group.

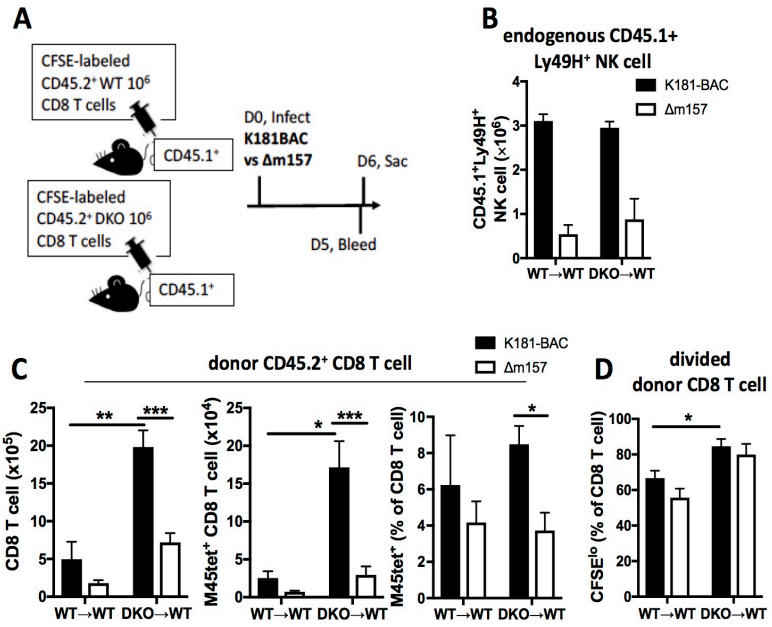


**Figure 0.6 Impact of WT m157-driven NK cells on antiviral CD8 T cell responses.**

CFSE-labeled total splenocytes containing $1\times 10^6$ total from naive WT ($CD45.2^+$) or DKO mice ($CD45.2^+$) mice were transferred into $CD45.1^+$ WT mice, followed with infection of $1\times 10^6$ PFU/mouse K181-BAC or Δm157 derivative the next day. Splenocytes were analyzed at 6 dpi (**A**). Numbers of endogenous $CD45.1^+$ $Ly49H^+$ NK cells in the recipients (**B**). Bar graphs comparing numbers of donor $CD45.2^+$ total CD8 T cells, and numbers as well as percentages of $CD45.2^+$ M45 specific cells (**C**). Bar graphs showing the percentages of $CFSE^{lo}$ divided cells within the transferred donor $CD45.2^+$ CD8 T cells in the recipients (**D**).

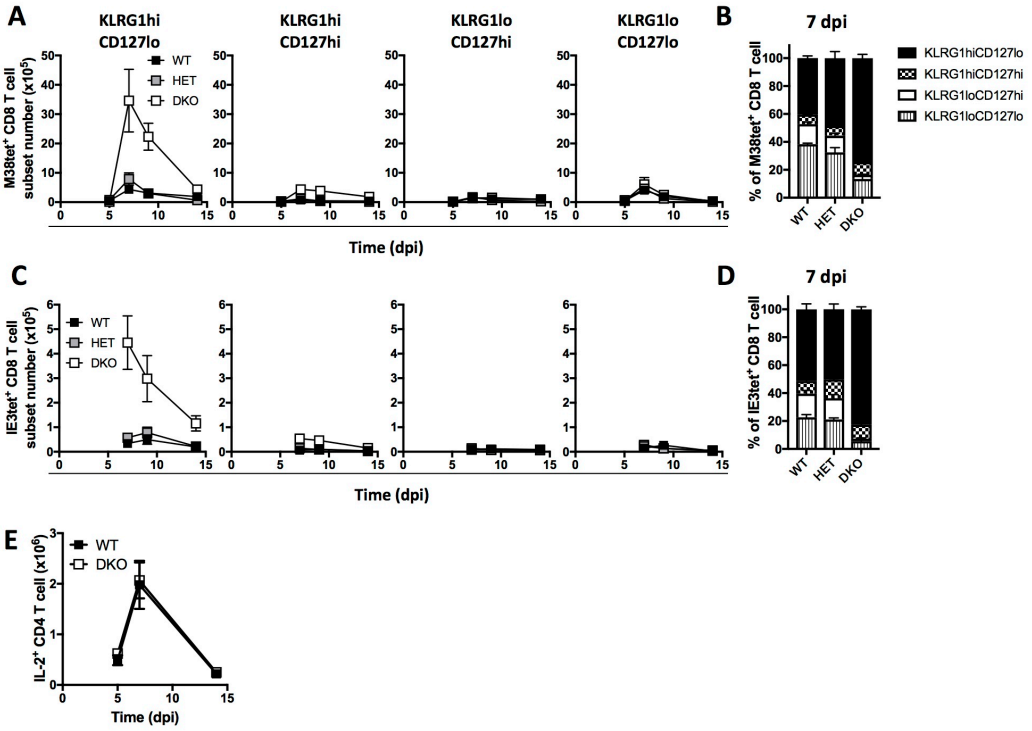


**Supplemental Figure 0.1 T cell responses during the acute phase of virus infection.**

Splenotypes were analyzed on indicated days post infection of K181-BAC. Graphs showing the numbers ± S.E.M. (A and C) and the proportions ± S.E.M. (B and D) of KLRG1$^{hi}$CD127$^{lo}$, KLRG1$^{hi}$CD127$^{hi}$, KLRG1$^{lo}$CD127$^{hi}$ or KLRG1$^{lo}$CD127$^{hi}$ subsets following gating on CD8 T cells positive to M38 (A and B) or IE3 tetramers (C and D). Graphs showing the mean percentages ± S.E.M of CD4 T cells that were IL-2$^{+}$ following stimulation of anti-CD3/CD28 for 5 h (E). Data represent at least two independent experiments with n = 5 mice per group.

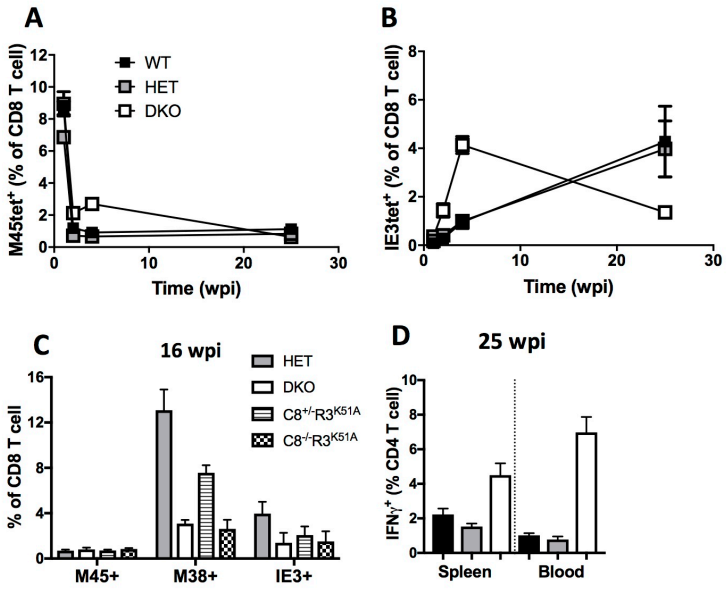


**Supplemental Figure 0.2 T cell responses during long-term infection.**

Conventional and inflationary CD8 T cell response in blood circulation on weeks 1, 2, 4, 25 post infection of K181-BAC, shown as percentages of M45- (A) and IE3- (B) specific subsets within the total CD8 T cell population. Bar graphs showing the percentages of blood circulating CD8 T cells specific to M45, M38 and IE3 tetramer staining at 16 wpi (C). Bar graphs showing mean percentages ± S.E.M of CD4 T cells that were IFN$\gamma^+$ from spleen or blood following stimulation of anti-CD3/CD28 for 5 h (D).Data are present as mean ± S.E.M. and represent three independent experiments with n = 5 mice per group.

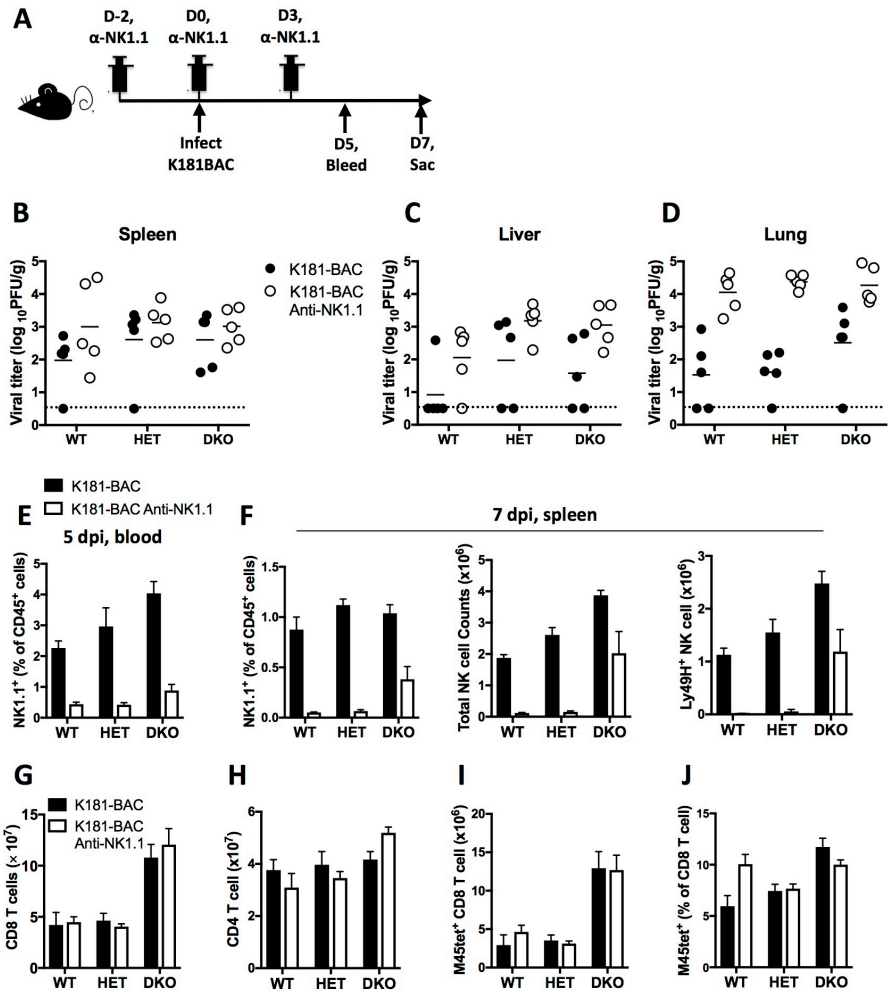


**Supplemental Figure 0.3. Impact of NK cell on antiviral CD8 T cell responses.**

Diagram showing experiment design (A). Viral titers at 7 dpi in spleen (B), liver (C) and lung (D) from anti-NK1.1 Ab treated and untreated mice. Dash lines showing limit of detection. (E – F) Analysis of NK cell levels in mice with or without the depletion Ab treatment. Bar graphs showing the percentages of $CD45^+CD3^-B220^-NK1.1^+$ total NK cells within the $CD45^+$ total leukocyte population in blood at 5 dpi (E, left panel) and in spleen at 7 dpi (E, right panel). Bar graphs showing the numbers of total and $Ly49H^+$ NK cells in spleen at 7 dpi (F). (G – J) Numbers of total CD8 (G) and CD4 (H) T cells, as well as percentages (I) and numbers (J) of CD8 T cells positive

for M45 tetramer staining. Data were present as mean ± S.E.M. and represent one experiment with n = 5 mice in each group.

# Chapter 4

Caspase-8 Restricts Ly49H$^+$ NK cell expansion following Murine Cytomegalovirus Infection

Yanjun Feng, Lisa Daley-Bauer, Marc Potempa, Linda Roback, Lewis Lanier, Edward Mocarski.

Data not generated by the Ph.D. candidate is indicated in the figure legends.

## 4.1 Abstract

NK cells are a group of innate immune cells essential for early viral control. NK cells have recently been demonstrated to possess adaptive immune cell features. Ligation of Ly49H activating receptor by MCMV viral antigen m157 drives the Ly49H$^+$ NK cells to undergo robust activation, a clonal expansion-like response, and subsequent memory formation. This process must be tightly controlled for the generation of an optimal antiviral immune response. As the central mediator of extrinsic death, caspase (Casp)8 drives apoptosis, keeps necroptosis in check, and regulates death-independent signaling transduction. A previous study has shown that combined elimination of Casp8 and RIPK3 leads to an amplified Ly49H$^+$ NK cells response when compared with *Casp8*$^{+/-}$ *Ripk3*$^{-/-}$ littermates and WT C57BL/6 mice. Here, we invoke an NK cell-autonomous role of Casp8 in restricting expansion during the acute phase of MCMV infection that is dispensable for memory development. Strikingly, total and Ly49H$^+$ NK cell populations are completely ablated once RIPK1 is eliminated together with Casp8 and RIPK3 following MCMV infection, even though this NK cell subset develops normal independent of RIPK1. Thus, in response to MCMV infection, Casp8 normally regulates the magnitude of adaptive NK cell responses, while RIPK1 function promotes overall NK cell numbers.

## 4.2 Introduction

NK cells are a population of innate lymphocytes that play an important role in early viral control. The NK antiviral response gain rapid control due to their capacity for a fast activation and a robust cytotoxic function (80). This fast activation, occurs without the requirement of a priming process, but instead depends on a signal transduced through the germline-encoded activating receptors that overrides the inhibitory signal induced by suppressive receptors (80). Although NK cells were initially defined as innate immune cells, several lines of evidence have indicated they also possess adaptive immune cell features following virus infection, including expansion, contraction, memory formation and a heightened recall responses (79). MCMV is a well-established model used to investigate antiviral NK cells. In C57BL/6 mice, ligation of the MCMV-encoded MHC class I like glycoprotein m157 to the Ly49H activating receptor triggers a robust proliferation of this NK cell subset and strong cytotoxic effector responses (94) that confer the early control of the virus (1, 300). Following the peak of the expansion, the majority of $Ly49H^+$ NK cells contract, leaving a small population that differentiates into memory cells (95). These adaptive immune features of NK cells have been described in human. HCMV seropositive individuals have 5% to 50% of the total NK cells as $CD94^+NKG2C^+$ NK cells, comparing to levels around 1% in HCMV serological negative individuals (99, 100). This feature is reminiscent of immune memory wherein antigen-specific cells increase to readily detectable levels, contrasting to their low numbers prior to infection. Expansion and persistence of this population has been reported in immunocompromised transplantation recipients (101). Thus, studies in mice using MCMV offer valuable insights of NK cell adaptive immune features and gain knowledge that can be applied to HCMV.

In addition to the Ly49H receptor, NK cell expansion is regulated by proinflammatory cytokines and co-stimulatory receptors. IL-12, Type I IFNs, IL-18 and IL-33 all play critical roles in supporting NK cell proliferation, cytotoxic function and memory formation (301). IL-12-triggered, STAT4-dependent signal transduction results in the upregulation of MyD88, which further induces IL-18 receptor upregulation for promoting NK cell proliferation (112). Type I IFN triggers the expression of transcription factors, including STAT1, STAT2, IRF8, IRF9, which are necessary to support the NK cell survival during the expansion phase (109-111). In addition, both IL-12 and type I IFN are important for NK cell cytotoxic function and IFNγ production (5, 108). NKG2D activation enhances Ly49H$^+$ NK expansion, although the signal through NKG2D by itself is not sufficient for NK cell proliferation (107). These data highlight the similarities between NK and T cells - both require a series of collaborating signals to achieve an optimal antiviral response including, signal one (TCR or Ly49H receptor) for proliferation initiation, and signal two (co-stimulation) and signal three (cytokines) (79). These factors combine to determine the levels, differentiation programs and longevity of NK cells through a balance of proliferation and death.

Lymphocyte death can be regulated by the intrinsic pathway or the extrinsic pathway (125). Upon virus infection, activation of the pro-apoptotic protein Bim initiates intrinsic apoptosis that drives antiviral T cell contraction (124, 202). A recent study has shown that elimination of Bim in NK cell population delays Ly49H$^+$ NK cell contraction and impairs memory pool generation (207, 314). The data suggest the important role of the intrinsic pathway in the shutdown of the acute NK cell responses and promoting memory differentiation. Extrinsic cell death is activated by cell surface TNF receptor superfamily DRs (including TNFR1, Fas, TRAIL), which trigger the cytosolic DISC formation. Several outcomes can occur upon DISC formation - Casp3-dependent apoptosis, RIPK3-mediated necroptosis when Casp8 is inhibited, and death-independent signaling

transduction (125). Casp8 was initially defined as a regulator that supports NK cell activation because cells carrying the enzymatic mutated Casp8 displayed defective NF-κB signaling following CD244 (or 2B4) and CD16 stimulation (164, 165). Later studies have indicated that this death-independent function of Casp8 has been confounded by its vital role in suppressing RIPK3-mediated necroptosis. Our recent study of DKO mice that lack Casp8 and RIPK3 function shows an enhanced Ly49H$^+$ NK cell accumulation compared to HET and WT controls during the acute phase of MCMV infection (233), suggesting an unexpected role of Casp8 in restricting Ly49H$^+$ NK cell expansion in a necroptosis-deficient background. However, the interpretation of these results are complicated by other environmental dysregulation in these mice (233), including the abnormal T cell accumulation and enhanced DCs numbers during MCMV infection (233).

In this study, we show that Casp8 plays a critical role in restricting Ly49H$^+$ NK cell accumulation as well as effector differentiation but is dispensable for memory NK cell development. While the previous study has shown that Ly49H$^+$ NK cell hyperaccumulation in DKO mice requires m157 MCMV antigen (Chapter 3), data from the current work demonstrates that this enhancement requires active virus replication. Further, using a co-transfer system, we demonstrate that Casp8 has a cell-autonomous function in restricting NK cell expansion. Strikingly, RIPK1 elimination together with Casp8 and RIPK3 completely ablates NK cell responses, even though *Ripk1*$^{-/-}$*Casp8*$^{-/-}$*Ripk3*$^{-/-}$ mice exhibit normal NK cell development during homeostasis (150). Finally, DKO NK cells have no defect in memory development, supported by the normal percentages of CD11b$^{lo}$CD27$^+$ and higher percentages of Ly6C$^+$ and KLRG1$^{hi}$ when compared with WT NK cells.

## 4.3 Results

*DKO NK cells hyperaccumulate in response MCMV infection but contract normally*

Previous studies have shown the enhanced accumulation of DKO Ly49H$^+$ NK cells in response to MCMV infection (233). To further investigate whether this enhancement is Ly49H$^+$ NK cell-specific, kinetics of Ly49H$^+$ and Ly49H$^-$ NK cells were analyzed. Splenocytes from WT, HET, and DKO mice were collected on indicated days post infection of MCMV K181-BAC and were assessed for total numbers and phenotype of NK cells. Total NK cell numbers were comparable on days 1.5, 3 and 5 post infection (Fig.4.1*A*), expanded to peak levels at 7 dpi that were higher in DKO mice than HET and WT controls, and contracted through days 9 and 14 post infection. The data suggest that Casp8 restricts NK cell numbers during the expansion phase but is dispensable for cell contraction. The MCMV-driven NK cell expansion is specifically attributable to the subset expressing Ly49H activating receptor (94). The numbers of this subset in DKO mice increased to significantly higher levels by 7 dpi as expected (233) (Fig. 4.1*B*), whereas the numbers of Ly49H$^-$ NK cells stayed comparable throughout the observed period (Fig. 4.1*C*). Consistent with the cell count analysis, the percentages of Ly49H$^+$ NK cells in DKO mice were significantly higher at 7 dpi compared to WT and HET controls, while the levels were comparable at 1.5 dpi independent of genotype (Fig. 4.1*D*). Upon infection, all three genotypes exhibited evident upregulation of KLRG1 on Ly49H$^+$ NK cells, suggesting NK cell maturation is independent of Casp8 or RIPK3 (Fig. 4.1*E*). However, a higher proportion of DKO Ly49H$^+$ NK cells upregulated KLRG1 at 7 dpi (Fig. 4.1*E*), a phenotype reminiscent of DKO CD8 T cells (Chapter 3, Fig. 3.1*F*). Taken together, Casp8 restricts Ly49H$^+$ NK cell accumulation following MCMV infection but plays no role in the contraction phase. This regulation of Casp8 is Ly49H$^+$ cell-specific.

*DKO NK cell hyperaccumulation is dependent on MCMV replication levels*

Next, we sought to investigate whether this phenotype of NK cells is dependent on MCMV replication levels. Infected mice were treated with CDV to compromise virus replication. NK cell responses were investigated at 7 dpi. CDV effectively suppressed viral load to undetectable levels (see Chapter 4, Fig. 4.3). This compromised antigen load reversed the heightened numbers of total DKO NK cell numbers to control levels (Fig. 4.2*A*). Interestingly, the numbers of Ly49H$^+$ cells in DKO mice trended lower than in WT and HET controls upon CDV treatment (Fig. 4.2*B*), in accordance with the reduced percentages (Fig. 4.2*C*). The decrease in virus replication compromised the extent of NK cell differentiation, indicated by the reduced percentages of KLRG1$^{hi}$ Ly49H$^+$ NK cells in CDV-treated mice when compared with non-treated mice, regardless of genotype (Fig. 4.2*D*). Notably, independent of CDV treatment, DKO mice exhibited higher percentages of KLRG1$^{hi}$ Ly49H$^+$ NK cells than control mice (Fig. 4.2*D*). These data suggest that the contribution of Casp8 to Ly49H$^+$ NK cell numbers is dependent on active virus infection. In contrast, Casp8 suppresses the cell differentiation independent of antigen load.

*Casp8 has a cell-autonomous impact on NK cell accumulation*

To further investigate whether Casp8 regulates NK cell through a cell-autonomous or cell-extrinsic mechanism, we co-transferred equal numbers of CD45.1$^+$ WT and CD45.2$^+$ DKO NK cells into Ly49H-deficient mice. Expansion and contraction of Ly49H$^+$ NK cells were measured in peripheral blood following MCMV infection. DKO cells exhibited increased expansion with a peak that was higher than WT controls (Fig. 4.3*A*). Following the peak of the NK cell response, Ly49H$^+$ NK cells from both genotypes contracted between days 14 and 28 post infection. Consistent with the enhanced accumulation, DKO cells made up the majority of total Ly49H$^+$

population throughout the infection (Fig. 4.3*B)*. Taken together, Casp8 has an NK cell-autonomous impact on restricting expansion but is dispensable for cell contraction.

*Contribution of Casp8 to NK cell proliferation and death.*

Lymphocyte numbers following virus infection are dictated by the balance between proliferation and death. We sought to investigate whether DKO NK cell hyperaccumulation is due to an increase in proliferation or a deficiency of death. Fas is an important DR that triggers Casp8-dependent extrinsic pathway (124). Both Ly49H$^+$ (Fig. 4.4*A*) and Ly49H$^-$ (Fig. 4.4*B*) NK cells upregulated Fas on the cell surface following infection, regardless of genotype. This increase was more evident on DKO Ly49H$^+$ and Ly49H$^-$ NK cells compared to WT controls on days 5 and 7 post infection. The Fas-Casp8 signaling axis regulates T cell proliferation and death upon TCR stimulation. Given the data from Chapter 3 showing that T cell hyperaccumulation is attributable to an increase in proliferation, we sought to investigate if enhanced Fas expression affects the NK cell proliferation when Casp8 is eliminated. Ki67 was utilized to measure dividing cells through day 7 post infection (298), the period of Ly49H$^+$ NK cell expansion. Overall, WT and DKO Ly49H$^+$ (Fig. 4.4*C*) and Ly49H$^-$ (Fig. 4.4*D*) NK cells exhibit comparable proliferation capacities throughout the observed period. Interestingly, while the proportions of Ki67$^+$ cells within the Ly49H$^-$ population dropped by 7 dpi in WT mice, the levels were sustained in DKO mice. These data show that Ly49H$^+$ NK cell hyperaccumulation in DKO mice is not due an increase in proliferation. FLICA was used to measure active Casp3, the apoptotic executioner downstream of Casp8 (125). Strikingly, the percentages of FLICA$^+$ cells within the Ly49H$^+$ population (Fig. 4.4*E*) were significantly lower than the percentages within the Ly49H$^-$ population (Fig. 4.4*F*), regardless of genotype. This suggests that Ly49H signal is important for NK cell survival during the expansion phase following MCMV infection. Curiously, DKO mice displayed higher percentages

of FLICA$^{+}$Ly49H$^{-}$ NK cells than WT controls throughout the observed period (Fig. 4.4*D*), most likely a consequence of Bim-dependent intrinsic death (124, 207). Taken together, DKO mice did not exhibit any death deficit or enhanced proliferation capacity that could account for the Ly49H$^{+}$ NK cell hyperaccumulation. Further analysis methods, including CFSE cell division measurement should be performed to confirm and extend the observation.

To investigate whether Ly49H$^{+}$ NK cell hyperaccumulation occurs with another necroptosis incompetent and Casp8-deficient strain, NK cells in C8$^{-/-}$R3$^{K51A}$ mice together with DKO and WT mice were analyzed at 7 dpi. Both Casp8-deficient mice developed higher numbers of total NK cells than the WT controls, ascribed to the enhanced Ly49H$^{+}$ subset numbers. RIPK1 is a pro-necroptotic kinase involved in regulating apoptosis and pro-survival signaling transduction (125). To understand whether RIPK1 contributes Ly49H$^{+}$ NK cell responses, *Ripk1*$^{-/-}$*Casp8*$^{-/-}$ *Ripk3*$^{-/-}$ mice were infected, and splenocytes were analyzed at 7 dpi. Interestingly, both the total and Ly49H$^{+}$ NK cell responses (Fig. 4.5*A-D*) were severely impaired in mice lacking RIPK1 at 7 dpi, even though these mice exhibit normal NK cell development during homeostasis (150). Whether the defect is an NK cell-intrinsic dysregulation or is due to environmental alteration dependent on RIPK1 remains to be clarified. Taken together, we demonstrate that Casp8 generally restricts NK cell accumulation during MCMV infection. Additionally, RIPK1 is required for supporting the NK cell responses.

*DKO mice exhibited normal memory NK development during long-term MCMV infection.*

Cytokines together with m157-driven Ly49H receptor signaling results in memory NK cell formation after the phase of contraction (301). Compared to naïve NK cells, these memory cells express high levels of markers related to differentiation and maturation (95). We sought to investigate whether the heightened acute response of Casp8-deficient NK cells affects memory

formation. NK cell numbers and memory cell differentiation markers were assessed in WT, DKO and *C8*$^{-/-}$*R3*$^{K51A}$ mice at 8 wpi. Both DKO and *C8*$^{-/-}$*R3*$^{K51A}$ mice exhibited lower numbers and percentages of Ly49H$^{+}$ NK cells than WT controls (Fig. 4.6*A-B*), despite the hyper-response during the acute phase of infection. Enhanced percentages of KLRG1hi Ly49H$^{+}$ NK cells were observed in the two Casp8-deficient genotypes when compared with WT controls (Fig. 4.6*C*), while the percentages of Ly6C$^{+}$ cells were comparable regardless of genotype (Fig. 4.6*D*), suggesting that there was no evident defect on the memory NK cell development despite Casp8-deficiency. Consistent with this observation, over 90% of the cells had a mature NK cell phenotype of CD27$^{lo}$CD11b$^{hi}$ in all three genotypes (Fig. 4.6*E*). Thus, Casp8 is dispensable for memory NK cell formation.

## 4.4 Discussion

Recent studies have highlighted the adaptive immune features of NK cells in mouse, human, and primate (79, 315). Like the virus-induced CD8 T cell response, signals through Ly49H receptor, cytokines and co-stimulatory molecules together induce NK cell proliferation, differentiation and memory development. However, the contribution of cell death pathway to NK cell responses remains to be fully explored (314). In the current study, we show that Casp8, a critical mediator of extrinsic death pathway (249), restricts NK cell expansion during the acute phase of MCMV infection but is dispensable for memory NK cell formation.

The magnitude of virus-specific lymphocyte responses are regulated by two apoptotic pathways – intrinsic and extrinsic death pathways (124). As a critical pro-apoptotic member that drives T cell contraction (115, 197), Bim also plays an important role in controlling Ly49H$^+$ NK cell numbers during the phase of expansion and memory development (207). The failure of NK cell contraction leads to a larger memory pool with a less mature phenotype. This work highlights that eliminating immature cells during the contraction helps to improve memory cell differentiation. Little work has been done to study the contribution of extrinsic pathway. Using DKO mice that have both the extrinsic apoptosis and necroptosis ablated (174), the current study shows an amplified Ly49H$^+$ NK cell response that peaks higher but undergoes normal contraction, with a pattern of enhanced terminal differentiation. However, this enhanced response does not lead to better viral control (233), again indicating the importance of controlling cell numbers to improve efficacy. Despite the increase in cell numbers, Ly49H$^+$ NK cells in DKO mice do not exhibit increased proliferation or death deficits. More experiments need to be conducted in the future for analysis of these two parameters.

Elimination of Bim or Casp8 together with RIPK3 enhances the magnitude of Ly49H$^+$ NK cell responses (207). However, while Bim-deficiency impairs memory NK cell development (207), memory cells in DKO mice do not show any phenotypic abnormality related to memory development defect. Perhaps this discrepancy can be ascribed to certain memory precursor NK cells that are regulated by Bim but not Casp8. In line with this hypothesis, Bim-elimination in T cells affects both terminal differentiated effector subsets and memory precursors during the acute phase of virus infection (201), whereas Casp8-deficiency (together with RIPK3) only affects the terminal differentiated effector subsets without clear impact on the memory precursors (Chapter 3). In addition, this discrepancy of memory NK cell formation may be attributable to a death-independent role of Casp8 in regulating cell differentiation. Casp8 has been shown to crosstalk with Akt-mTOR pathway (316), which is important for NK cell activation (317, 318). Disruption of Casp8 may interfere with NK or other adaptive immune cell differentiation through the Akt-mTOR signaling axis.

The function of Casp8 in NK cells was initially described in patients with a Casp8 catalytic mutant (164, 165). NK cells from these individuals have a defect in NF-κB activation following CD16 or CD244 ligation. Later studies have clarified  attributable to the unleashed RIPK3-mediated necroptosis due to Casp8-deficiency (166, 167, 176). The dual elimination of Casp8 together with RIPK3 rescues this defect and leads to enhanced Ly49H$^+$ NK cells response upon MCMV infection. These data support that a Casp8 function in NK cells beyond necroptosis suppression. Further experiments are needed to explore the precise spatial and temporal mechanism of Casp8 in the regulation of NK cell activation. Similar to TCR, Ly49H receptor activation triggers the formation of the CARMA-MALT1-BCL10 complex that subsequently drives NF-κB activation (83). Studies of T cells have shown that this complex recruits FADD and

Casp8 through the DD interactions between FADD and MALT1 (83, 165, 232). Given the similarity between TCR- and Ly49H - initiated pathways, a complex may form directly that is associated with Ly49H. Another hypothesis is that Casp8 locates downstream of DRs, which act as co-stimulatory receptors (234) to regulate Ly49H signaling transduction.

## 4.5 Materials and Methods

*Mice, viruses and experimental infection*

DKO (174) and $C8^{-/-}R3^{K51A}$ (148) mice were generated as described previously and backcrossed to be > 97% C57BL/6 background. DKO and HET littermates were generated from mating DKO and HET mice. *Ripk1*$^{-/-}$*Casp8*$^{-/-}$*Ripk3*$^{-/-}$ mice were generated as described previously (150). C57BL/6 WT mice were from The Jackson Laboratory and maintained at Emory University Division of Animal Resources, and experimental procedures were conducted in accordance with the National Institutes of Health and Emory University Institutional Animal Care and Use Committee guidelines. K181-BAC virus strain was propagated in NIH3T3 fibroblasts. The cell culture medium was purified and concentrated for virus collection. The virus was stored at -80 °C until use. K181-BAC-derived Δm157 was kindly provided by C. Biron (Brown University) and propagated the same way as K181-BAC strain. Mice were i.p. inoculated with $1 \times 10^6$ PFU virus per mouse.

*Plaque assay*

Homogenized tissue in DMEM medium were overlaid on NIH3T3 cells plated in 6-well plates. On day 4 post infection, cells were fixed with methanol and stained with Giemsa for visualizing plaques.

*Abs*

For flow cytometry, Abs to CD16/CD32 (FcγRII/III; Clone 2.4G2), CD45 (Clone 30-F11), CD45.1 (Clone A20), CD45.2 (Clone 104), CD11b (Clone M1/70), NK1.1 (Clone PK136), B220 (Clone RA3-6B2), CD3ε (Clone 17A2), CD3ε (Clone 145-2C11), CD8 (Clone 53-6.7), KLRG1 (Clone 2F1), Ki67 (Clone SolA15) were from BD PharMingen; and CD3ε (Clone 17A2) were

from BioLegend; and Ly49H (Clone 3D10) was from eBioscience. For FLICA or Annexin V analysis, splenocytes harvested from mice were stained with FLICA (BD Bioscience) or Annexin V (BD Bioscience).

*NK cell adoptive transfer*

Equal numbers ($1 \times 10^6$) of purified NK cells from naïve $CD45.1^+$ WT or $CD45.2^+$ DKO mice were mixed (1:1) and adoptively transfer through the intravenous route into Ly49H-deficient recipients on the day before MCMV infection (95).

*Flow cytometry*

Spleens were harvested from euthanized mice, and were mashed through metal sieves for organ disruption. Cells mixture were then incubated with red blood cell lysis buffer and then passed through a 100 mm strainer. In all experiments, $2 \times 10^6$ viable cells, as determined by on a hemacytometer by trypan blue exclusion, were stained with antibodies specific for surface and intracellular proteins and were prepared for detection by flow cytometer (BD LSRII cytometer and FACSDiva Software; BD Biosciences). For Ki67 detection, splenocytes were stained directly *ex vivo*, with antibodies for detection of surface markers and intracellular Ki67 protein. Data were analyzed with FlowJo (TreeStar), and graphed with Prism 7 (GraphPad).

## 4.6 Figures and Figure Legends

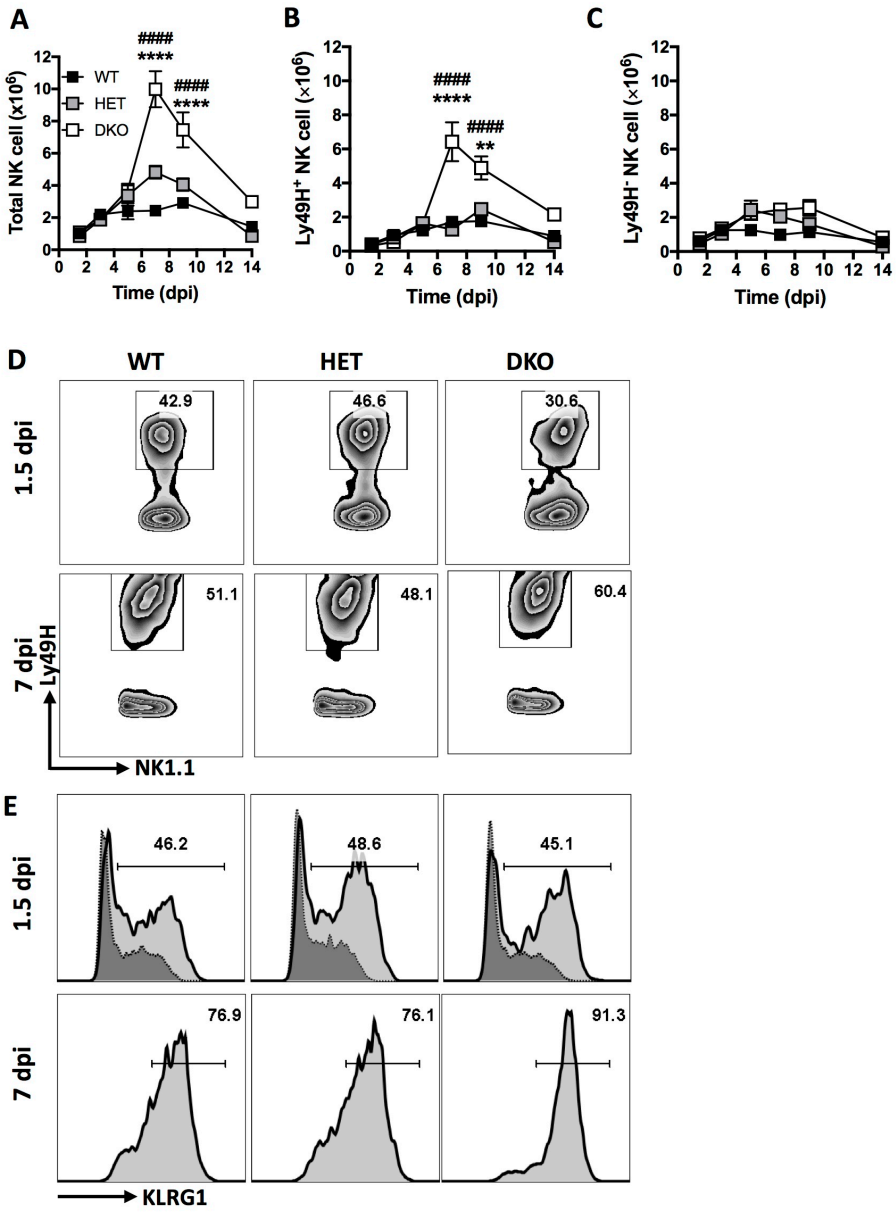


**Figure 0.1 NK cell expansion, contraction, and differentiation during the acute phase of MCMV infection.**

Six- to eight-week-old WT, HET, and DKO mice were i.p. inoculated with $1\times 10^6$ PFU/mouse MCMV K181-BAC strain per mouse. Spleens were processed on day 1.5, 3, 5, 7, 9 and 14 post infection and stained with antibodies specific for the indicated cell-surface markers. Splenic

$CD45^+B220^-CD3^-NK1.1^+$ NK cells were gated to identify $Ly49H^+$ and $Ly49H^-$ NK cells. Graphs comparing numbers of total (**A**), $Ly49H^+$ (**B**), and $L49H^-$ (**C**) NK cells. Data are present as mean numbers ± S.E.M.. Representative flow plots comparing the frequencies of $Ly49H^+$ subset out of total NK cells (**D**). Representative histograms showing the frequencies of $Ly49H^+$ NK cells expressing KLRG1 (**E**). Data represent at least two independent experiments using n = 5 mice per group. Significant differences between DKO and WT (*) or HET (#) mice are indicated as **, $p < 0.01$; *** or ###, $p < 0.001$; **** or ####, $p < 0.0001$.

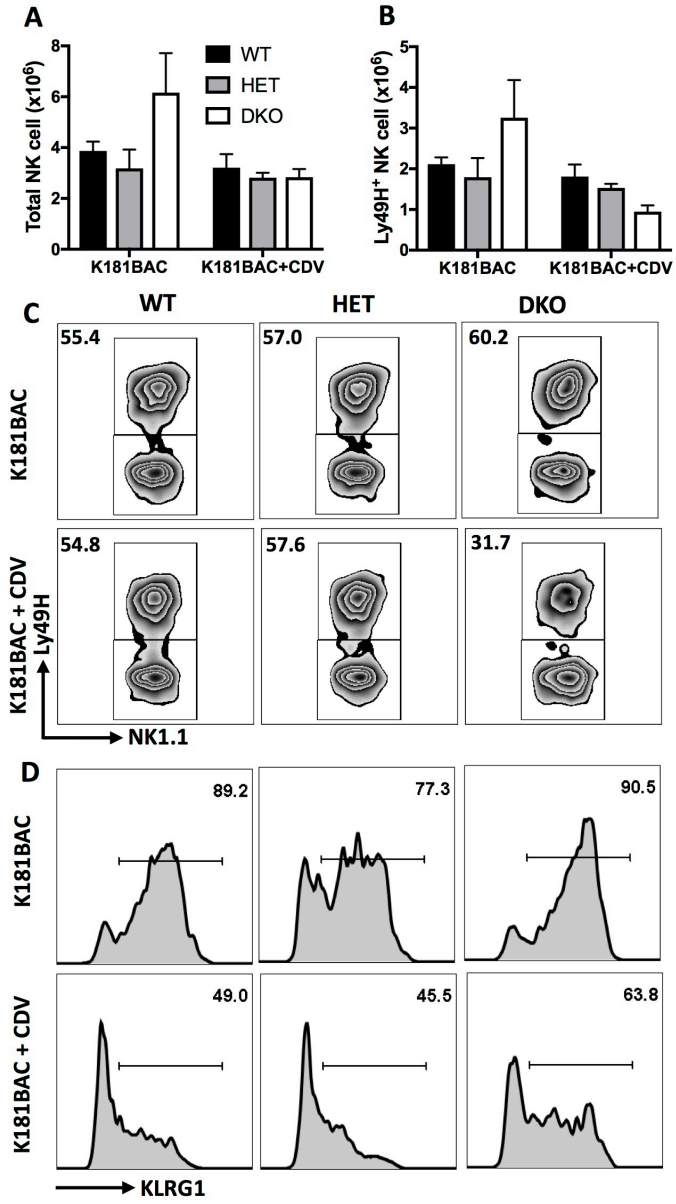


**Figure 0.2 Patterns of NK cell responses when antigen levels were compromised**.

Mice were i.p. inoculated with 5 mg/kg/day CDV in PBS, starting from 3 day prior to infection. All groups were sacrificed and splenocytes were analyzed at 7 dpi. (A – B) Bar graphs comparing the numbers of total (A) and Ly49H$^+$ (B) NK cells. Data are present as mean ± S.E.M. Representative flow plots showing the percentages of Ly49H$^+$ cells within the total NK population

(C). Representative histograms showing the percentages Ly49H$^{+}$ NK cells expressing KLRG1 (D). Data represent two independent experiments with n = 4 mice per group.

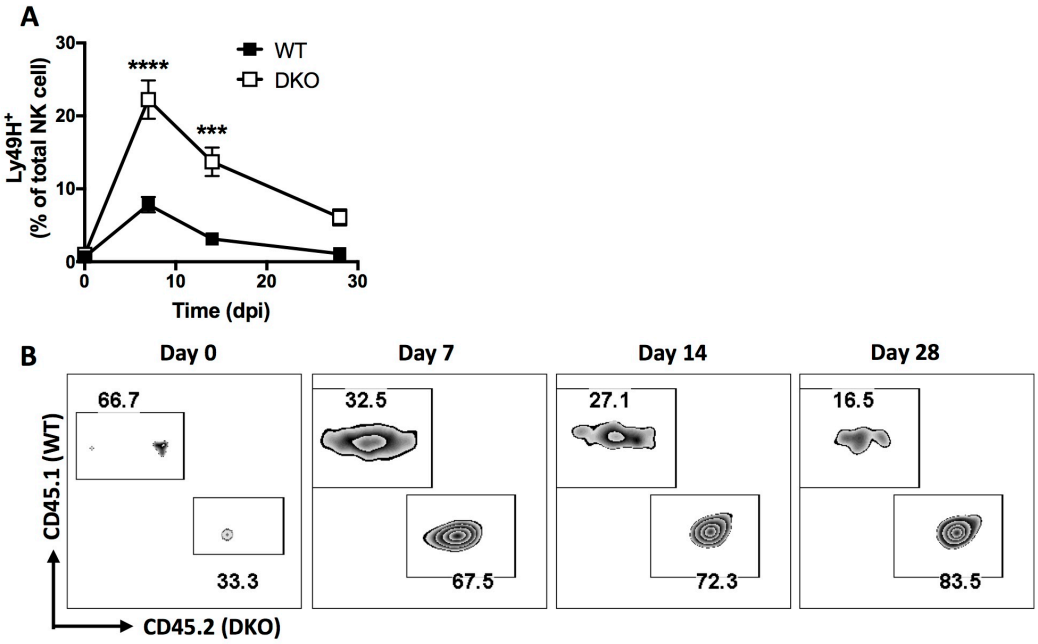


**Figure 0.3 Cell-autonomous impact of Casp8 on NK cell expansion and contraction during the acute phase of MCMV infection.**

Equal numbers of the purified TCRβ$^-$NK1.1$^+$ cells from CD45.1$^+$ WT mice and CD45.2$^+$ DKO mice were co-transferred into Ly49H-deficient recipients, followed with MCMV infection the next day. Graph showing the percentages ± S.E.M. of Ly49H$^+$ cells in blood on days 0, 7, 14, and 28 post infection. Representative plots showing the ratios of WT and DKO Ly49H$^+$ NK cells in blood of the recipients on the indicated days post infection. Data represent one experiment with n = 3 mice per group. Data in this figure were generated by M. Potempa.

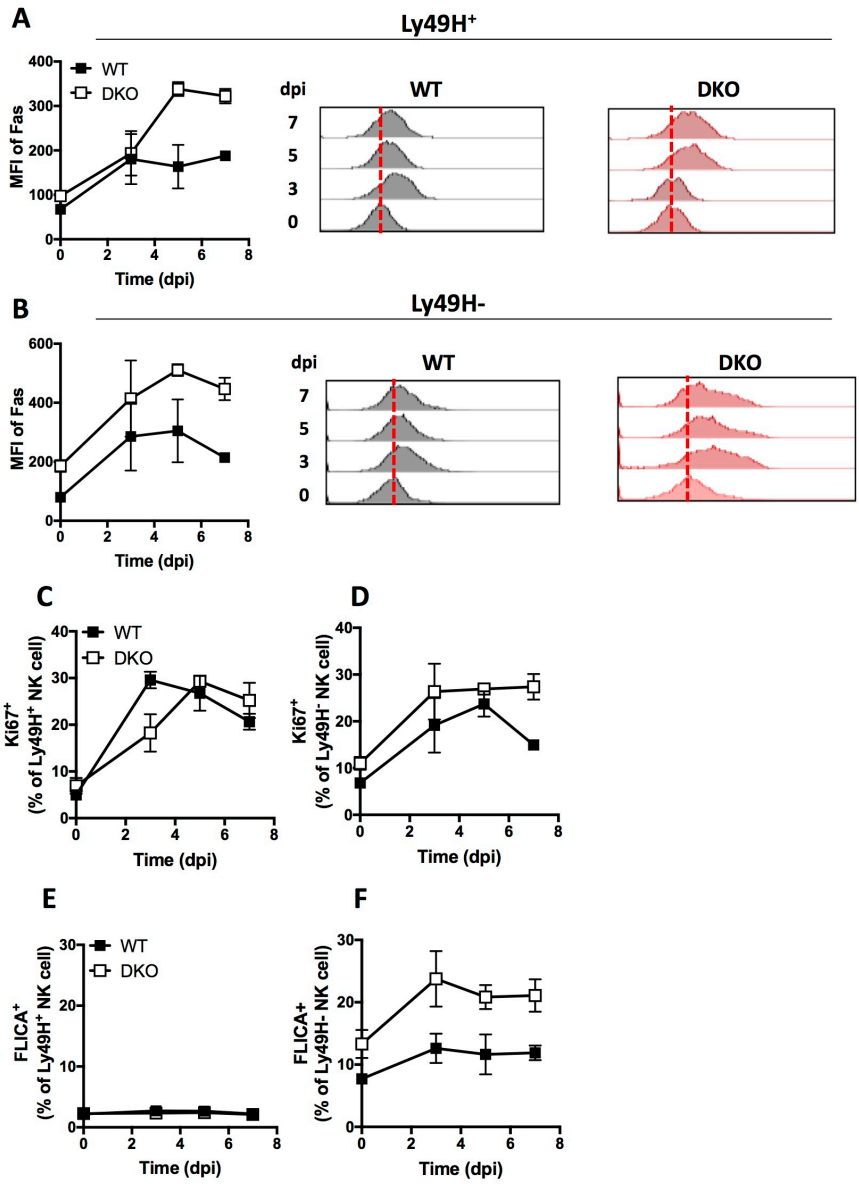


**Figure 0.4 Impact of Casp8 on NK cell proliferation and death.**

WT and DKO mice were infected with K181-BAC as described in Figure 1. Splenocytes from mock treated or infected mice were assessed on days 3, 5, 7 post infection. Graphs and representative histograms showing the median fluorescent intensity levels of Fas on $Ly49H^+$ (**A**), and $L49H^-$ (**B**) NK cells over time. Graphs comparing the percentages of $Ki67^+$ cells within $Ly49H^+$ (**C**), and $L49H^-$ (**D**) NK populations. Graphs comparing the percentages of $FLICA^+$ cells

within Ly49H$^{+}$ (**E**), and L49H$^{-}$ (**F**) NK populations. Data are present as mean ± S.E.M. and represent two independent experiments with mice $n \geq 3$ in each group.

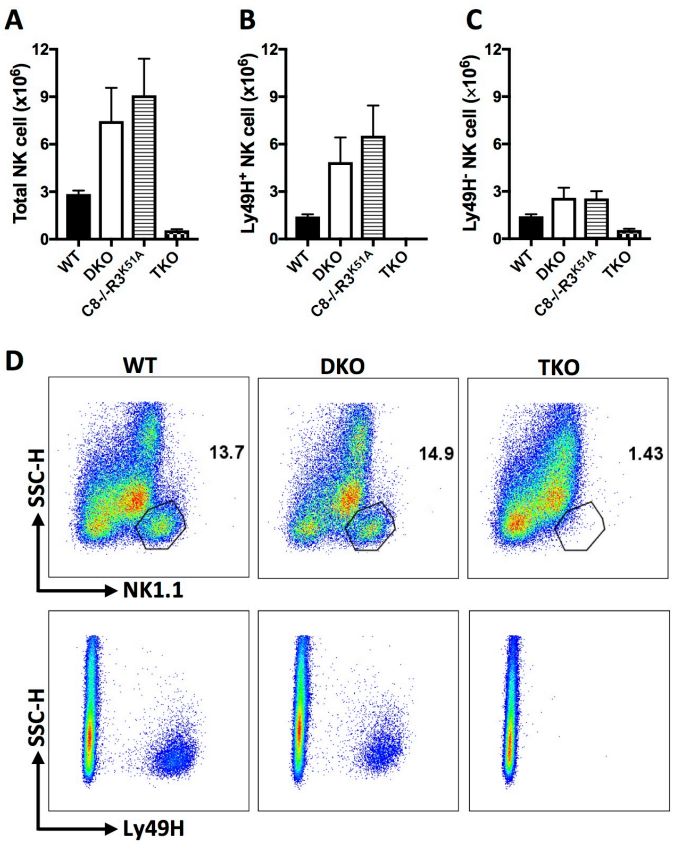


**Figure 0.5 Assessment of NK cell responses in another Casp8-deficienct strain and the contribution of RIPK1 to the response.**

WT, DKO, *C8*$^{-/-}$*R3*$^{K51A}$ and *Ripk1*$^{-/-}$*Casp8*$^{-/-}$*Ripk3*$^{-/-}$ mice were infected with MCMV as described in Fig. 1. Bar graphs comparing the mean numbers ± S.E.M. of the splenic total (**A**), Ly49H$^{+}$ (**B**), and L49H$^{-}$ (**C**) NK cells at 7 dpi. Representative flow plots showing the percentages of CD45$^{+}$CD3$^{-}$B220$^{-}$ cells expressing NK1.1 (**D**) or Ly49H (**E**). Combined data of n = 7 mice from two independent experiments are shown.

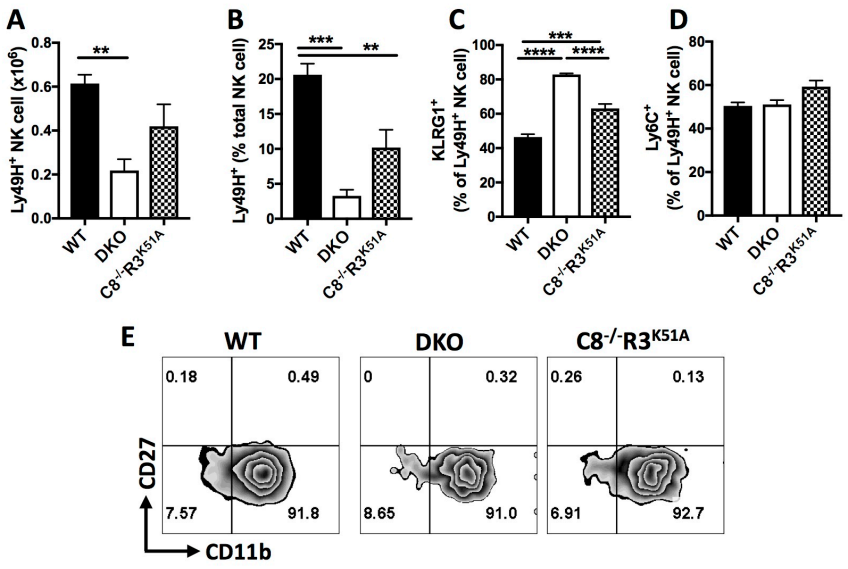


**Figure 0.6 Phenotype of NK cells in long-term infected Casp8-deficient mice.**

WT, DKO, *C8*$^{-/-}$*R3*$^{K51A}$ mice were infected and splenocytes were analyzed at 60 dpi. Bar graphs comparing the numbers (**A**) and percentages (**B**) of Ly49H$^{+}$ NK cells. Graphs comparing the percentages of KLRG1$^{hi}$ (**C**) and Ly6C$^{hi}$ (**D**) cells within the Ly49H$^{+}$ NK population. Representative flow plots depicting CD27 versus CD11b expression on the NK cell subset (**E**). Data are present as mean ± S.E.M. and represent one experiment with mice n = 5 in each group.

## Chapter 5. Discussion and future directions

Virus infection triggers robust innate and adaptive immune cell activation and effector cell cytotoxic function for controlling infection. An optimal immune response is tightly regulated by cell proliferation and death. Casp8 is a key mediator in the generation of an optimal anti-viral immune responses. Casp8 has the potential to initiate apoptosis, to suppresses necroptosis, and to regulate death-independent signaling transduction. In activated lymphocytes, one essential function of Casp8 is to restrict RIPK3-mediated necroptosis, given that compromised Casp8 function leads to the unleashing of necroptosis following TCR stimulation. The assessment of any death-independent role of Casp8 following lymphocyte activation requires a necroptosis-deficient setting. In addition, recent studies have shown that Casp8-deficient mice exhibit hypocytokine responses to Yersinia and influenza A and with disparate susceptibility to bacterial versus viral infections. The crucial functions of Casp8 together with the observations in infected Casp8-deficient mice leave the impression that Casp8 likely contributes significantly to the development of host immunity. In this dissertation, I used MCMV, natural mouse pathogen to study the contribution of Casp8 to antiviral immunity. In Chapter 2, I demonstrate that DKO mice exhibit robust innate and adaptive immune responses with functional cytotoxic NK and CD8 T cells that control MCMV infection. The striking differences between the current natural herpesvirus pathogen and previous cross-species bacterial and influenza studies is likely attributed to the species-specific regulation of Casp8. In Chapter 3 and 4, I demonstrate an unexpected NK and CD8 T cell-autonomous function of Casp8 in restricting the expansion of both cell types during the acute phase. Notably, while the impact on proliferation is T cell-autonomous, the enhanced CD8 T cell numbers requires a robust m157-driven $Ly49H^+$ NK cell response that supports T cell survival. Therefore, Chapter 3 highlights an unexpected T cell-autonomous Casp8 function that

facilitates crosstalk between NK and CD8 T cells and keeps CD8 T cells in check. Taken together, Casp8 contributes to the suppression of NK and CD8 T cell expansion but is dispensable for the generation of innate and adaptive immune responses during infection with this natural mouse pathogen.

*A similar contribution of Casp8 in NK cells and CD8 T cells.* DKO mice mount enhanced responses of both virus-specific CD8 T cells and Ly49H$^+$ NK cells during the acute phase of MCMV infection. Adoptive transfer experiments demonstrate that hyperaccumulation occurs independently of the DKO environment following infection, indicating that the cell-autonomous functions of Casp8 in NK and CD8 T cells act to restrict the magnitude of the response. Stimulation of TCR or Ly49H triggers a similar type of signaling cascade in both of these lymphocyte subpopulations (80, 83) where phosphorylation of ITAMs at receptor cytosolic tails leads to recruitment and activation of ZAP-70, which subsequently phosphorylates to activate PLC-γ for CARMA-MALT1-BCL10 formation. Elimination of CARMA, MALT1 or BCL10 impairs both NK and T cell activation (82, 83), suggesting the indispensable role of this platform for activation signaling transduction in both cell types. Studies of T cells have shown a DISC-like complex forms in association with CARMA-MALT1-BCL10 through the DD interactions between FADD and MALT1 (83, 165, 232). Given that a similar signaling platform is induced upon NK cell activation, FADD, together with Casp8, are likely to be recruited to the NK cell activating receptor-associated complex. Notably, mutations resulting in the disruptions of catalytic activities of Casp8 unleash necroptosis in the activated NK cells, a similar defect occurs within the activated T cells (165). This observation demonstrates that an important function of Casp8 in both lymphocyte subsets is suppressing necroptosis. Furthermore, these data also suggest that the mechanism behind the regulatory function of Casp8 and signaling platform involved is analogous in NK and T cell. It

remains unclear whether Casp8 regulates TCR or NK activating receptor signaling transduction independent of DRs (133, 249). It has been shown that elimination of Fas or TNFR1 does not rescue *Casp8*$^{-/-}$ T cells from necroptotic death upon TCR stimulation (personal communication with Hedrick, UCSD), indicating that DISC forms independent of these DRs.

*Intrinsic and extrinsic death pathways in controlling virus-specific T cell responses.* Upon infection, antigen-specific CD8 T cells undergo dramatic clonal expansion and differentiation into effector subsets with either cytotoxic functions or memory differentiation potential (202). After the peak of the acute response, the vast majority of the terminal-differentiated cells contract, leaving the memory precursors that then differentiate into memory cells. MCMV antigen-specific Ly49H$^{+}$ NK cells follow a kinetic similar virus-specific CD8 T cells (79). This system ensures a robust response to combat pathogens as well as induces shutdown of these activities to avoid excess tissue damage. Intrinsic apoptosis plays a dominant role in controlling NK and CD8 T cell numbers; elimination of Bim, or Bax together with Bak results in increased numbers of KLRG1$^{hi}$ and KLRG1$^{lo}$ subsets during the expansion and contraction phases (201). Bim-deficient Ly49H$^{+}$ NK cells display a slower contraction and impaired memory differentiation (207). In contrast to the dominant role of intrinsic apoptosis, extrinsic pathway has a less prominent impact on the magnitude of T cell responses during viral infection (115). Earlier studies have shown that *lpr* mice exhibit normal CD8 T cell numbers throughout the acute phase of virus infection; however, elimination of virus-specific CD8 T cells during persistent virus infection (e.g., MHV-68) requires the collaboration of Bim with Fas (116, 227). This was supported by the data that mice with combined deficiency of Bim and Fas maintained higher MHV-68-specific CD8 T cell numbers in compared to levels in Bim- or Fas-eliminated strains (116, 227). One shortcoming of using *lpr* mice is that multiple DRs can trigger the same downstream pathway for initiating apoptosis. DKO

mice with the extrinsic pathway completely ablated avoid any problem of DR redundancy. Data in Chapters 3 and 4 showed that combined deficiency of Casp8 and RIPK3 leads to hyperaccumulation of antiviral CD8 T cells and Ly49H$^+$ NK cells that peaked higher than WT mice, but had no impact on cell contraction. Further, the dying cell event assessment indicated no defect of Casp3 activation despite Casp8 and RIPK3 deficiency, suggesting that the cell death during contraction phase is driven by intrinsic pathway, a mechanism remaining intact in this genotype. These observations reinforce that the intrinsic pathway acts dominant in activing Casp3-dependent apoptosis and driving both antiviral CD8 T cell and Ly49H$^+$ NK cell contraction.

*An unexpected critical role of extrinsic cell death for suppressing proliferation.* In Chapter 3, enhanced proliferation capacity of DKO CD8 T cells reveals a death-independent function of Casp8 in suppressing proliferation on a necroptosis-compromised background. Previous studies have indicated contribution of extrinsic pathway to suppress T cell homeostatic proliferation. The abnormal B220$^+$CD3$^+$ T cells and the normal CD8 T cells in DKO and *lpr* mice exhibit enhanced homeostatic proliferation (149, 243), leading to the accumulation of these lymphocytes and the development of ALPS. Notably, overexpression of cell cycle inhibitor p21 reverses this abnormal T cell accumulation in *lpr* mice (243), demonstrating that Fas-mediated signal normally dampens T cell homeostatic proliferation to prevent the lymphoid hyperplasia. Casp8 is placed directly downstream of Fas. In line with this hypothesis, Casp8 may normally dampen T cell proliferation through regulating p21 during homeostasis and virus infection. Certainly, challenges remain for distinguishing whether this increased accumulation is due to enhanced proliferation or defective death of the proliferated cells. Important to note, adult *Casp3*$^{-/-}$ or *Casp3*$^{-/-}$*Casp7*$^{-/-}$ mice do not develop the abnormal B220$^+$CD3$^+$ T cells (242), suggesting that this dysregulation cannot be

simply explained as an apoptotic defect. These data suggest that extrinsic pathway may regulate cell cycle regulators to suppress T cell proliferation.

Casp8 elimination in hepatocytes improves liver regeneration, attributable to the enhanced NF-κB activation that drives earlier expression of cell cycle progression proteins (237). RIPK1 is an important pro-necroptotic kinase also involved in innate immune signaling transduction (150). Compromising Casp8 catalytic activities in myeloid cells leads to RIPK1- and RIPK3-dependent prolonged NF-κB and Erk activation and enhanced proinflammatory cytokine production (238, 239). When signal transduction in DKO CD8 T cells was evaluated in a preliminary experiment, in comparison with WT and *Casp8*$^{DA/DA}$ (Fig. 5.1.), phosphorylated IκBα induced by TCR activation leads to the disassociation of p65/p50 heterodimers, which then translocate into nucleus to activate NF-κB, consistent with published observations (319). Phospho-IκBα expression was detected in all three genotypes by 5 min post stimulation with anti-CD3/CD28 or CD28 alone, although protein levels were higher in WT cells than DKO and *Casp8*$^{DA/DA}$ cells. This signal was transient and decreased by 15 min post stimulation. Similar to the pattern of phospho-IκBα, phospho-p65 expression was detected in by 5 min, when the levels were higher in WT cells and decreased with time. Notably, DKO CD8 T cells exhibited prolonged p65 phosphorylation, a pattern not observed with *Casp8*$^{DA/DA}$ cells. This prolonged phosphorylation of p65 correlated with enhanced DKO cell proliferation, suggesting that scaffold function or the basal catalytic activities of Casp8 contribute to the proper termination of signaling. Interesting, *Ripk1*$^{-/-}$*Casp8*$^{-/-}$*Ripk3*$^{-/-}$ mice exhibited normal CD8 T cell response comparable WT mice in response to MCMV infection (150); however, *Ripk1*$^{-/-}$*Casp8*$^{-/-}$*Ripk3*$^{-/-}$ or *Ripk1*$^{-/-}$*Fadd*$^{-/-}$*Ripk3*$^{-/-}$ CD8 T cells exhibit enhanced proliferation (151, 152). These data suggest that Casp8 may be required for proper shutdown of NF-κB activation independent of RIPK1; certainly, assessment with more time points-post

stimulation is required for confirm this thought. The enhanced total and Ly49H$^+$ NK cell responses in DKO mice is completely ablated to undetectable once RIPK1 is eliminated (Chapter 4), despite the normal NK cell numbers in naïve *Ripk1*$^{-/-}$*Casp8*$^{-/-}$*Ripk3*$^{-/-}$ mice (150). Given the critical role RIPK1 in regulating the cytokine milieu, this defect can be due to a NK cell-autonomous impact or environmental alteration due to the lack of RIPK1.

*DKO CD4 T cell defect that may lead to persistent virus replication in salivary glands of DKO mice.* The lack of Casp8 together with RIPK3 enhances the accumulation of CD8 T cells but has no effect on CD4 T cells, suggesting a distinctive role of Casp8 in the two T cell subsets. Interestingly, preliminary data show a defect of DKO CD4 T cells in culture. While CD4 T cells from 6- to 8-week-old DKO mice proliferate robustly upon TCR stimulation in culture, cells isolated from ageing (age > 10-week-old) adults exhibit a profound defect in proliferation (Fig. 5.2. *A*). T cell stimulation leads to the upregulation of IL-2 α-subunit CD25 that forms the high affinity IL-2R along with β-subunit CD122 and γ-subunit (320). CD4 T cell produces IL-2, which can act in an autocrine or paracrine fashion by binding to the IL-2R to promote T cell proliferation (320). Upregulation of CD25 on DKO CD4 T cells is impaired in comparison with WT and HET controls at 24 and 48 hr post stimulation (Fig. 5.2. *C* and *D*). Further, lower percentages of DKO CD4 T cells produce IL-2 (Fig. 5.2. *E*) as well as IFNγ (Fig. 5.2. *F*) and TNF (Fig. 5.2. *G*). This impaired IL-2 production and CD25 upregulation correlates with the observed DKO CD4 T cell hypo-proliferation. In contrast to the *in vitro* defect, DKO CD4 T cells respond robustly in mice following virus infection and display no defect in IL-2 production, suggesting certain environmental factors *in vivo* reverse the defect observed *in vitro*. MCMV control in SGs dependent on CD4 T cells, specifically IFNγ-producing CD4 T cells (65, 66). Notably, active virus replication is detected long-term (25 wpi) in the SGs of infected DKO mice, suggesting a possible

CD4 T cell tissue-specific defect that is not observed in spleens or blood circulation. A cell-intrinsic function of ASC-Casp8 inflammation has been shown using the experimental autoimmune encephalomyelitis (EAE) model (321). ASC in CD4 T cells is required for sustaining Th17 proliferation and survival in the brain but not in secondary lymphoid organs. ASC-Casp8 inflammasome-dependent IL-1β production from Th17 acts in an autocrine manner for supporting these helper cells (321). In line with this hypothesis, a Casp8-intrinsic function may support CD4 T cell proliferation in SG but may be supplanted by some environmental factors in spleens and blood circulation. In contrast to CD4 T cells, DKO CD8 T cells proliferate robustly upon TCR stimulation in culture or *in vivo*. These data suggest that CD4 and CD8 T cells have different needs from Casp8 to respond to environmental stimuli, an intriguing result remains to be clarified.

*An opposite contribution of Casp8 to inflationary CD8 T cells during the acute phase versus long-term infection.* It is unclear why the enhanced inflationary CD8 T cell responses are not sustained in long-term infected DKO mice. Signaling through the two TNF superfamily receptors, OX40 and 4-1BB, is required for an optimal inflationary CD8 T cell response (54, 56). 4-1BB-elimination leads to enhanced inflationary subsets accumulation by day 7 post infection that contract overtime (56), a phenotype similar to DKO mice. Although 4-1BB does not directly signal through FADD/Casp8 (133), stimulation of this receptor may increase cell surface expression of Fas, which subsequently recruits Casp8 to regulate inflationary CD8 T cell responses. Cytokine milieu makes a significant contribution to memory inflation. IL-2 is required for the optimal inflationary CD8 T cell responses (59), whereas IL-10 suppresses the magnitude (57). We observed no defect of IL-2 secretion from CD4 T cell in DKO mice through the course of infection, suggesting the impaired memory inflation is independent of IL-2. DKO, as well as *lpr* mice, display increased serum IL-10 levels as they age (149, 322), which may depress memory inflation. Curiously, DKO mice

exhibit persistent virus replication in SGs, a phenotype that may be a consequence or a cause of the hypo-inflationary CD8 T cell responses (75). A previous study has shown that virus persistence in SG is not required for the generation and maintenance of the inflationary responses (323); however, whether persistent MCMV replication in this organ dampens memory inflation remains unclear.

*MCMV infection and the abnormal T cell generation.* $B220^{+}CD3^{+}$ abnormal T cells accumulate in naïve aging DKO mice (174, 233), reminiscent of Fas signaling-deficient *lpr* mice (264). Surprisingly, MCMV infection depresses this accumulation by 25 wpi in DKO mice. This beneficial impact of MCMV on ameliorating the accumulation of the abnormal T cells was unexpected because previous studies suggested that herpesvirus infection (including HSV-1, MCMV or MHV-68) exacerbates this lymphoid hyperproliferative syndrome (116, 227, 229). However, previous studies all ended around 2 mpi, while we observed a decrease of the abnormal T cells later, by 4 to 6 mpi (16 to 25 wpi). Therefore, the discrepancy may be owing to the length of the infection. Strikingly, the abnormal T cells further decreased in numbers once IFNγ receptor is eliminated along with Casp8 and RIPK3 (*Ifngr*$^{-/-}$*Casp8*$^{-/-}$*Ripk3*$^{-/-}$) (Fig. 5.3. *A*). This result is consistent with the known contribution of IFNγ in promoting abnormal T cell proliferation in *lpr* mice (324). However, *Ifngr*$^{-/-}$*Casp8*$^{-/-}$*Ripk3*$^{-/-}$ mice exhibited higher levels of persistent virus replication in SGs (Fig. 5.3. *B*) and lungs (Fig. 5.3. *C*) than DKO mice at 25 wpi. This observation adds more complexity to the question of whether the decrease in abnormal T cell numbers is due to IFNγ elimination or higher levels of virus replication. HCMV persistence has been shown to alter the immune response threshold to heterologous virus infection, which leads to an enhanced adaptive immune response to influenza vaccination or infection with either *Listeria monocytogenes* or *Yersinia pestis* infection (325, 326). No matter the mechanism, these data

suggest an underappreciated impact of this natural herpesvirus on ameliorating autoimmune syndromes.

*Conclusion*. The magnitude of T cell responses to virus infection represents a balance of proliferation and death. Caspase-8 is an autoactivated protease that controls extrinsic cell death pathways. Any cell death-independent functions of caspase-8 remain to be fully explored. By modulating Casp8 on a RIPK3-eliminated background to avoid the confounding impact of necroptotic death, my work highlights a Casp8 function in restricting the extent of CD8 T cell proliferation in response to a natural mouse herpesvirus infection (Fig. 5.4). This regulation of Casp8 is dependent on NK cells, possibly through the crosstalk with DCs that dictate antigen stimulation to CD8 T cells. Similar to CD8 T cells, NK cells hyper-expand following MCMV infection in the lack of Casp8. This suppressive function of Casp8 is NK cell-autonomous. Taken together, my work shows that Casp8 has a crucial impact on lymphocyte population in general, significantly further our current understanding of Casp8 as a crucial player for innate cell defense and innate immune signaling transduction.

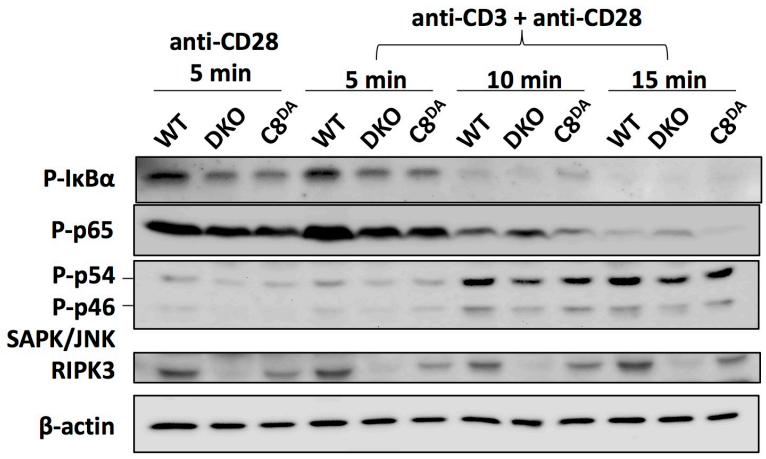


**Figure 0.1. Assessment of signaling mechanism following TCR stimulation.**

Purified spleniCD44$^{lo}$ CD8 T cells were activated for 5, 10, 15 min using 10 μg/ml of plate-bound anti-CD3 and 2 μg/ml soluble anti-CD28. Cells were harvested for immunoblot analysis. Data represent two independent experiments.

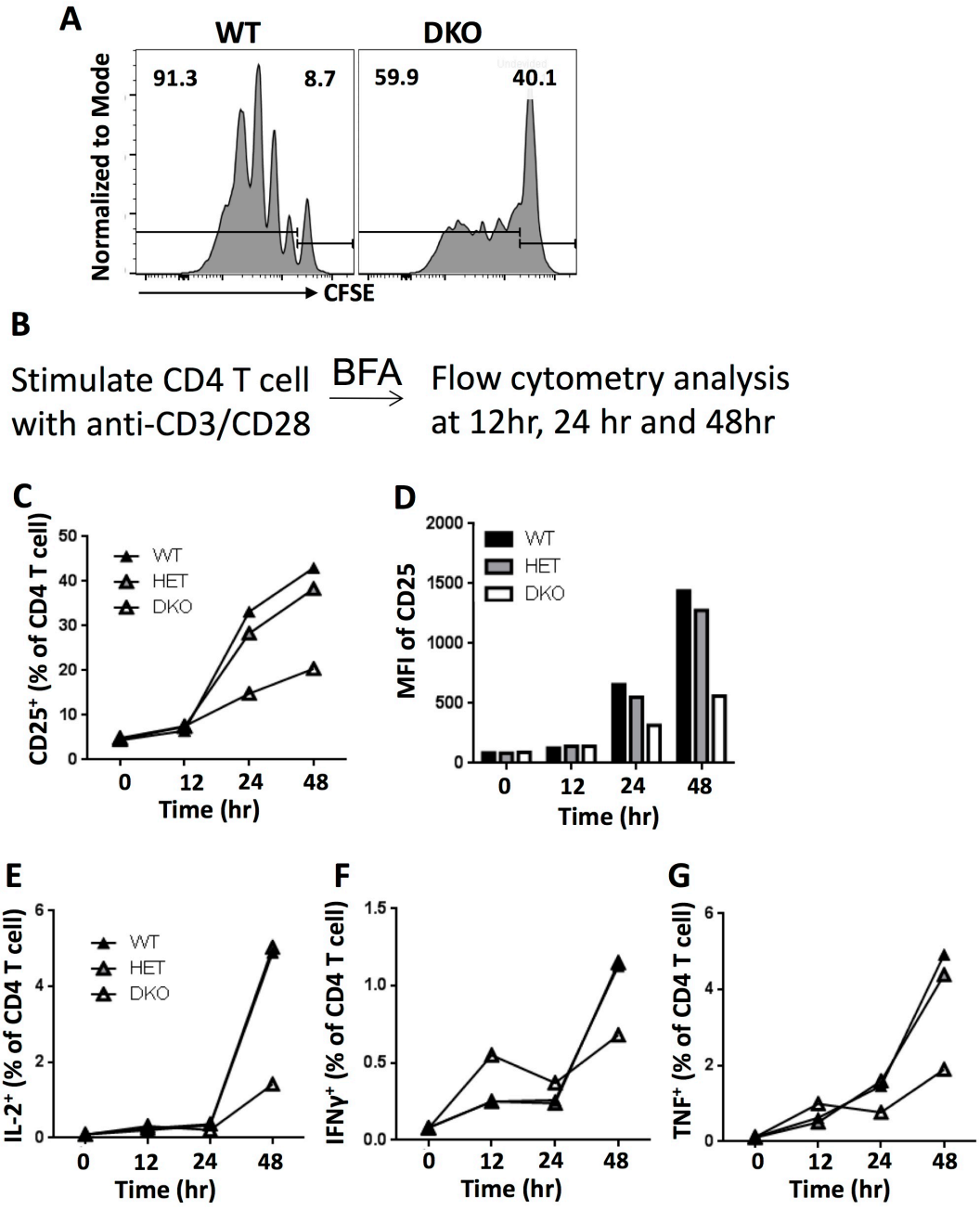


**Figure 0.2 CD4 T cell proliferation and cytokine production following TCR stimulation**.

CFSE-labeled purified splenic CD4 T cells from 12 week-old mice were stimulated by 10 μg/ml of plate-bound anti-CD3 and 2 μg/ml soluble anti-CD28 for 72 hr. Representative flow plots showing CFSE distribution of 7-AAD$^-$ CD4 T cells (A). (B – G) Surface marker and cytokine analysis. Purified splenic CD4 T cells from 12 week-old mice were stimulated by 10 μg/ml of

plate-bound anti-CD3 and 2 μg/ml soluble anti-CD28 for 0, 12, 24 or 48 hr. Brefeldin A was added in culture 5 hour before harvest (B). Graphs showing the percentages of $CD25^{+}$ CD4 T cells (C) and the median fluorescent intensity of CD25 (D). Graphs showing the percentages of IL-2 (E), IFNγ (F), and TNF (G) producing CD4 T cells.

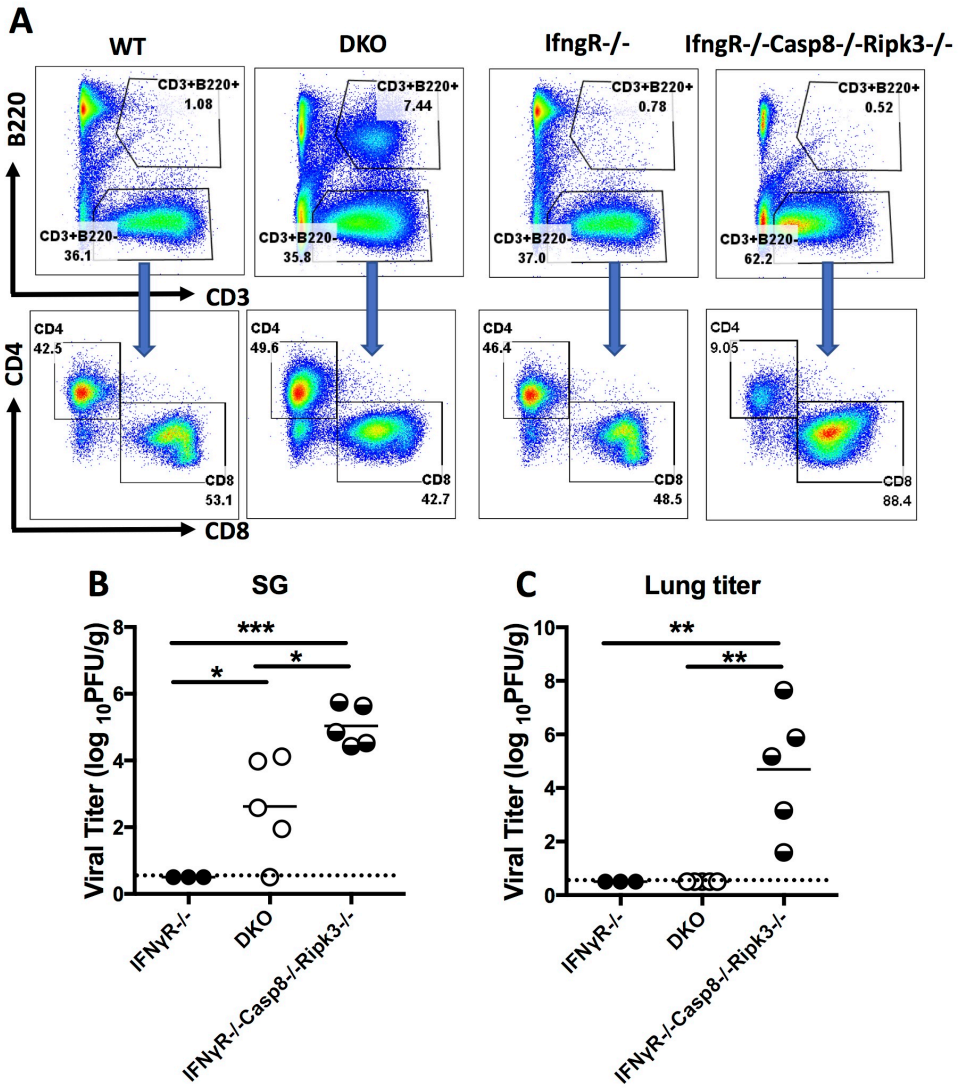


**Figure 0.3 Assessment of the abnormal T cell and virus titers in long-term infected mice.**

WT, DKO, *IfngR*$^{-/-}$ and *IfngR*$^{-/-}$*Casp8* $^{-/-}$ *Ripk3* $^{-/-}$ mice were infected with K181-BAC for 25 weeks. Representative flow plots showing the proportions of CD3$^{+}$B220$^{+}$ abnormal T cells and normal CD3$^{+}$B220$^{-}$ T cells in spleens after gating on CD45$^{+}$ leukocytes. Normal T cells were further broken down to CD4 and CD8 T cells (**A**). Graphs showing the virus titers in SGs (**B**) and lungs (**C**).

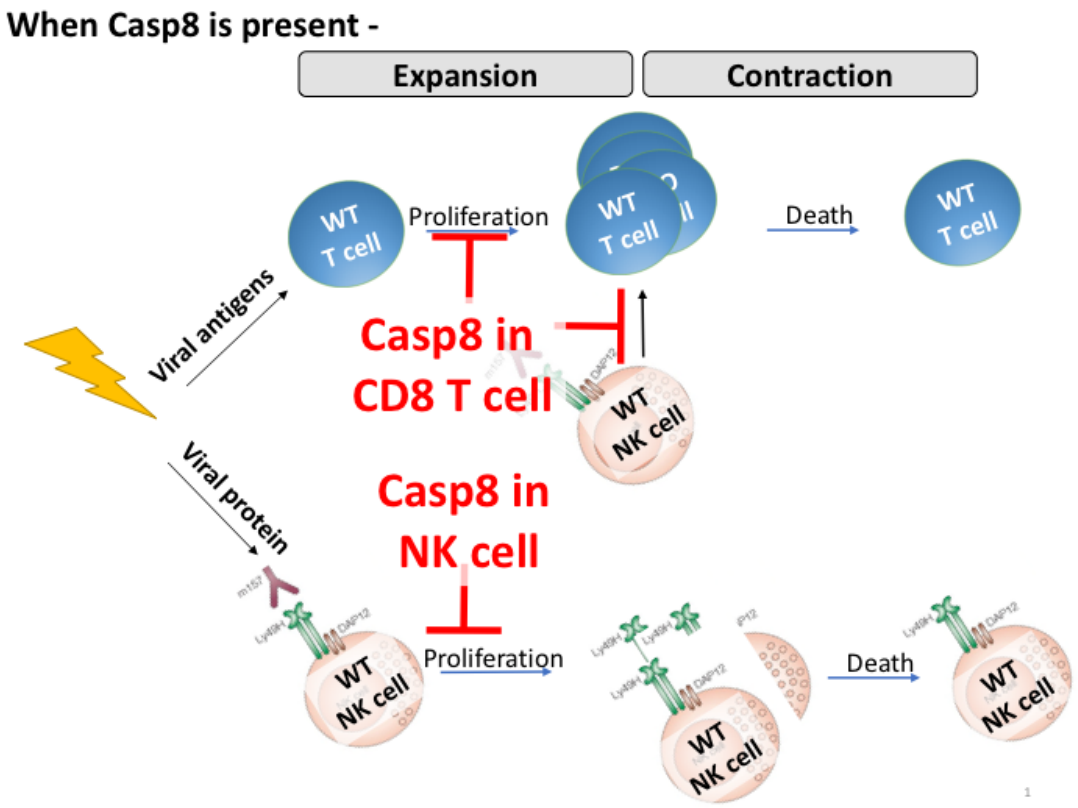


**Figure 5.4 Schematic of how Casp8 regulates CD8 T cell and NK cell.**

## References


1. Picarda G & Benedict CA (2018) Cytomegalovirus: Shape-Shifting the Immune System. *Journal of immunology (Baltimore, Md. : 1950)* 200(12):3881-3889.
2. Klenerman P & Oxenius A (2016) T cell responses to cytomegalovirus. *Nature reviews. Immunology*.
3. Loewendorf A & Benedict CA (2010) Modulation of host innate and adaptive immune defenses by cytomegalovirus: timing is everything. *Journal of internal medicine* 267(5):483-501.
4. Banks TA*, et al.* (2005) A lymphotoxin-IFN-beta axis essential for lymphocyte survival revealed during cytomegalovirus infection. *Journal of immunology (Baltimore, Md. : 1950)* 174(11):7217-7225.
5. Orange JS & Biron CA (1996) An absolute and restricted requirement for IL-12 in natural killer cell IFN-gamma production and antiviral defense. Studies of natural killer and T cell responses in contrasting viral infections. *Journal of immunology (Baltimore, Md. : 1950)* 156(3):1138-1142.
6. Dalod M*, et al.* (2003) Dendritic cell responses to early murine cytomegalovirus infection: subset functional specialization and differential regulation by interferon alpha/beta. *The Journal of experimental medicine* 197(7):885-898.
7. Dalod M*, et al.* (2002) Interferon alpha/beta and interleukin 12 responses to viral infections: pathways regulating dendritic cell cytokine expression in vivo. *The Journal of experimental medicine* 195(4):517-528.
8. Pallmer K & Oxenius A (2016) Recognition and Regulation of T Cells by NK Cells. *Frontiers in immunology* 7:251.

9. Andrews DM, Andoniou CE, Granucci F, Ricciardi-Castagnoli P, & Degli-Esposti MA (2001) Infection of dendritic cells by murine cytomegalovirus induces functional paralysis. *Nature immunology* 2(11):1077-1084.

10. Munks MW, Pinto AK, Doom CM, & Hill AB (2007) Viral interference with antigen presentation does not alter acute or chronic CD8 T cell immunodominance in murine cytomegalovirus infection. *Journal of immunology (Baltimore, Md. : 1950)* 178(11):7235-7241.

11. Mintern JD*, et al.* (2006) Viral interference with B7-1 costimulation: a new role for murine cytomegalovirus fc receptor-1. *Journal of immunology (Baltimore, Md. : 1950)* 177(12):8422-8431.

12. Loewendorf A*, et al.* (2004) Identification of a mouse cytomegalovirus gene selectively targeting CD86 expression on antigen-presenting cells. *Journal of virology* 78(23):13062-13071.

13. Loewendorf AI*, et al.* (2011) The mouse cytomegalovirus glycoprotein m155 inhibits CD40 expression and restricts CD4 T cell responses. *Journal of virology* 85(10):5208-5212.

14. Benedict CA, Loewendorf A, Garcia Z, Blazar BR, & Janssen EM (2008) Dendritic cell programming by cytomegalovirus stunts naive T cell responses via the PD-L1/PD-1 pathway. *Journal of immunology (Baltimore, Md. : 1950)* 180(7):4836-4847.

15. Alexandre YO, Cocita CD, Ghilas S, & Dalod M (2014) Deciphering the role of DC subsets in MCMV infection to better understand immune protection against viral infections. *Frontiers in microbiology* 5:378.

16. Snyder CM, Allan JE, Bonnett EL, Doom CM, & Hill AB (2010) Cross-presentation of a spread-defective MCMV is sufficient to prime the majority of virus-specific CD8+ T cells. *PloS one* 5(3):e9681.

17. Snyder CM, Cho KS, Bonnett EL, Allan JE, & Hill AB (2011) Sustained CD8+ T cell memory inflation after infection with a single-cycle cytomegalovirus. *PLoS pathogens* 7(10):e1002295.

18. Hildner K*, et al.* (2008) Batf3 deficiency reveals a critical role for CD8alpha+ dendritic cells in cytotoxic T cell immunity. *Science (New York, N.Y.)* 322(5904):1097-1100.

19. Munks MW*, et al.* (2006) Four distinct patterns of memory CD8 T cell responses to chronic murine cytomegalovirus infection. *Journal of immunology (Baltimore, Md. : 1950)* 177(1):450-458.

20. Torti N, Walton SM, Murphy KM, & Oxenius A (2011) Batf3 transcription factor-dependent DC subsets in murine CMV infection: differential impact on T-cell priming and memory inflation. *European journal of immunology* 41(9):2612-2618.

21. Tussiwand R*, et al.* (2012) Compensatory dendritic cell development mediated by BATF-IRF interactions. *Nature* 490(7421):502-507.

22. Kaech SM & Cui W (2012) Transcriptional control of effector and memory CD8+ T cell differentiation. *Nature reviews. Immunology* 12(11):749-761.

23. Hanke T, Corral L, Vance RE, & Raulet DH (1998) 2F1 antigen, the mouse homolog of the rat "mast cell function-associated antigen", is a lectin-like type II transmembrane receptor expressed by natural killer cells. *European journal of immunology* 28(12):4409-4417.

24. Voehringer D, Koschella M, & Pircher H (2002) Lack of proliferative capacity of human effector and memory T cells expressing killer cell lectinlike receptor G1 (KLRG1). *Blood* 100(10):3698-3702.

25. Henson SM & Akbar AN (2009) KLRG1--more than a marker for T cell senescence. *Age (Dordr)* 31(4):285-291.

26. Wherry EJ, Barber DL, Kaech SM, Blattman JN, & Ahmed R (2004) Antigen-independent memory CD8 T cells do not develop during chronic viral infection. *Proceedings of the National Academy of Sciences of the United States of America* 101(45):16004-16009.

27. Schluns KS, Kieper WC, Jameson SC, & Lefrancois L (2000) Interleukin-7 mediates the homeostasis of naive and memory CD8 T cells in vivo. *Nature immunology* 1(5):426-432.

28. Obar JJ*, et al.* (2011) Pathogen-induced inflammatory environment controls effector and memory CD8+ T cell differentiation. *Journal of immunology (Baltimore, Md. : 1950)* 187(10):4967-4978.

29. Plumlee CR*, et al.* (2015) Early Effector CD8 T Cells Display Plasticity in Populating the Short-Lived Effector and Memory-Precursor Pools Following Bacterial or Viral Infection. *Scientific reports* 5:12264.

30. Joshi NS*, et al.* (2007) Inflammation directs memory precursor and short-lived effector CD8(+) T cell fates via the graded expression of T-bet transcription factor. *Immunity* 27(2):281-295.

31. Xin A*, et al.* (2016) A molecular threshold for effector CD8(+) T cell differentiation controlled by transcription factors Blimp-1 and T-bet. *Nature immunology* 17(4):422-432.

32. Kaech SM*, et al.* (2003) Selective expression of the interleukin 7 receptor identifies effector CD8 T cells that give rise to long-lived memory cells. *Nature immunology* 4(12):1191-1198.

33. Herndler-Brandstetter D*, et al.* (2018) KLRG1(+) Effector CD8(+) T Cells Lose KLRG1, Differentiate into All Memory T Cell Lineages, and Convey Enhanced Protective Immunity. *Immunity* 48(4):716-729 e718.

34. Yuzefpolskiy Y, Baumann FM, Kalia V, & Sarkar S (2015) Early CD8 T-cell memory precursors and terminal effectors exhibit equipotent in vivo degranulation. *Cellular & molecular immunology* 12(4):400-408.

35. Jameson SC & Masopust D (2018) Understanding Subset Diversity in T Cell Memory. *Immunity* 48(2):214-226.

36. Parish IA & Kaech SM (2009) Diversity in CD8(+) T cell differentiation. *Current opinion in immunology* 21(3):291-297.

37. Snyder CM*, et al.* (2008) Memory inflation during chronic viral infection is maintained by continuous production of short-lived, functional T cells. *Immunity* 29(4):650-659.

38. Sylwester AW*, et al.* (2005) Broadly targeted human cytomegalovirus-specific CD4+ and CD8+ T cells dominate the memory compartments of exposed subjects. *The Journal of experimental medicine* 202(5):673-685.

39. Klenerman P & Oxenius A (2016) T cell responses to cytomegalovirus. *Nature reviews. Immunology* 16(6):367-377.

40. Jonjic S, Pavic I, Lucin P, Rukavina D, & Koszinowski UH (1990) Efficacious control of cytomegalovirus infection after long-term depletion of CD8+ T lymphocytes. *Journal of virology* 64(11):5457-5464.

41. Del Val M*, et al.* (1991) Protection against lethal cytomegalovirus infection by a recombinant vaccine containing a single nonameric T-cell epitope. *Journal of virology* 65(7):3641-3646.

42. Holtappels R*, et al.* (2004) Cytomegalovirus misleads its host by priming of CD8 T cells specific for an epitope not presented in infected tissues. *The Journal of experimental medicine* 199(1):131-136.

43. Halle S*, et al.* (2016) In Vivo Killing Capacity of Cytotoxic T Cells Is Limited and Involves Dynamic Interactions and T Cell Cooperativity. *Immunity* 44(2):233-245.

44. Riddell SR*, et al.* (1992) Restoration of viral immunity in immunodeficient humans by the adoptive transfer of T cell clones. *Science (New York, N.Y.)* 257(5067):238-241.

45. Smith CJ, Turula H, & Snyder CM (2014) Systemic Hematogenous Maintenance of Memory Inflation by MCMV Infection. *PLoS pathogens* 10(7).

46. Koffron AJ*, et al.* (1998) Cellular localization of latent murine cytomegalovirus. *Journal of virology* 72(1):95-103.

47. Redeker A, Welten SP, & Arens R (2014) Viral inoculum dose impacts memory T-cell inflation. *European journal of immunology* 44(4):1046-1057.

48. Quinn M*, et al.* (2015) Memory T cells specific for murine cytomegalovirus re-emerge after multiple challenges and recapitulate immunity in various adoptive transfer scenarios. *Journal of immunology (Baltimore, Md. : 1950)* 194(4):1726-1736.

49. Dekhtiarenko I, Jarvis MA, Ruzsics Z, & Cicin-Sain L (2013) The context of gene expression defines the immunodominance hierarchy of cytomegalovirus antigens. *Journal of immunology (Baltimore, Md. : 1950)* 190(7):3399-3409.

50. Grzimek NK, *et al.* (1999) In vivo replication of recombinant murine cytomegalovirus driven by the paralogous major immediate-early promoter-enhancer of human cytomegalovirus. *Journal of virology* 73(6):5043-5055.

51. Hutchinson S, *et al.* (2011) A dominant role for the immunoproteasome in CD8+ T cell responses to murine cytomegalovirus. *PLoS One* 6(2):e14646.

52. Dekhtiarenko I, *et al.* (2016) Peptide Processing Is Critical for T-Cell Memory Inflation and May Be Optimized to Improve Immune Protection by CMV-Based Vaccine Vectors. *PLoS pathogens* 12(12):e1006072.

53. Arens R, *et al.* (2011) Differential B7-CD28 costimulatory requirements for stable and inflationary mouse cytomegalovirus-specific memory CD8 T cell populations. *Journal of immunology (Baltimore, Md. : 1950)* 186(7):3874-3881.

54. Humphreys IR, *et al.* (2007) OX40 costimulation promotes persistence of cytomegalovirus-specific CD8 T Cells: A CD4-dependent mechanism. *Journal of immunology (Baltimore, Md. : 1950)* 179(4):2195-2202.

55. Welten SP, *et al.* (2013) CD27-CD70 costimulation controls T cell immunity during acute and persistent cytomegalovirus infection. *Journal of virology* 87(12):6851-6865.

56. Humphreys IR, *et al.* (2010) Biphasic role of 4-1BB in the regulation of mouse cytomegalovirus-specific CD8(+) T cells. *European journal of immunology* 40(10):2762-2768.

57. Jones M*, et al.* (2010) IL-10 restricts memory T cell inflation during cytomegalovirus infection. *Journal of immunology (Baltimore, Md. : 1950)* 185(6):3583-3592.

58. Popovic B*, et al.* (2017) IL-33/ST2 pathway drives regulatory T cell dependent suppression of liver damage upon cytomegalovirus infection. *PLoS pathogens* 13(4):e1006345.

59. Bachmann MF, Wolint P, Walton S, Schwarz K, & Oxenius A (2007) Differential role of IL-2R signaling for CD8+ T cell responses in acute and chronic viral infections. *European journal of immunology* 37(6):1502-1512.

60. Baumann NS*, et al.* (2018) Tissue maintenance of CMV-specific inflationary memory T cells by IL-15. *PLoS pathogens* 14(4):e1006993.

61. Delpoux A*, et al.* (2018) Continuous activity of Foxo1 is required to prevent anergy and maintain the memory state of CD8(+) T cells. *The Journal of experimental medicine* 215(2):575-594.

62. Michelini RH, Doedens AL, Goldrath AW, & Hedrick SM (2013) Differentiation of CD8 memory T cells depends on Foxo1. *The Journal of experimental medicine* 210(6):1189-1200.

63. Arens R*, et al.* (2008) Cutting edge: murine cytomegalovirus induces a polyfunctional CD4 T cell response. *Journal of immunology (Baltimore, Md. : 1950)* 180(10):6472-6476.

64. Welten SPM, Redeker A, Toes REM, & Arens R (2016) Viral Persistence Induces Antibody Inflation without Altering Antibody Avidity. *Journal of virology* 90(9):4402-4411.

65. Jonjic S, Mutter W, Weiland F, Reddehase MJ, & Koszinowski UH (1989) Site-restricted persistent cytomegalovirus infection after selective long-term depletion of CD4+ T lymphocytes. *The Journal of experimental medicine* 169(4):1199-1212.

66. Walton SM*, et al.* (2011) Absence of cross-presenting cells in the salivary gland and viral immune evasion confine cytomegalovirus immune control to effector CD4 T cells. *PLoS pathogens* 7(8):e1002214.

67. Verma S*, et al.* (2015) Cytomegalovirus-Specific CD4 T Cells Are Cytolytic and Mediate Vaccine Protection. *Journal of virology* 90(2):650-658.

68. Jeitziner SM, Walton SM, Torti N, & Oxenius A (2013) Adoptive transfer of cytomegalovirus-specific effector CD4+ T cells provides antiviral protection from murine CMV infection. *European journal of immunology* 43(11):2886-2895.

69. Einsele H*, et al.* (2002) Infusion of cytomegalovirus (CMV)-specific T cells for the treatment of CMV infection not responding to antiviral chemotherapy. *Blood* 99(11):3916-3922.

70. Gordon CL*, et al.* (2017) Tissue reservoirs of antiviral T cell immunity in persistent human CMV infection. *The Journal of experimental medicine* 214(3):651-667.

71. Thom JT, Weber TC, Walton SM, Torti N, & Oxenius A (2015) The Salivary Gland Acts as a Sink for Tissue-Resident Memory CD8(+) T Cells, Facilitating Protection from Local Cytomegalovirus Infection. *Cell reports* 13(6):1125-1136.

72. Turner DL*, et al.* (2014) Lung niches for the generation and maintenance of tissue-resident memory T cells. *Mucosal immunology* 7(3):501-510.

73. Lu X, Pinto AK, Kelly AM, Cho KS, & Hill AB (2006) Murine Cytomegalovirus Interference with Antigen Presentation Contributes to the Inability of CD8 T Cells To Control Virus in the Salivary Gland. *Journal of virology* 80(8):4200-4202.

74. Smith CJ, Caldeira-Dantas S, Turula H, & Snyder CM (2015) Murine CMV Infection Induces the Continuous Production of Mucosal Resident T Cells. *Cell reports* 13(6):1137-1148.

75. Thom JT & Oxenius A (2016) Tissue-resident memory T cells in cytomegalovirus infection. *Current opinion in virology* 16:63-69.

76. Mackay LK*, et al.* (2013) The developmental pathway for CD103(+)CD8+ tissue-resident memory T cells of skin. *Nature immunology* 14(12):1294-1301.

77. Mueller SN & Mackay LK (2016) Tissue-resident memory T cells: local specialists in immune defence. *Nature reviews. Immunology* 16(2):79-89.

78. Laidlaw BJ*, et al.* (2014) CD4+ T cell help guides formation of CD103+ lung-resident memory CD8+ T cells during influenza viral infection. *Immunity* 41(4):633-645.

79. Sun JC & Lanier LL (2011) NK cell development, homeostasis and function: parallels with CD8(+) T cells. *Nature reviews. Immunology* 11(10):645-657.

80. Lanier LL (2008) Up on the tightrope: natural killer cell activation and inhibition. *Nature immunology* 9(5):495-502.

81. Orr MT*, et al.* (2009) Ly49H signaling through DAP10 is essential for optimal natural killer cell responses to mouse cytomegalovirus infection. *The Journal of experimental medicine* 206(4):807-817.

82. Gross O*, et al.* (2008) Multiple ITAM-coupled NK-cell receptors engage the Bcl10/Malt1 complex via Carma1 for NF-kappaB and MAPK activation to selectively control cytokine production. *Blood* 112(6):2421-2428.

83. Juilland M & Thome M (2018) Holding All the CARDs: How MALT1 Controls CARMA/CARD-Dependent Signaling. *Frontiers in immunology* 9:1927.

84. Kim S*, et al.* (2002) In vivo developmental stages in murine natural killer cell maturation. *Nature immunology* 3(6):523-528.

85. Kim S*, et al.* (2005) Licensing of natural killer cells by host major histocompatibility complex class I molecules. *Nature* 436(7051):709-713.

86. Johansson S*, et al.* (2005) Natural killer cell education in mice with single or multiple major histocompatibility complex class I molecules. *The Journal of experimental medicine* 201(7):1145-1155.

87. Fernandez NC*, et al.* (2005) A subset of natural killer cells achieves self-tolerance without expressing inhibitory receptors specific for self-MHC molecules. *Blood* 105(11):4416-4423.

88. Orr MT & Lanier LL (2010) Natural killer cell education and tolerance. *Cell* 142(6):847-856.

89. Brodin P, Lakshmikanth T, Johansson S, Karre K, & Hoglund P (2009) The strength of inhibitory input during education quantitatively tunes the functional responsiveness of individual natural killer cells. *Blood* 113(11):2434-2441.

90. Joncker NT, Fernandez NC, Treiner E, Vivier E, & Raulet DH (2009) NK cell responsiveness is tuned commensurate with the number of inhibitory receptors for self-

MHC class I: the rheostat model. *Journal of immunology (Baltimore, Md. : 1950)* 182(8):4572-4580.

91. Sun JC (2010) Re-educating natural killer cells. *The Journal of experimental medicine* 207(10):2049-2052.

92. Joncker NT, Shifrin N, Delebecque F, & Raulet DH (2010) Mature natural killer cells reset their responsiveness when exposed to an altered MHC environment. *The Journal of experimental medicine* 207(10):2065-2072.

93. Elliott JM, Wahle JA, & Yokoyama WM (2010) MHC class I-deficient natural killer cells acquire a licensed phenotype after transfer into an MHC class I-sufficient environment. *The Journal of experimental medicine* 207(10):2073-2079.

94. Smith HR*, et al.* (2002) Recognition of a virus-encoded ligand by a natural killer cell activation receptor. *Proceedings of the National Academy of Sciences of the United States of America* 99(13):8826-8831.

95. Sun JC, Beilke JN, & Lanier LL (2009) Adaptive immune features of natural killer cells. *Nature* 457(7229):557-561.

96. Dokun AO*, et al.* (2001) Specific and nonspecific NK cell activation during virus infection. *Nature immunology* 2(10):951-956.

97. Mitrovic M*, et al.* (2012) The NK cell response to mouse cytomegalovirus infection affects the level and kinetics of the early CD8(+) T-cell response. *Journal of virology* 86(4):2165-2175.

98. Adams EJ*, et al.* (2007) Structural elucidation of the m157 mouse cytomegalovirus ligand for Ly49 natural killer cell receptors. *Proceedings of the National Academy of Sciences of the United States of America* 104(24):10128-10133.

99. Guma M*, et al.* (2004) Imprint of human cytomegalovirus infection on the NK cell receptor repertoire. *Blood* 104(12):3664-3671.

100. Guma M*, et al.* (2006) Human cytomegalovirus infection is associated with increased proportions of NK cells that express the CD94/NKG2C receptor in aviremic HIV-1-positive patients. *J Infect Dis* 194(1):38-41.

101. Lopez-Verges S*, et al.* (2011) Expansion of a unique CD57(+)NKG2Chi natural killer cell subset during acute human cytomegalovirus infection. *Proceedings of the National Academy of Sciences of the United States of America* 108(36):14725-14732.

102. Kuijpers TW*, et al.* (2008) Human NK cells can control CMV infection in the absence of T cells. *Blood* 112(3):914-915.

103. Chambers BJ, Salcedo M, & Ljunggren HG (1996) Triggering of natural killer cells by the costimulatory molecule CD80 (B7-1). *Immunity* 5(4):311-317.

104. Barao I (2012) The TNF receptor-ligands 4-1BB-4-1BBL and GITR-GITRL in NK cell responses. *Frontiers in immunology* 3:402.

105. Benson DM, Jr.*, et al.* (2010) The PD-1/PD-L1 axis modulates the natural killer cell versus multiple myeloma effect: a therapeutic target for CT-011, a novel monoclonal anti-PD-1 antibody. *Blood* 116(13):2286-2294.

106. Nandi D, Gross JA, & Allison JP (1994) CD28-mediated costimulation is necessary for optimal proliferation of murine NK cells. *Journal of immunology (Baltimore, Md. : 1950)* 152(7):3361-3369.

107. Nabekura T*, et al.* (2017) Cutting Edge: NKG2D Signaling Enhances NK Cell Responses but Alone Is Insufficient To Drive Expansion during Mouse Cytomegalovirus Infection. *Journal of immunology (Baltimore, Md. : 1950)* 199(5):1567-1571.

108. Nguyen KB*, et al.* (2002) Coordinated and distinct roles for IFN-alpha beta, IL-12, and IL-15 regulation of NK cell responses to viral infection. *Journal of immunology (Baltimore, Md. : 1950)* 169(8):4279-4287.

109. Madera S*, et al.* (2016) Type I IFN promotes NK cell expansion during viral infection by protecting NK cells against fratricide. *The Journal of experimental medicine* 213(2):225-233.

110. Geary CD*, et al.* (2018) Non-redundant ISGF3 Components Promote NK Cell Survival in an Auto-regulatory Manner during Viral Infection. *Cell reports* 24(8):1949-1957 e1946.

111. Adams NM*, et al.* (2018) Transcription Factor IRF8 Orchestrates the Adaptive Natural Killer Cell Response. *Immunity* 48(6):1172-1182 e1176.

112. Madera S & Sun JC (2015) Cutting edge: stage-specific requirement of IL-18 for antiviral NK cell expansion. *Journal of immunology (Baltimore, Md. : 1950)* 194(4):1408-1412.

113. Nabekura T, Girard JP, & Lanier LL (2015) IL-33 receptor ST2 amplifies the expansion of NK cells and enhances host defense during mouse cytomegalovirus infection. *Journal of immunology (Baltimore, Md. : 1950)* 194(12):5948-5952.

114. Tait SW & Green DR (2010) Mitochondria and cell death: outer membrane permeabilization and beyond. *Nature reviews. Molecular cell biology* 11(9):621-632.

115. Li KP*, et al.* (2017) Dying to protect: cell death and the control of T-cell homeostasis. *Immunological reviews* 277(1):21-43.

116. Hughes PD*, et al.* (2008) Apoptosis regulators Fas and Bim cooperate in shutdown of chronic immune responses and prevention of autoimmunity. *Immunity* 28(2):197-205.

117. Youle RJ & Strasser A (2008) The BCL-2 protein family: opposing activities that mediate cell death. *Nature reviews. Molecular cell biology* 9(1):47-59.

118. Chen L*, et al.* (2005) Differential targeting of prosurvival Bcl-2 proteins by their BH3-only ligands allows complementary apoptotic function. *Molecular cell* 17(3):393-403.

119. Willis SN*, et al.* (2007) Apoptosis initiated when BH3 ligands engage multiple Bcl-2 homologs, not Bax or Bak. *Science (New York, N.Y.)* 315(5813):856-859.

120. Dijkers PF, Medema RH, Lammers JW, Koenderman L, & Coffer PJ (2000) Expression of the pro-apoptotic Bcl-2 family member Bim is regulated by the forkhead transcription factor FKHR-L1. *Current biology : CB* 10(19):1201-1204.

121. Nakano K & Vousden KH (2001) PUMA, a novel proapoptotic gene, is induced by p53. *Molecular cell* 7(3):683-694.

122. Narita M*, et al.* (1998) Bax interacts with the permeability transition pore to induce permeability transition and cytochrome c release in isolated mitochondria. *Proceedings of the National Academy of Sciences of the United States of America* 95(25):14681-14686.

123. Li P*, et al.* (1997) Cytochrome c and dATP-dependent formation of Apaf-1/caspase-9 complex initiates an apoptotic protease cascade. *Cell* 91(4):479-489.

124. Bouillet P & O'Reilly LA (2009) CD95, BIM and T cell homeostasis. *Nature reviews. Immunology* 9(7):514-519.

125. Tummers B & Green DR (2017) Caspase-8: regulating life and death. *Immunological reviews* 277(1):76-89.

126. Fu TM*, et al.* (2016) Cryo-EM Structure of Caspase-8 Tandem DED Filament Reveals Assembly and Regulation Mechanisms of the Death-Inducing Signaling Complex. *Molecular cell* 64(2):236-250.

127. Boatright KM*, et al.* (2003) A unified model for apical caspase activation. *Molecular cell* 11(2):529-541.

128. Krueger A, Schmitz I, Baumann S, Krammer PH, & Kirchhoff S (2001) Cellular FLICE-inhibitory protein splice variants inhibit different steps of caspase-8 activation at the CD95 death-inducing signaling complex. *The Journal of biological chemistry* 276(23):20633-20640.

129. Micheau O*, et al.* (2002) The long form of FLIP is an activator of caspase-8 at the Fas death-inducing signaling complex. *The Journal of biological chemistry* 277(47):45162-45171.

130. Kang TB*, et al.* (2008) Mutation of a self-processing site in caspase-8 compromises its apoptotic but not its nonapoptotic functions in bacterial artificial chromosome-transgenic mice. *Journal of immunology (Baltimore, Md. : 1950)* 181(4):2522-2532.

131. Wei MC*, et al.* (2001) Proapoptotic BAX and BAK: a requisite gateway to mitochondrial dysfunction and death. *Science (New York, N.Y.)* 292(5517):727-730.

132. Yin XM*, et al.* (1999) Bid-deficient mice are resistant to Fas-induced hepatocellular apoptosis. *Nature* 400(6747):886-891.

133. Mocarski ES, Upton JW, & Kaiser WJ (2012) Viral infection and the evolution of caspase 8-regulated apoptotic and necrotic death pathways. *Nature reviews. Immunology* 12(2):79-88.

134. Ea CK, Deng L, Xia ZP, Pineda G, & Chen ZJ (2006) Activation of IKK by TNFalpha requires site-specific ubiquitination of RIP1 and polyubiquitin binding by NEMO. *Molecular cell* 22(2):245-257.

135. Bertrand MJ*, et al.* (2008) cIAP1 and cIAP2 facilitate cancer cell survival by functioning as E3 ligases that promote RIP1 ubiquitination. *Molecular cell* 30(6):689-700.

136. Varfolomeev EE*, et al.* (1998) Targeted disruption of the mouse Caspase 8 gene ablates cell death induction by the TNF receptors, Fas/Apo1, and DR3 and is lethal prenatally. *Immunity* 9(2):267-276.

137. Wang L, Du F, & Wang X (2008) TNF-alpha induces two distinct caspase-8 activation pathways. *Cell* 133(4):693-703.

138. Vucic D, Dixit VM, & Wertz IE (2011) Ubiquitylation in apoptosis: a post-translational modification at the edge of life and death. *Nature reviews. Molecular cell biology* 12(7):439-452.

139. Moriwaki K & Chan FK (2013) RIP3: a molecular switch for necrosis and inflammation. *Genes & development* 27(15):1640-1649.

140. Sun L*, et al.* (2012) Mixed lineage kinase domain-like protein mediates necrosis signaling downstream of RIP3 kinase. *Cell* 148(1-2):213-227.

141. Dondelinger Y*, et al.* (2014) MLKL compromises plasma membrane integrity by binding to phosphatidylinositol phosphates. *Cell reports* 7(4):971-981.

142. Ros U*, et al.* (2017) Necroptosis Execution Is Mediated by Plasma Membrane Nanopores Independent of Calcium. *Cell reports* 19(1):175-187.

143. Lin Y, Devin A, Rodriguez Y, & Liu ZG (1999) Cleavage of the death domain kinase RIP by caspase-8 prompts TNF-induced apoptosis. *Genes & development* 13(19):2514-2526.

144. Feng S*, et al.* (2007) Cleavage of RIP3 inactivates its caspase-independent apoptosis pathway by removal of kinase domain. *Cell Signal* 19(10):2056-2067.

145. Oberst A, *et al.* (2011) Catalytic activity of the caspase-8-FLIP(L) complex inhibits RIPK3-dependent necrosis. *Nature* 471(7338):363-367.

146. Holler N, *et al.* (2000) Fas triggers an alternative, caspase-8-independent cell death pathway using the kinase RIP as effector molecule. *Nature immunology* 1(6):489-495.

147. Newton K, *et al.* (2014) Activity of protein kinase RIPK3 determines whether cells die by necroptosis or apoptosis. *Science (New York, N.Y.)* 343(6177):1357-1360.

148. Mandal P, *et al.* (2014) RIP3 induces apoptosis independent of pronecrotic kinase activity. *Molecular cell* 56(4):481-495.

149. Alvarez-Diaz S, *et al.* (2016) The Pseudokinase MLKL and the Kinase RIPK3 Have Distinct Roles in Autoimmune Disease Caused by Loss of Death-Receptor-Induced Apoptosis. *Immunity* 45(3):513-526.

150. Kaiser WJ, *et al.* (2014) RIP1 suppresses innate immune necrotic as well as apoptotic cell death during mammalian parturition. *Proceedings of the National Academy of Sciences of the United States of America* 111(21):7753-7758.

151. Dowling JP, Nair A, & Zhang J (2015) A novel function of RIP1 in postnatal development and immune homeostasis by protecting against RIP3-dependent necroptosis and FADD-mediated apoptosis. *Frontiers in Cell and Developmental Biology* 3.

152. Dillon CP, *et al.* (2014) RIPK1 blocks early postnatal lethality mediated by caspase-8 and RIPK3. *Cell* 157(5):1189-1202.

153. Rickard JA, *et al.* (2014) RIPK1 regulates RIPK3-MLKL-driven systemic inflammation and emergency hematopoiesis. *Cell* 157(5):1175-1188.

154. Cook WD, *et al.* (2014) RIPK1- and RIPK3-induced cell death mode is determined by target availability. *Cell death and differentiation* 21(10):1600-1612.

155. Remijsen Q*, et al.* (2014) Depletion of RIPK3 or MLKL blocks TNF-driven necroptosis and switches towards a delayed RIPK1 kinase-dependent apoptosis. *Cell death & disease* 5:e1004.

156. Kaiser WJ*, et al.* (2013) Toll-like receptor 3-mediated necrosis via TRIF, RIP3, and MLKL. *The Journal of biological chemistry* 288(43):31268-31279.

157. Upton JW, Kaiser WJ, & Mocarski ES (2012) DAI/ZBP1/DLM-1 complexes with RIP3 to mediate virus-induced programmed necrosis that is targeted by murine cytomegalovirus vIRA. *Cell host & microbe* 11(3):290-297.

158. Upton JW, Kaiser WJ, & Mocarski ES (2008) Cytomegalovirus M45 cell death suppression requires receptor-interacting protein (RIP) homotypic interaction motif (RHIM)-dependent interaction with RIP1. *The Journal of biological chemistry* 283(25):16966-16970.

159. Guo H, Kaiser WJ, & Mocarski ES (2015) Manipulation of apoptosis and necroptosis signaling by herpesviruses. *Medical microbiology and immunology* 204(3):439-448.

160. Lin J*, et al.* (2016) RIPK1 counteracts ZBP1-mediated necroptosis to inhibit inflammation. *Nature* 540(7631):124-128.

161. Newton K*, et al.* (2016) RIPK1 inhibits ZBP1-driven necroptosis during development. *Nature* 540(7631):129-133.

162. Rajput A*, et al.* (2011) RIG-I RNA helicase activation of IRF3 transcription factor is negatively regulated by caspase-8-mediated cleavage of the RIP1 protein. *Immunity* 34(3):340-351.

163. Schock SN*, et al.* (2017) Induction of necroptotic cell death by viral activation of the RIG-I or STING pathway. *Cell death and differentiation* 24(4):615-625.

164. Chun HJ*, et al.* (2002) Pleiotropic defects in lymphocyte activation caused by caspase-8 mutations lead to human immunodeficiency. *Nature* 419(6905):395-399.

165. Su H*, et al.* (2005) Requirement for caspase-8 in NF-kappaB activation by antigen receptor. *Science (New York, N.Y.)* 307(5714):1465-1468.

166. Ch'en IL, Tsau JS, Molkentin JD, Komatsu M, & Hedrick SM (2011) Mechanisms of necroptosis in T cells. *The Journal of experimental medicine* 208(4):633-641.

167. Ch'en IL*, et al.* (2008) Antigen-mediated T cell expansion regulated by parallel pathways of death. *Proceedings of the National Academy of Sciences of the United States of America* 105(45):17463-17468.

168. Čičin-Šain L*, et al.* (2008) Dominant-Negative FADD Rescues the In Vivo Fitness of a Cytomegalovirus Lacking an Antiapoptotic Viral Gene. *Journal of virology* 82(5):2056-2064.

169. Upton JW, Kaiser WJ, & Mocarski ES (2010) Virus inhibition of RIP3-dependent necrosis. *Cell host & microbe* 7(4):302-313.

170. Daley-Bauer LP*, et al.* (2017) Mouse cytomegalovirus M36 and M45 death suppressors cooperate to prevent inflammation resulting from antiviral programmed cell death pathways. *Proceedings of the National Academy of Sciences of the United States of America*.

171. Skaletskaya A*, et al.* (2001) A cytomegalovirus-encoded inhibitor of apoptosis that suppresses caspase-8 activation. *Proceedings of the National Academy of Sciences of the United States of America* 98(14):7829-7834.

172. McCormick AL, Skaletskaya A, Barry PA, Mocarski ES, & Goldmacher VS (2003) Differential function and expression of the viral inhibitor of caspase 8-induced apoptosis

(vICA) and the viral mitochondria-localized inhibitor of apoptosis (vMIA) cell death suppressors conserved in primate and rodent cytomegaloviruses. *Virology* 316(2):221-233.

173. McCormick AL & Mocarski ES (2013) Cell death pathways controlled by cytomegaloviruses. *Cytomegaloviruses: From Molecular Pathogenesis to Intervention*, ed Reddehase MJ (Caister Scientific Press, Norfolk, United Kingdom), Vol I, pp 263-276.

174. Kaiser WJ*, et al.* (2011) RIP3 mediates the embryonic lethality of caspase-8-deficient mice. *Nature* 471(7338):368-372.

175. Gunther C*, et al.* (2011) Caspase-8 regulates TNF-alpha-induced epithelial necroptosis and terminal ileitis. *Nature* 477(7364):335-339.

176. Hedrick SM, Ch'en IL, & Alves BN (2010) Intertwined pathways of programmed cell death in immunity. *Immunological reviews* 236:41-53.

177. Sears N, Sen GC, Stark GR, & Chattopadhyay S (2011) Caspase-8-mediated cleavage inhibits IRF-3 protein by facilitating its proteasome-mediated degradation. *The Journal of biological chemistry* 286(38):33037-33044.

178. Cuda CM*, et al.* (2014) Caspase-8 acts as a molecular rheostat to limit RIPK1- and MyD88-mediated dendritic cell activation. *Journal of immunology (Baltimore, Md. : 1950)* 192(12):5548-5560.

179. Cuda CM*, et al.* (2015) Conditional deletion of caspase-8 in macrophages alters macrophage activation in a RIPK-dependent manner. *Arthritis research & therapy* 17:291.

180. Weng D*, et al.* (2014) Caspase-8 and RIP kinases regulate bacteria-induced innate immune responses and cell death. *Proceedings of the National Academy of Sciences of the United States of America* 111(20):7391-7396.

181. Gurung P*, et al.* (2014) FADD and caspase-8 mediate priming and activation of the canonical and noncanonical Nlrp3 inflammasomes. *Journal of immunology (Baltimore, Md. : 1950)* 192(4):1835-1846.

182. Philip NH*, et al.* (2016) Activity of Uncleaved Caspase-8 Controls Anti-bacterial Immune Defense and TLR-Induced Cytokine Production Independent of Cell Death. *PLoS pathogens* 12(10):e1005910.

183. Philip NH*, et al.* (2014) Caspase-8 mediates caspase-1 processing and innate immune defense in response to bacterial blockade of NF-kappaB and MAPK signaling. *Proceedings of the National Academy of Sciences of the United States of America* 111(20):7385-7390.

184. Nogusa S*, et al.* (2016) RIPK3 Activates Parallel Pathways of MLKL-Driven Necroptosis and FADD-Mediated Apoptosis to Protect against Influenza A Virus. *Cell host & microbe* 20(1):13-24.

185. Hartmann BM*, et al.* (2017) Pandemic H1N1 influenza A viruses suppress immunogenic RIPK3-driven dendritic cell death. *Nature communications* 8(1):1931.

186. Jorgensen I, Rayamajhi M, & Miao EA (2017) Programmed cell death as a defence against infection. *Nature reviews. Immunology* 17(3):151-164.

187. Antonopoulos C*, et al.* (2015) Caspase-8 as an Effector and Regulator of NLRP3 Inflammasome Signaling. *The Journal of biological chemistry* 290(33):20167-20184.

188. Chung H, *et al.* (2016) NLRP3 regulates a non-canonical platform for caspase-8 activation during epithelial cell apoptosis. *Cell death and differentiation* 23(8):1331-1346.

189. Gringhuis SI, *et al.* (2012) Dectin-1 is an extracellular pathogen sensor for the induction and processing of IL-1beta via a noncanonical caspase-8 inflammasome. *Nature immunology* 13(3):246-254.

190. Kang S, *et al.* (2015) Caspase-8 scaffolding function and MLKL regulate NLRP3 inflammasome activation downstream of TLR3. *Nature communications* 6:7515.

191. Sarhan J, *et al.* (2018) Caspase-8 induces cleavage of gasdermin D to elicit pyroptosis during Yersinia infection. *Proceedings of the National Academy of Sciences of the United States of America* 115(46):E10888-E10897.

192. Kuida K, *et al.* (1996) Decreased apoptosis in the brain and premature lethality in CPP32-deficient mice. *Nature* 384(6607):368-372.

193. Lakhani SA, *et al.* (2006) Caspases 3 and 7: key mediators of mitochondrial events of apoptosis. *Science (New York, N.Y.)* 311(5762):847-851.

194. Knudson CM, Tung KS, Tourtellotte WG, Brown GA, & Korsmeyer SJ (1995) Bax-deficient mice with lymphoid hyperplasia and male germ cell death. *Science (New York, N.Y.)* 270(5233):96-99.

195. Lindsten T, *et al.* (2000) The combined functions of proapoptotic Bcl-2 family members bak and bax are essential for normal development of multiple tissues. *Molecular cell* 6(6):1389-1399.

196. Bouillet P*, et al.* (1999) Proapoptotic Bcl-2 relative Bim required for certain apoptotic responses, leukocyte homeostasis, and to preclude autoimmunity. *Science (New York, N.Y.)* 286(5445):1735-1738.

197. Hildeman DA*, et al.* (2002) Activated T cell death in vivo mediated by proapoptotic bcl-2 family member bim. *Immunity* 16(6):759-767.

198. Pellegrini M, Belz G, Bouillet P, & Strasser A (2003) Shutdown of an acute T cell immune response to viral infection is mediated by the proapoptotic Bcl-2 homology 3-only protein Bim. *Proceedings of the National Academy of Sciences of the United States of America* 100(24):14175-14180.

199. Wojciechowski S*, et al.* (2006) Bim mediates apoptosis of CD127(lo) effector T cells and limits T cell memory. *European journal of immunology* 36(7):1694-1706.

200. Fischer SF, Belz GT, & Strasser A (2008) BH3-only protein Puma contributes to death of antigen-specific T cells during shutdown of an immune response to acute viral infection. *Proceedings of the National Academy of Sciences of the United States of America* 105(8):3035-3040.

201. Kurtulus S*, et al.* (2015) Bim controls IL-15 availability and limits engagement of multiple BH3-only proteins. *Cell death and differentiation* 22(1):174-184.

202. Kurtulus S, Tripathi P, & Hildeman DA (2012) Protecting and rescuing the effectors: roles of differentiation and survival in the control of memory T cell development. *Frontiers in immunology* 3:404.

203. Petschner F*, et al.* (1998) Constitutive expression of Bcl-xL or Bcl-2 prevents peptide antigen-induced T cell deletion but does not influence T cell homeostasis after a viral infection. *European journal of immunology* 28(2):560-569.

204. Tripathi P*, et al.* (2010) STAT5 is critical to maintain effector CD8+ T cell responses. *Journal of immunology (Baltimore, Md. : 1950)* 185(4):2116-2124.

205. Rubinstein MP*, et al.* (2008) IL-7 and IL-15 differentially regulate CD8+ T-cell subsets during contraction of the immune response. *Blood* 112(9):3704-3712.

206. Huntington ND*, et al.* (2007) Interleukin 15-mediated survival of natural killer cells is determined by interactions among Bim, Noxa and Mcl-1. *Nature immunology* 8(8):856-863.

207. Min-Oo G, Bezman NA, Madera S, Sun JC, & Lanier LL (2014) Proapoptotic Bim regulates antigen-specific NK cell contraction and the generation of the memory NK cell pool after cytomegalovirus infection. *The Journal of experimental medicine* 211(7):1289-1296.

208. Brunner T*, et al.* (1995) Cell-autonomous Fas (CD95)/Fas-ligand interaction mediates activation-induced apoptosis in T-cell hybridomas. *Nature* 373(6513):441-444.

209. Dhein J, Walczak H, Baumler C, Debatin KM, & Krammer PH (1995) Autocrine T-cell suicide mediated by APO-1/(Fas/CD95). *Nature* 373(6513):438-441.

210. Ju ST*, et al.* (1995) Fas(CD95)/FasL interactions required for programmed cell death after T-cell activation. *Nature* 373(6513):444-448.

211. Rieux-Laucat F*, et al.* (1995) Mutations in Fas associated with human lymphoproliferative syndrome and autoimmunity. *Science (New York, N.Y.)* 268(5215):1347-1349.

212. Fisher GH*, et al.* (1995) Dominant interfering Fas gene mutations impair apoptosis in a human autoimmune lymphoproliferative syndrome. *Cell* 81(6):935-946.

213. Watanabe-Fukunaga R, Brannan CI, Copeland NG, Jenkins NA, & Nagata S (1992) Lymphoproliferation disorder in mice explained by defects in Fas antigen that mediates apoptosis. *Nature* 356(6367):314-317.

214. Takahashi T*, et al.* (1994) Generalized lymphoproliferative disease in mice, caused by a point mutation in the Fas ligand. *Cell* 76(6):969-976.

215. Bidere N, Su HC, & Lenardo MJ (2006) Genetic disorders of programmed cell death in the immune system. *Annual review of immunology* 24:321-352.

216. Sneller MC*, et al.* (1992) A novel lymphoproliferative/autoimmune syndrome resembling murine lpr/gld disease. *The Journal of clinical investigation* 90(2):334-341.

217. Zhou T*, et al.* (1996) Greatly accelerated lymphadenopathy and autoimmune disease in lpr mice lacking tumor necrosis factor receptor I. *Journal of immunology (Baltimore, Md. : 1950)* 156(8):2661-2665.

218. Adachi M*, et al.* (1996) Enhanced and accelerated lymphoproliferation in Fas-null mice. *Proceedings of the National Academy of Sciences of the United States of America* 93(5):2131-2136.

219. Cruz AC*, et al.* (2016) Fas/CD95 prevents autoimmunity independently of lipid raft localization and efficient apoptosis induction. *Nature communications* 7:13895.

220. Kang TB*, et al.* (2004) Caspase-8 serves both apoptotic and nonapoptotic roles. *Journal of immunology (Baltimore, Md. : 1950)* 173(5):2976-2984.

221. Zhang H*, et al.* (2011) Functional complementation between FADD and RIP1 in embryos and lymphocytes. *Nature* 471(7338):373-376.

222. Lu JV*, et al.* (2011) Complementary roles of Fas-associated death domain (FADD) and receptor interacting protein kinase-3 (RIPK3) in T-cell homeostasis and antiviral

immunity. *Proceedings of the National Academy of Sciences of the United States of America* 108(37):15312-15317.

223. Walsh CM*, et al.* (1998) A role for FADD in T cell activation and development. *Immunity* 8(4):439-449.

224. Salmena L*, et al.* (2003) Essential role for caspase 8 in T-cell homeostasis and T-cell-mediated immunity. *Genes & development* 17(7):883-895.

225. Beisner DR, Ch'en IL, Kolla RV, Hoffmann A, & Hedrick SM (2005) Cutting edge: innate immunity conferred by B cells is regulated by caspase-8. *Journal of immunology (Baltimore, Md. : 1950)* 175(6):3469-3473.

226. Tripathi P, Koss B, Opferman JT, & Hildeman DA (2013) Mcl-1 antagonizes Bax/Bak to promote effector CD4(+) and CD8(+) T-cell responses. *Cell death and differentiation* 20(8):998-1007.

227. Weant AE*, et al.* (2008) Apoptosis regulators Bim and Fas function concurrently to control autoimmunity and CD8+ T cell contraction. *Immunity* 28(2):218-230.

228. Masson F, Kupresanin F, Mount A, Strasser A, & Belz GT (2011) Bid and Bim collaborate during induction of T cell death in persistent infection. *Journal of immunology (Baltimore, Md. : 1950)* 186(7):4059-4066.

229. Fleck M*, et al.* (1998) Apoptosis mediated by Fas but not tumor necrosis factor receptor 1 prevents chronic disease in mice infected with murine cytomegalovirus. *The Journal of Clinical Investigation* 102(7):1431-1443.

230. Kawadler H, Gantz MA, Riley JL, & Yang X (2008) The paracaspase MALT1 controls caspase-8 activation during lymphocyte proliferation. *Molecular cell* 31(3):415-421.

231. Misra RS, *et al.* (2007) Caspase-8 and c-FLIPL associate in lipid rafts with NF-kappaB adaptors during T cell activation. *The Journal of biological chemistry* 282(27):19365-19374.

232. Arechiga AF, *et al.* (2005) Cutting edge: FADD is not required for antigen receptor-mediated NF-kappaB activation. *Journal of immunology (Baltimore, Md. : 1950)* 175(12):7800-7804.

233. Feng Y, *et al.* (2018) Remarkably Robust Antiviral Immune Response despite Combined Deficiency in Caspase-8 and RIPK3. *Journal of immunology (Baltimore, Md. : 1950)*.

234. Paulsen M & Janssen O (2011) Pro- and anti-apoptotic CD95 signaling in T cells. *Cell Commun Signal* 9:7.

235. Paulsen M, *et al.* (2011) Modulation of CD4+ T-cell activation by CD95 co-stimulation. *Cell death and differentiation* 18(4):619-631.

236. Strauss G, *et al.* (2009) CD95 co-stimulation blocks activation of naive T cells by inhibiting T cell receptor signaling. *The Journal of experimental medicine* 206(6):1379-1393.

237. Freimuth J, *et al.* (2013) Loss of caspase-8 in hepatocytes accelerates the onset of liver regeneration in mice through premature nuclear factor kappa B activation. *Hepatology* 58(5):1779-1789.

238. Najjar M, *et al.* (2016) RIPK1 and RIPK3 Kinases Promote Cell-Death-Independent Inflammation by Toll-like Receptor 4. *Immunity* 45(1):46-59.

239. Rebe C, *et al.* (2007) Caspase-8 prevents sustained activation of NF-kappaB in monocytes undergoing macrophagic differentiation. *Blood* 109(4):1442-1450.

240. Podmirseg SR, *et al.* (2016) Caspases uncouple p27(Kip1) from cell cycle regulated degradation and abolish its ability to stimulate cell migration and invasion. *Oncogene* 35(35):4580-4590.

241. Eymin B, *et al.* (1999) Caspase-induced proteolysis of the cyclin-dependent kinase inhibitor p27Kip1 mediates its anti-apoptotic activity. *Oncogene* 18(34):4839-4847.

242. Woo M, *et al.* (2003) Caspase-3 regulates cell cycle in B cells: a consequence of substrate specificity. *Nature immunology* 4(10):1016-1022.

243. Daszkiewicz L, *et al.* (2015) Distinct p21 requirements for regulating normal and self-reactive T cells through IFN-gamma production. *Scientific reports* 5:7691.

244. Yosefzon Y, *et al.* (2018) Caspase-3 Regulates YAP-Dependent Cell Proliferation and Organ Size. *Molecular cell* 70(4):573-587 e574.

245. Ding AX, *et al.* (2016) CasExpress reveals widespread and diverse patterns of cell survival of caspase-3 activation during development in vivo. *Elife* 5.

246. Gudipaty SA, Conner CM, Rosenblatt J, & Montell DJ (2018) Unconventional Ways to Live and Die: Cell Death and Survival in Development, Homeostasis, and Disease. *Annu Rev Cell Dev Biol* 34:311-332.

247. Sun G, *et al.* (2017) A molecular signature for anastasis, recovery from the brink of apoptotic cell death. *J Cell Biol* 216(10):3355-3368.

248. Chan FK, Luz NF, & Moriwaki K (2015) Programmed necrosis in the cross talk of cell death and inflammation. *Annual review of immunology* 33:79-106.

249. Mocarski ES, Kaiser WJ, Livingston-Rosanoff D, Upton JW, & Daley-Bauer LP (2014) True grit: programmed necrosis in antiviral host defense, inflammation, and immunogenicity. *Journal of immunology (Baltimore, Md. : 1950)* 192(5):2019-2026.

250. Mocarski ES, Guo H, & Kaiser WJ (2015) Necroptosis: The Trojan horse in cell autonomous antiviral host defense. *Virology* 479-480:160-166.

251. Micheau O & Tschopp J (2003) Induction of TNF receptor I-mediated apoptosis via two sequential signaling complexes. *Cell* 114(2):181-190.

252. Feoktistova M*, et al.* (2011) cIAPs block Ripoptosome formation, a RIP1/caspase-8 containing intracellular cell death complex differentially regulated by cFLIP isoforms. *Molecular cell* 43(3):449-463.

253. He S, Liang Y, Shao F, & Wang X (2011) Toll-like receptors activate programmed necrosis in macrophages through a receptor-interacting kinase-3-mediated pathway. *Proceedings of the National Academy of Sciences of the United States of America* 108(50):20054-20059.

254. Tenev T*, et al.* (2011) The Ripoptosome, a signaling platform that assembles in response to genotoxic stress and loss of IAPs. *Molecular cell* 43(3):432-448.

255. Omoto S*, et al.* (2015) Suppression of RIP3-dependent necroptosis by human cytomegalovirus. *The Journal of biological chemistry* 290(18):11635-11648.

256. Li M & Beg AA (2000) Induction of necrotic-like cell death by tumor necrosis factor alpha and caspase inhibitors: novel mechanism for killing virus-infected cells. *Journal of virology* 74(16):7470-7477.

257. Cho YS*, et al.* (2009) Phosphorylation-driven assembly of the RIP1-RIP3 complex regulates programmed necrosis and virus-induced inflammation. *Cell* 137(6):1112-1123.

258. Koehler H*, et al.* (2017) Inhibition of DAI-dependent necroptosis by the Z-DNA binding domain of the vaccinia virus innate immune evasion protein, E3. *Proceedings of the National Academy of Sciences of the United States of America* 114(43):11506-11511.

259. Thapa RJ, *et al.* (2016) DAI Senses Influenza A Virus Genomic RNA and Activates RIPK3-Dependent Cell Death. *Cell host & microbe* 20(5):674-681.

260. Kuriakose T, *et al.* (2016) ZBP1/DAI is an innate sensor of influenza virus triggering the NLRP3 inflammasome and programmed cell death pathways. *Science immunology* 1(2):aag2045.

261. Guo H, *et al.* (2015) Herpes simplex virus suppresses necroptosis in human cells. *Cell host & microbe* 17(2):243-251.

262. Guo H, *et al.* (2018) Species-independent contribution of ZBP1/DAI/DLM-1-triggered necroptosis in host defense against HSV1. *Cell death & disease* 9(8):816.

263. Sneller MC, *et al.* (1997) Clincal, immunologic, and genetic features of an autoimmune lymphoproliferative syndrome associated with abnormal lymphocyte apoptosis. *Blood* 89(4):1341-1348.

264. Zheng L, Li J, & Lenardo M (2017) Restimulation-induced cell death: new medical and research perspectives. *Immunological reviews* 277(1):44-60.

265. Durai V & Murphy KM (2016) Functions of Murine Dendritic Cells. *Immunity* 45(4):719-736.

266. Schraml BU & Reis e Sousa C (2015) Defining dendritic cells. *Current opinion in immunology* 32:13-20.

267. Kang TB, Yang SH, Toth B, Kovalenko A, & Wallach D (2013) Caspase-8 blocks kinase RIPK3-mediated activation of the NLRP3 inflammasome. *Immunity* 38(1):27-40.

268. Cuda CM, *et al.* (2012) Requirement of myeloid cell-specific Fas expression for prevention of systemic autoimmunity in mice. *Arthritis and rheumatism* 64(3):808-820.

269. Katagiri T, Cohen PL, & Eisenberg RA (1988) The lpr gene causes an intrinsic T cell abnormality that is required for hyperproliferation. *The Journal of experimental medicine* 167(3):741-751.

270. Andrews DM, Scalzo AA, Yokoyama WM, Smyth MJ, & Degli-Esposti MA (2003) Functional interactions between dendritic cells and NK cells during viral infection. *Nature immunology* 4(2):175-181.

271. Selgrade MK, Nedrud JG, Collier AM, & Gardner DE (1981) Effects of cell source, mouse strain, and immunosuppressive treatment on production of virulent and attenuated murine cytomegalovirus. *Infection and immunity* 33(3):840-847.

272. Livingston-Rosanoff D*, et al.* (2012) Antiviral T cell response triggers cytomegalovirus hepatitis in mice. *Journal of virology* 86(23):12879-12890.

273. Andrews DM*, et al.* (2010) Innate immunity defines the capacity of antiviral T cells to limit persistent infection. *The Journal of experimental medicine* 207(6):1333-1343.

274. Walton S, Mandaric S, & Oxenius A (2013) CD4 T cell responses in latent and chronic viral infections. *Frontiers in immunology* 4:105.

275. Jonjic S*, et al.* (1994) Antibodies are not essential for the resolution of primary cytomegalovirus infection but limit dissemination of recurrent virus. *The Journal of experimental medicine* 179(5):1713-1717.

276. Stranges PB*, et al.* (2007) Elimination of antigen-presenting cells and autoreactive T cells by Fas contributes to prevention of autoimmunity. *Immunity* 26(5):629-641.

277. Varanasi V, Khan AA, & Chervonsky AV (2014) Loss of the death receptor CD95 (Fas) expression by dendritic cells protects from a chronic viral infection. *Proceedings of the National Academy of Sciences of the United States of America* 111(23):8559-8564.

278. Cho BK, Rao VP, Ge Q, Eisen HN, & Chen J (2000) Homeostasis-stimulated proliferation drives naive T cells to differentiate directly into memory T cells. *The Journal of experimental medicine* 192(4):549-556.

279. Menard C*, et al.* (2003) Role of murine cytomegalovirus US22 gene family members in replication in macrophages. *Journal of virology* 77(10):5557-5570.

280. Mandal P*, et al.* (2018) Caspase-8 Collaborates with Caspase-11 to Drive Tissue Damage and Execution of Endotoxic Shock. *Immunity* 49(1):42-55.e46.

281. Autenrieth IB, Tingle A, Reske-Kunz A, & Heesemann J (1992) T lymphocytes mediate protection against Yersinia enterocolitica in mice: characterization of murine T-cell clones specific for Y. enterocolitica. *Infection and immunity* 60(3):1140-1149.

282. Rathinam VA & Fitzgerald KA (2011) Innate immune sensing of DNA viruses. *Virology* 411(2):153-162.

283. Redwood AJ*, et al.* (2005) Use of a murine cytomegalovirus K181-derived bacterial artificial chromosome as a vaccine vector for immunocontraception. *Journal of virology* 79(5):2998-3008.

284. Handke W*, et al.* (2013) Viral inhibition of BAK promotes murine cytomegalovirus dissemination to salivary glands. *Journal of virology* 87(6):3592-3596.

285. Manning WC, Stoddart CA, Lagenaur LA, Abenes GB, & Mocarski ES (1992) Cytomegalovirus determinant of replication in salivary glands. *Journal of virology* 66(6):3794-3802.

286. Sangster MY*, et al.* (2000) Analysis of the virus-specific and nonspecific B cell response to a persistent B-lymphotropic gammaherpesvirus. *Journal of immunology (Baltimore, Md. : 1950)* 164(4):1820-1828.

287. Daley-Bauer LP, Wynn GM, & Mocarski ES (2012) Cytomegalovirus impairs antiviral CD8+ T cell immunity by recruiting inflammatory monocytes. *Immunity* 37(1):122-133.

288. Torti N, Walton SM, Brocker T, Rulicke T, & Oxenius A (2011) Non-hematopoietic cells in lymph nodes drive memory CD8 T cell inflation during murine cytomegalovirus infection. *PLoS pathogens* 7(10):e1002313.

289. Shalini S, Dorstyn L, Dawar S, & Kumar S (2015) Old, new and emerging functions of caspases. *Cell death and differentiation* 22(4):526-539.

290. Kennedy NJ, Kataoka T, Tschopp J, & Budd RC (1999) Caspase Activation Is Required for T Cell Proliferation. *The Journal of experimental medicine* 190(12):1891-1896.

291. Newton K, Harris AW, Bath ML, Smith KG, & Strasser A (1998) A dominant interfering mutant of FADD/MORT1 enhances deletion of autoreactive thymocytes and inhibits proliferation of mature T lymphocytes. *The EMBO journal* 17(3):706-718.

292. Tsau JS, Huang X, Lai CY, & Hedrick SM (2018) The Effects of Dendritic Cell Hypersensitivity on Persistent Viral Infection. *Journal of immunology (Baltimore, Md. : 1950)* 200(4):1335-1346.

293. Wallach D & Kang TB (2018) Programmed Cell Death in Immune Defense: Knowledge and Presumptions. *Immunity* 49(1):19-32.

294. Crouse J, Xu HC, Lang PA, & Oxenius A (2015) NK cells regulating T cell responses: mechanisms and outcome. *Trends in immunology* 36(1):49-58.

295. Simon CO*, et al.* (2006) CD8 T cells control cytomegalovirus latency by epitope-specific sensing of transcriptional reactivation. *Journal of virology* 80(21):10436-10456.

296. Polic B*, et al.* (1998) Hierarchical and redundant lymphocyte subset control precludes cytomegalovirus replication during latent infection. *The Journal of experimental medicine* 188(6):1047-1054.

297. Lenzo JC, Shellam GR, & Lawson CM (2001) Ganciclovir and Cidofovir Treatment of Cytomegalovirus-Induced Myocarditis in Mice. *Antimicrobial Agents and Chemotherapy* 45(5):1444-1449.

298. Scholzen T & Gerdes J (2000) The Ki-67 protein: from the known and the unknown. *J Cell Physiol* 182(3):311-322.

299. Leverrier S, Salvesen GS, & Walsh CM (2011) Enzymatically active single chain caspase-8 maintains T-cell survival during clonal expansion. *Cell death and differentiation* 18(1):90-98.

300. Vivier E*, et al.* (2011) Innate or adaptive immunity? The example of natural killer cells. *Science (New York, N.Y.)* 331(6013):44-49.

301. Lam VC & Lanier LL (2017) NK cells in host responses to viral infections. *Curr Opin Immunol* 44:43-51.

302. Robbins SH*, et al.* (2007) Natural killer cells promote early CD8 T cell responses against cytomegalovirus. *PLoS pathogens* 3(8):e123.

303. Sun JC & Lanier LL (2008) Cutting edge: viral infection breaks NK cell tolerance to "missing self". *Journal of immunology (Baltimore, Md. : 1950)* 181(11):7453-7457.

304. Arase H, Mocarski ES, Campbell AE, Hill AB, & Lanier LL (2002) Direct recognition of cytomegalovirus by activating and inhibitory NK cell receptors. *Science (New York, N.Y.)* 296(5571):1323-1326.

305. Schuster IS*, et al.* (2014) TRAIL+ NK cells control CD4+ T cell responses during chronic viral infection to limit autoimmunity. *Immunity* 41(4):646-656.

306. Schuster IS, Coudert JD, Andoniou CE, & Degli-Esposti MA (2016) "Natural Regulators": NK Cells as Modulators of T Cell Immunity. *Frontiers in immunology* 7:235.

307. Nandakumar S, Woolard SN, Yuan D, Rouse BT, & Kumaraguru U (2008) Natural killer cells as novel helpers in anti-herpes simplex virus immune response. *Journal of virology* 82(21):10820-10831.

308. Bell BD*, et al.* (2008) FADD and caspase-8 control the outcome of autophagic signaling in proliferating T cells. *Proceedings of the National Academy of Sciences of the United States of America* 105(43):16677-16682.

309. Thome M, Charton JE, Pelzer C, & Hailfinger S (2010) Antigen receptor signaling to NF-kappaB via CARMA1, BCL10, and MALT1. *Cold Spring Harb Perspect Biol* 2(9):a003004.

310. Qiao Q*, et al.* (2013) Structural architecture of the CARMA1/Bcl10/MALT1 signalosome: nucleation-induced filamentous assembly. *Molecular cell* 51(6):766-779.

311. Salvesen GS & Walsh CM (2014) Functions of caspase 8: the identified and the mysterious. *Semin Immunol* 26(3):246-252.

312. Snyder CM*, et al.* (2009) CD4+ T cell help has an epitope-dependent impact on CD8+ T cell memory inflation during murine cytomegalovirus infection. *Journal of immunology (Baltimore, Md. : 1950)* 183(6):3932-3941.

313. Yamada Y*, et al.* (1991) The pathogenicity of ribonucleotide reductase-null mutants of herpes simplex virus type 1 in mice. *J Infect Dis* 164(6):1091-1097.

314. Min-Oo G, Kamimura Y, Hendricks DW, Nabekura T, & Lanier LL (2013) NK cells: walking three paths down memory lane. *Trends in immunology* 34(6):251-258.

315. Lau CM & Sun JC (2018) The widening spectrum of immunological memory. *Curr Opin Immunol* 54:42-49.

316. Arechiga AF*, et al.* (2007) A Fas-associated death domain protein/caspase-8-signaling axis promotes S-phase entry and maintains S6 kinase activity in T cells responding to IL-2. *Journal of immunology (Baltimore, Md. : 1950)* 179(8):5291-5300.

317. Marcais A*, et al.* (2017) High mTOR activity is a hallmark of reactive natural killer cells and amplifies early signaling through activating receptors. *Elife* 6.

318. Marcais A*, et al.* (2014) The metabolic checkpoint kinase mTOR is essential for IL-15 signaling during the development and activation of NK cells. *Nature immunology* 15(8):749-757.

319. Brownlie RJ & Zamoyska R (2013) T cell receptor signalling networks: branched, diversified and bounded. *Nature reviews. Immunology* 13(4):257-269.

320. Marchingo JM*, et al.* (2014) T cell signaling. Antigen affinity, costimulation, and cytokine inputs sum linearly to amplify T cell expansion. *Science (New York, N.Y.)* 346(6213):1123-1127.

321. Martin BN*, et al.* (2016) T cell-intrinsic ASC critically promotes T17-mediated experimental autoimmune encephalomyelitis. *Nature immunology*.

322. Prud'homme GJ, Kono DH, & Theofilopoulos AN (1995) Quantitative polymerase chain reaction analysis reveals marked overexpression of interleukin-1 beta, interleukin-1 and interferon-gamma mRNA in the lymph nodes of lupus-prone mice. *Mol Immunol* 32(7):495-503.

323. Loewendorf AI, Arens R, Purton JF, Surh CD, & Benedict CA (2011) Dissecting the requirements for maintenance of the CMV-specific memory T-cell pool. *Viral Immunol* 24(4):351-355.

324. Balomenos D, Rumold R, & Theofilopoulos AN (1998) Interferon-gamma is required for lupus-like disease and lymphoaccumulation in MRL-lpr mice. *The Journal of clinical investigation* 101(2):364-371.

325. Barton ES*, et al.* (2007) Herpesvirus latency confers symbiotic protection from bacterial infection. *Nature* 447(7142):326-329.

326. Furman D*, et al.* (2015) Cytomegalovirus infection improves immune responses to influenza. *Science translational medicine* 7(281):281ra243.